

AD-A151 234

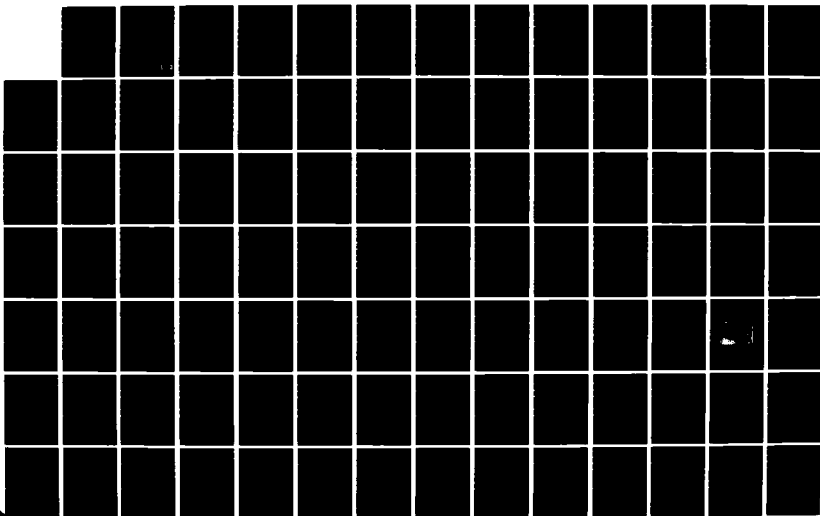
FIELD-INDUCED PHENOMENA IN ELECTRICAL INSULATION(U)
STATE UNIV OF NEW YORK AT BUFFALO DEPT OF ELECTRICAL
AND COMPUTER ENGINEERING J R LAGHARI ET AL. 29 SEP 84
AFOSR-TR-85-0129 AFOSR-83-0344

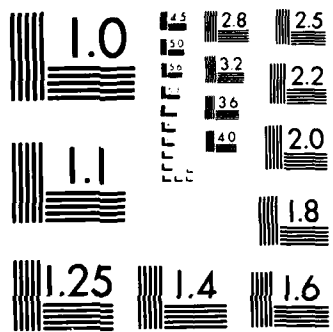
1/2

UNCLASSIFIED

F/G 28/3

NL





MICROCOPY RESOLUTION TEST CHART
NATIONAL BUREAU OF STANDARDS 1963-A

3

AD-A151 234

REPORT DOCUMENTATION PAGE

1. REPORT SECURITY CLASSIFICATION Unclassified		16. RESTRICTIVE MARKINGS	
2. SECURITY CLASSIFICATION AUTHORITY		3. DISTRIBUTION STATEMENT (AVAILABILITY STATEMENT) DISTRIBUTION STATEMENT A Approved for public release Distribution Unlimited	
3. DECLASSIFICATION/DOWNGRADING SCHEDULE		4. PERFORMING ORGANIZATION REPORT NUMBER(S)	
5. MONITORING ORGANIZATION REPORT NUMBER(S) AFOSR-TR- 85-0129		6. NAME OF PERFORMING ORGANIZATION State University of NY at Buffalo Dept. of Elect. & Computer Engr.	
7. NAME OF MONITORING ORGANIZATION Air Force Office of Scientific Research		8. OFFICE SYMBOL <i>If applicable</i>	
9. ADDRESS (City, State, and ZIP Code) 4232 Ridge Lea Road Amherst, New York 14226		10. NAME OF MONITORING ORGANIZATION Directorate of Physical & Geophysical Science Bolling Air Force Base, Washington, DC 20332	
11. NAME OF FUNDING SPONSORING ORGANIZATION Air Force Office of Scientific Re		12. OFFICE SYMBOL <i>If applicable</i>	
13. PROCUREMENT INSTRUMENT IDENTIFICATION NUMBER Contract AFOSR 830344		14. SOURCE OF FUNDING NOS. PROGRAM ELEMENT NO. PROJECT NO. TASK NO. WORK UNIT NO.	
15. ADDRESS (City, State, and ZIP Code) Directorate of Physical & Geophysical Science Bolling Air Force Base, Washington, DC 20332		16. TITLE (Include Security Classification) FIELD-INDUCED PHENOMENA IN ELECTRICAL INSULATION	
17. PERSONAL AUTHOR(S) J.R. Laghari, W.J. Sarjeant and R. K. Gupta			
18a. TYPE OF REPORT Annual Scientific		18b. TIME COVERED FROM 9/30/83 TO 9/29/84	
19. DATE OF REPORT (Yr., Mo., Day) 1984, October 26 SEPT. 27		20. PAGE COUNT 119	
21. SUPPLEMENTARY NOTATION			
22. COSATI CODES FIELD GROUP SUB GR		23. SUBJECT TERMS (Continue on reverse if necessary; use block numbers) Field, Electrical Insulation, Pulse Voltage, Corona-Inception, Corona-Extinction, Partial Discharge, Breakdown Temperature Rise.	
24. ABSTRACT (Continue on reverse if necessary; use block numbers) A review and an interpretation of the existing literature on dielectrics and dielectric breakdown was completed. Experiments were planned in light of the above interpretation and an experimental system was designed and developed. Experiments were then conducted on the time-to-break and breakdown of composite laminate insulation structures under pulsed and alternating voltages. Corona inception and extinction signatures were simultaneously obtained and evaluated. In view of the future experiments planned, theoretical and computer studies were carried out to determine the rise in temperature of laminate insulation structures under pulsed loads. All this was performed and is reported in this start-up phase first annual scientific report.			
25. DISTRIBUTION STATEMENT (AVAILABILITY OF ABSTRACT) UNCLASSIFIED Major Henry Pugh		26. ABSTRACT SECURITY CLASSIFICATION Unclassified (202) 767-4906	

DTIC FILE COPY

DTIC ELECTE
S MAR 11 1985 D

B

Unclassified

SCIENTIFIC
FIRST ANNUAL REPORT
(Start-Up Phase)
September 29, 1984

FIELD-INDUCED PHENOMENA
IN ELECTRICAL INSULATION

Approved for public release;
distribution unlimited.

Grant Number: AFOSR-830344
Starting Date: September 30, 1983
Submitted To: Dr. H. Pugh
Major, USAF
Directorate of Physical and
Geophysical Sciences
Air Force Office of Scientific
Research
Bolling Air Force Base
Washington, D.C. 20332
Submitted By: J. R. Laghari, W. J. Sarjeant and
R. K. Gupta*
Department of Electrical and
Computer Engineering
State University of New York at Buffalo
4232 Ridge Lea Road
Amherst, New York 14226
Telephone Number (716) 831-3164
*Department of Chemical Engineering

ABSTRACT

A review and an interpretation of the existing literature on dielectrics and dielectric breakdown was completed. Experiments were planned in light of the above interpretation and an experimental system was designed and developed. Experiments were then conducted on the time-to-break and breakdown of composite laminate insulation structures under pulsed and alternating voltages. Corona inception and extinction signatures were simultaneously obtained and evaluated. In view of the future experiments planned, theoretical and computer studies were carried out to determine the rise in temperature of laminate insulation structures under pulsed loads. All this was performed and is reported in this start-up phase first annual scientific report.

Approved For	<input checked="" type="checkbox"/>
Noted	<input type="checkbox"/>
Reviewed	<input type="checkbox"/>
Used	<input type="checkbox"/>
Justified	<input type="checkbox"/>
PER CALL TO	
By	
Distribution	
Availability	
Dist	S:
A-1	

AIR FORCE OFFICE OF SCIENTIFIC ASSESSMENT (AFSC)
NOTICE OF DISCONTINUATION
This report is discontinued and is
applicable to AFSC Form 100-12.
Distribution
MATTHEW J. [unclear]
Chief, Technical Information Division



SCIENTIFIC
FIRST ANNUAL REPORT
(Start-Up Phase)

TABLE OF CONTENTS

<u>Section</u>	<u>Page</u>
ABSTRACT.	i
LIST OF FIGURES	iv
LIST OF TABLES.	vi
RESEARCH OBJECTIVE.	vii
1. SUMMARY	1
1.1 Interpretation and Review of Literature.	1
1.2 Experimental Work.	1
1.2.1 Alternating Voltages	1
1.2.2 Corona Inception/Extinction Voltages	2
1.2.3 Pulse Voltages	2
1.3 Theoretical Work	3
2. INTERPRETATION AND REVIEW OF LITERATURE	3
2.1 Introduction	3
2.2 Characteristics of a Dielectric.	5
2.3 Solid Dielectrics.	17
2.4 Liquid Dielectrics	27
2.5 Composite Laminate Insulation Structures	35
2.6 Conclusions.	37
3. EXPERIMENTAL WORK	39
3.1 Test Cell and Electrode System	39
3.2 Sample Preparation	41
3.3 High Voltage Supplies and Measuring System	43
3.4 Experimental Results	49
3.4.1 Dielectric Constant and Dielectric Loss.	49
3.4.2 Complex Modulus and Mechanical $\tan \delta_m$	49
3.4.3 Alternating Voltage.	51
3.4.4 Corona Inception/Extinction Voltages	65
3.4.5 Pulse Voltages	69

<u>Section</u>	<u>Page</u>
4. THEORETICAL WORK.	86
4.1 Problem Formulation.	86
4.2 Initial and Boundary Conditions.	87
4.3 Steady State	88
4.4 Dimensionless Formulation.	88
4.5 Application to Composites.	90
4.6 Method of Solution	90
4.7 Material Properties Used	94
4.8 Method of Solution	94
4.9 Effect of Maximum Values of P_1 and P_2	97
4.10 Check of the Solution Scheme	97
4.11 Effect of Number of Layers at Fixed Values of L, W and H.	99
4.12 Effect of L and W Keeping H Constant	101
4.13 Effect of Changing H	101
4.14 Concluding Remarks	104
5. CONCLUSIONS (Year-1 Activity)	105
6. EXPERIMENTS IN PROGRESS	106
7. OTHER SUPPORTING INFORMATION.	107
7.1 Papers Presented	107
7.2 Personnel Supported.	107
8. REFERENCES.	108
9. APPENDICES	
A. Properties of Dielectrics Used.	114
B. Standard Deviations and Breakdown Voltages.	115
C. Solution of Two Dimensional Poisson Equation	117

LIST OF FIGURES

<u>Figure</u>		<u>Page</u>
2.1	Variation of breakdown strength with time of stressing. . .	7
3.1	Test fixture and electrodes mounted in the test chamber (A: test electrodes, B: test sample, C: test fixture, D: high voltage lead, E: high voltage feed through (banana plug), F: ground connection (banana plug)	40
3.2	Block diagram of the impregnation cycle	42
3.3	Circuit and test set up	44
3.4	Rise of applied voltage as a function of time ($t_s = 0, 15,$ 30, 60, 90 seconds)	46
3.5	Dissipation factor ($\tan \delta$) and relative dielectric constant (ϵ) of 1-mil polypropylene film at 21 °C as a function of frequency	50
3.6	Complex Modulus of a 3-mil polypropylene film as a function of temperature at 110 Hz.	52
3.7	Mechanical $\tan \delta_m$ of a 3-mil polypropylene film as a function of temperature at 110 Hz	53
3.8	Breakdown voltage of Mylar, Teflon and Polypropylene in a one layer structure in air under non-uniform field as a function of t_s	54
3.9	Breakdown voltage of Mylar, Teflon and Polypropylene for a 3-layer structure in air under non-uniform field as a function of t_s	55
3.10	Damage on a 3-mil polypropylene film tested under non- uniform field in air.	58
3.11	Breakdown voltage of polypropylene in air under uniform and non-uniform fields as a function of thickness	59
3.12	Breakdown voltage of polypropylene under uniform field as a function of t_s	61
3.13	Breakdown voltage of polypropylene with and without a void in the center layer of a 3-layer structure under uniform as a function of t_s	62
3.14	Corona Inception Voltage (CIV) and Corona Extinction Volt- age (CEV), at 60 Hz ac, 1 kV/sec. as a function of number of Mylar sheets, each 3-mil thick	66

<u>Figure</u>		<u>Page</u>
3.15	Corona Inception Voltage (CIV) and Corona Extinction Voltage (CEV), at 60 Hz ac, 1 kV/sec, as a function of number of Polypropylene paper sheets, each 2-mil thick	67
3.16	Corona Inception Voltage (CIV) and Corona Extinction Voltage (CEV), at 60 Hz ac, 1 kV/sec, as a function of number of Polypropylene sheets, each 2-mil thick	68
3.17	Typical waveforms for (a) pulsed and (b) ramped voltages.	71
3.18	Breakdown voltage vs. pulsewidth for 1 sheet of 3-mil (76.2 μ m) Mylar tested in Fluorinert. Risetime, t_r , is 0.1 μ s.	75
3.19	Breakdown voltage vs. pulsewidth for 2 sheets of 1-mil (25.4 μ m) Mylar tested in air. Risetime, t_r , is 0.1 μ s	76
3.20	Breakdown voltage vs. pulsewidth for 1 sheet of 1-mil (25.4 μ m) Polypropylene impregnated in Castor Oil. Samples were submerged in Castor Oil during tests and t_r was 0.1 μ s	77
3.21	Breakdown voltage vs. pulsewidth for 1 sheet of 1-mil (25.4 μ m) Polypropylene impregnated in Castor Oil. Samples were submerged in Transformer Oil during tests and t_r was 0.1 μ s.	78
3.22	Breakdown voltage vs. pulsewidth for 1 sheet of 1-mil (25.4 μ m) Polypropylene impregnated in Castor Oil. Samples were tested in air and t_r was 0.1 μ s.	79
3.23	Breakdown voltage vs leading-edge risetime for 1 sheet of 3-mil (76.2 μ m) Mylar. Samples were submerged in Fluorinert during tests	81
3.24	Breakdown voltage vs leading-edge risetime for 2 sheets of 1-mil (25.4 μ m) Mylar. Samples were tested in air.	82
3.25	Number of pulses to breakdown vs leading-edge risetime for 2 sheets of 1-mil (25.4 μ m) Mylar. Samples were tested in air and the applied voltage, V_a , was 10 kV.	84
3.26	Number of pulses to breakdown vs pulsewidth for 2 sheets of 1-mil (25.4 μ m) Mylar. Samples were tested in air and the risetime, t_r , was 0.1 μ s. The applied voltage, V_a , was 10 kV	85
4.1	Geometry of the system.	89
4.2	The flowchart of the Fortran program for the calculation of the steady state temperature profiles in the multilayer systems with heat generation.	96

<u>Figure</u>		<u>Page</u>
4.3	Dependence of the evaluated temperature vs. numbers of the terms in the summations in Equation 4.25.	98
4.4	Scheme 1.	100
4.5	Scheme 2.	0
4.6	Dependence of the temperature on the dimensions of the system ($L=W=DIM$, $H=1. * 10^{-2}m$) (scheme 2)	102
4.7	Dependence of the temperature on height ($L=0.1 m$, $w=0.1 m$) for different X - positions (scheme 2).	103

LIST OF TABLES

<u>Table</u>		<u>Page</u>
2.1	Some solid dielectrics with their properties.	18
2.2	Some liquid dielectrics with their properties	29
3.1	Summary of Experiment Descriptions.	72

RESEARCH OBJECTIVE

- o To establish a theoretical and experimental base in order to predict the influence of long-term electric field stress on dielectric behavior and breakdown.

FIELD INDUCED PHENOMENA IN ELECTRICAL INSULATION

Scientific

First Annual Report

(Start-Up Phase)

1. SUMMARY

Since the Grant started on September 30, 1983, progress has been made in the following areas:

1.1 Interpretation and Review of Literature

An interpretation and review of literature on the electrical properties of insulating materials was carried out in depth. The search revealed that more database is required, especially in the area of laminated-insulation breakdown, before any well-defined experimental or theoretical work could be carried out to understand the influence of electric field in dielectrics.

1.2 Experimental Work

Experimental work was carried out in the following areas:

1.2.1 Alternating Voltages

The rate of rise of the applied voltage was varied and the breakdown voltage of laminated and single structures (Mylar, Teflon or Polypropylene), impregnated with a suitable dielectric (air or castor oil), was determined under both uniform and non-uniform fields. The influence of a defect or a void in the laminate structure on the long-term dielectric strength was also evaluated. Results indicated that

(i) Composite laminate structures gave higher dielectric strength as compared with simple-layer structures. (ii) Partial discharges greatly reduced dielectric strength and life. (iii) Certain impregnants especially when matched with a suitable material, gave better corona performances and dielectric strengths.

1.2.2 Corona Inception/Extinction Voltages

Using a partial discharge detector the corona signatures from laminated structures were evaluated. The dielectrics used were Mylar, Polyethylene and Polypropylene. The number of layers varied from 1 to 4. The impregnants used were Fluorinert (FC-72) and air. Results showed that Fluorinert gave better corona performance of the insulating materials. Also, this performance improved by increasing the number of layers. This observation was quite consistent with the observations made earlier under Alternating Voltages.

1.2.3 Pulse Voltages

The MIT Mod-9 pulser was used to determine the time-to-break and the breakdown voltage of laminate structures. Two types of voltage pulses were used, viz pulse and ramp voltages, the variables being the rise-time, the pulsewidth and the applied voltage. The materials tested were Mylar and Polypropylene. The impregnants used were Fluorinert, castor-oil and air. A "threshold voltage" was found in Fluorinert below which breakdown would not occur irrespective of the number of pulses. This was not found in air. The pulse-width was found to have

very little effect on the dielectric strength under existing experimental conditions. The pulse rise-time may, however, influence time-to-break of insulation in certain cases.

1.3 Theoretical Work

A theoretical model using a finite sine transform method was developed to calculate the temperature increase in each layer of a composite laminate structure. Results were presently obtained for a polypropylene dielectric and a fluorinert impregnant placed between aluminum electrodes. It was found that the maximum temperature rise would be about 5.5 °C (at the center of a sandwiched block) when the block dimensions were 0.1 m x 0.01 m x 0.05 m. Details of this work are described later.

2. INTERPRETATION AND REVIEW OF LITERATURE

2.1 Introduction

Almost all electrical equipment depends on insulation in some form to maintain the flow of current in the proper channel as well as for the safety of operating personnel. It is well known that most of the failures in electrical apparatus occur due to the electrical breakdown of the insulating medium. Therefore, understanding the mechanism of the failure of the electrical insulation and dielectrics is important for the design of reliable high voltage apparatus.

Insulating materials, in general, are used in almost all existing electrical or non-electrical systems. Of those, the ones employed in electrical applications cover a very broad area which makes it extremely

There are other factors, not discussed here, which might indirectly influence the behavior of dielectrics and their properties. Some of these factors, such as density, surface tension, pour and flash points, electrode effects and other mechanical aspects could lead to electrical failure, especially in aged insulation. Also the effects of dirt contamination or additives (stabilizers) and environmental stability are equally important.

2.3 Solid Dielectrics

Solid dielectrics differ very widely in their properties as well as their chemical composition and therefore, the choice of the dielectric depends greatly on the application where it is to be used. In apparatus where the dielectric is to be lapped, for example, it is desirable to use polymers with high tensile modulus because it increases the accuracy of lapping and ensures that the dielectric will not suffer damage during reeling.^[30] In this section, only those solid dielectrics which have found extensive use in power capacitors will be discussed. These solid dielectrics along with their properties are given in Table 2.1. It is important, however, to note that these properties were obtained from different sources where the experimental conditions were not necessarily the same.

Kraft paper, which is mostly impregnated with chlorinated biphenyls, for small capacitor units, and with mineral oils for large units, has been used for a long time as the dielectric of ac power capacitors.^[31] It is also used where very low loss is not essential, such as in power-factor correction of inductive loads and fluorescent lighting circuits.

partial discharges, a low viscosity liquid will be desired because it helps prevent partial discharges by helping to maintain complete impregnation and thus exclude gases. Generally, the viscosity for most liquid dielectrics decreases with an increase in the temperature.

h. Moisture Content

All insulating materials, to some extent, absorb moisture. To operate them at their greatest dielectric efficiency, this moisture must be effectively removed. Removal of this moisture is usually done in the early fabrication and processing stages of the material. Water has little effect on organic materials which do not wet and have no affinity for the water, such as hydrocarbons, polytetrafluoroethylene, silicone rubbers and non-polar materials (unless they are impure). Impregnation of fibrous materials with a suitable liquid dielectric is a satisfactory way of preventing the major effects of moisture, but does not entirely avoid them.^[3]

The breakdown voltage, as well as many other electrical and mechanical properties, are very much affected by the moisture content of the dielectric, generally because of the chemical activity accelerated by the presence of this moisture.^[4] The loss tangent increases with moisture content, as was mentioned previously for dense paper. Also, the breakdown voltage and the corona inception voltage of transformer and silicone oil, respectively, shows a dramatic decrease with increase in water content.^[8] These effects should be considered seriously, especially where these liquid dielectrics act as impregnants in laminate insulation structures.

f. Thermal Stability

Thermal stability is another important factor which has to be considered in selecting insulating materials. Thermal stability is determined by all of the thermal properties of a dielectric. In particular, thermal conductivity, the glass-transition temperature, the melting point and the thermal coefficient of expansion are important properties. It has been mentioned before that some of the dielectric properties undergo changes due to increased temperature. There is usually an increase in the dielectric loss, a decrease in dielectric strength and a change in electrical stress distribution. It has been found that the effects of the rise in temperature of about 10 °C could halve the life expectancy of an insulating system.^[29]

Materials differ very widely in their thermal stability and are usually classified according to their temperature limit. The presence of foreign elements in a dielectric may also significantly influence its degradation rate. For example, the rate of deterioration of rubber and petroleum oil is greatly increased by the presence of oxygen, while this is not the case with mica, asbestos and cellulose. Cellulosic materials, however, deteriorate more rapidly in the presence of nitrogen.^[12]

g. Viscosity

Viscosities of liquid dielectrics differ from one to another and their selection depends on the purpose for which the liquid is being used. For example, in applications in which the material is subject to

capacitors. A partial discharge is, by definition, a discharge that bridges a part of a dielectric which is usually in a gaseous phase. The gas may be a permanent void caused by some imperfection, poor impregnation for example, or be produced by the continuous degradation or by high energy densities within the insulating system. The applied voltage at which discharges begin, as voltage is raised, is called the discharge inception voltage (DIV); the value at which they cease on reducing the voltage is called the discharge extinction voltage (DEV). The partial-discharge characteristics of an insulating system depend on many factors, such as: the ability of the liquid impregnant, if used, to produce and absorb gas under high electrical stress conditions, the hydrostatic pressure and temperature, the electrode design, the type of voltage applied, its frequency or repetition rate and its rise time, and the composition and processing of the dielectric.

As the hydrostatic pressure increases, the DIV and DEV values increase. This has been shown for polypropylene films by Shaw, et.al.^[26] Also, an increase in dielectric thickness and surface roughness corresponds to an increase in partial discharge values. The DIV and DEV usually increase with thickness, such as for Mylar,^[27] and with surface roughness, such as for polypropylene.^[18] For the case of paper-polypropylene film, the DIV and DEV exhibit a decrease with an increase in temperature while on the other hand for polypropylene (PP) film alone, they experience an increase with temperature.^[28] An important characteristic of the partial discharges is that they have a cumulative effect. Therefore, precautions should be taken in order to avoid an early failure in the insulating system.

$$\sigma = \sigma_0 \exp (-b/T) \quad (2.3)$$

where σ is the electrical conductivity, T is the temperature, and σ_0 and b are empirical constants.

The ac conductivity of liquid paraffin, silicone and mineral oil usually increases with temperature as given in the data by Hippel.^[12] Also, the conductivity of some insulating materials changes under the exposure of X-rays or gamma rays, where they experience a deterioration in their properties and some recovery occurs after the removal of the radiating source. The electrical conductivity σ as a function of radiation intensity could be expressed as^[12]

$$\sigma = \sigma_b (I/I_b)^n \quad (2.4)$$

where σ_b is the normal conductivity (at background irradiation rate), I_b is the background intensity of irradiation, I is the intensity of gamma irradiation, and n is a constant.

Existence of impurities such as contamination, sludge, or additives as well as the chemical compounds that form under discharges also cause a great change in the conductivity of the insulating system.^[12]

e. Resistance to Partial Discharge

Premature breakdown of insulation occurs, generally, at relatively low ac electric stress due to erosion, chemical degradation or deterioration resulting from partial discharges.^[25] The partial discharge characteristics of the insulating system influence the reliability of the system and this is especially true for high voltage

the $\tan \delta$ -voltage characteristics for polypropylene typically shows a decrease in $\tan \delta$ with an increase in voltage, attaining a minimum at about 6.8 kV and then increasing beyond that voltage;^[18] however, for the case of low-density polyethylene, $\tan \delta$ remains almost constant up to about 10 kV followed by a very sharp increase as the voltage is increased further. In the case of temperature, usually, the higher the temperature, the greater is the increase in $\tan \delta$.^[19] The loss angle of most dielectrics, especially polymers, usually shows an increase with frequency such as in the case of Teflon;^[20] however, for other insulants, like Mineral oil, $\tan \delta$ exhibits a linear decrease with an increase in the frequency at a constant temperature.^[21] It has been found that under alternating voltages, $\tan \delta$ is time dependent,^[22] where it tends to decrease with time of stress and under ac-dc mixed voltages conditions, the decrease is much more steeper than the ac case. Another important factor that influences the loss tangent of a dielectric is its moisture content, where it has been reported that the loss angle of both unimpregnated and oil-impregnated dense paper increases significantly with the moisture content.^[23]

d. Electrical Conductivity

The electrical conductivity of an insulating material increases with the voltage gradient and with increasing temperature. As the temperature increases, the viscosity goes down causing a rise in the mobility of the ions and hence an increase in the conductivity. The relation between conductivity and temperature can be expressed as follows^[24]

iv) Temperature, humidity, pressure, moisture content and other ambient conditions such as radiation could also influence the dielectric strength. Generally speaking, the dielectric strength of an insulating material reduces with temperature.^[14] The degree of decrease depends on the dielectric material involved as well as its crystallinity. For example, with high-density polyethylene polymer, the higher the crystallinity, the lower is the electric strength at a certain temperature.^[14] It has been also shown that the breakdown voltage increases with the partial pressure of the water vapor in the material.^[6]

b. Dielectric Constant

Dielectric constant or permittivity is a measure or indication of how freely the charges (or dipoles) within the dielectric could move (or rotate). Its value depends on the number of atoms or molecules per unit volume and the ability of each to be polarized. For most dielectrics, permittivity depends greatly on frequency, temperature, molecular weight as well as the density of the dielectric. The permittivity decreases as the frequency increases. At higher temperatures, this decrease usually tends to be sharper as is found in the case of PVC.^[15] Also, at a constant frequency, it decreases with an increase in temperature due to thermal expansion, such as for Teflon,^[16] while an increase in the density results in an increase in the permittivity.^[17]

c. Loss Factor

The loss factor of an insulating material is defined as the product of its dielectric constant and its dissipation factor, where the dissipation factor ($\tan \delta$ or D) is the tangent of the loss angle. $\tan \delta$ depends on the voltage applied, frequency and temperature. For example,

shortest rise time. This happens because the space charge formation times are less than the breakdown formative time lags.^[6] Therefore, short pulses have the highest breakdown voltages followed by ac, and then by dc. Also, breakdown voltages are sufficiently lower if the high field electrode is the cathode.^[6] This again occurs due to electron or negative charge injection caused by field emission from the cathode. It has also been determined^[11] that the breakdown voltages reduces slightly with pulse width. This decrease, is however, more rapidly at higher temperatures, as in the case of polyparabanic acid (PPA) film, where breakdown voltage reduces from 6 kV for a 0.5 μ sec pulse width to 4 kV for a 1000 μ sec pulse width at 250 °C.

ii) System geometry which includes uniformity of the electric field developed, electrode material and configuration, presence of voids and imbedded materials or impurities in the dielectric. It is well known that the more uniform the field, the higher is the breakdown voltage. Also, it has been reported that the greater the separation between the electrodes, the higher is the voltage to cause breakdown.^[12]

iii) Thickness and type of insulation (crystal, glass, polymer, composite) as well as the area of the specimen. It has generally been shown that the dielectric strength decreases with the area of the specimen used.^[13] Also, the dielectric strength per unit thickness decreases with an increase in thickness. This happens because the probability for a field emitted electron to find a weak spot or passage in the dielectric is also greater.

dielectric permittivity, dielectric loss, duty cycle of the applied voltage and the ambient conditions. An important characteristic of thermal breakdown is that the breakdown voltage does not increase in proportion to insulation thickness and that is because the greater the thickness, the more slowly heat is removed from the central region.

Breakdown due to partial discharges results from degradation or erosion of the dielectric caused by these discharges. These are usually initiated in the cavities or voids existing within the insulation or between the dielectric and the electrodes. The field intensity in these voids tends to be higher than that in the insulation medium itself because of the fact that their dielectric constant is lower than that of the dielectric. The dielectric breaks down when the voltage across the cavity exceeds its breakdown value causing discharges, resulting in the formation of chemical products that degrade the material.

In solid dielectrics, any form of breakdown may occur depending on the value of the field strength and its duration. While the electric strength of liquids mostly depends on the presence of moisture, gas pockets, or solid impurities, in gases, it is greatly affected by the temperature and pressure.

The value of the dielectric strength depends on the following:

- i) Type of the voltage applied, methods of excitation (penetrating charged particle or electron beam, electrical circuit), conditions of excitation (intensity, wave form),^[10] polarity, frequency or repetition rate, rise time, pulse width and total duration. Generally speaking the data indicates that breakdown voltages are the highest for voltages of the

ceed the lattice ionizing energy. If this process continues, formation of electron avalanche takes place resulting in a streamer. The fields at the streamer tips are estimated to be about 10^9 V/m (25 kV/mil).^[8]

Thermal breakdown usually occurs at high temperatures where the rate of heat generated exceeds the rate of heat removal. Most dielectrics show increasing electrical conductivity and decreasing thermal conductivity as the temperature increases.^[9] At high temperatures, the heat generated by conduction currents raises the dielectric temperature, which in turn gives rise to the conduction current leading to a thermal runaway and thus causing breakdown. Also, the thermal stress, resulting from increasing temperature, weakens the insulation by a slow process of aging which probably gives rise to partial discharges and hence accelerates the failure. The relation between the heat input to a specimen which must equal to the heat conducted away plus the heat used to raise the temperature T is given as^[6]

$$\sigma E^2 = C_v \frac{dT}{dt} + \text{div} (K \text{ grad } T) \quad (2.2)$$

where C_v is the specific heat/unit volume of specimen, K is the thermal conductivity, σ is the electrical conductivity, and E is the electric stress.

In the case of dc voltages, heat is generated inside the dielectric due to the conduction current while for ac conditions, it results from the dipole relaxation which depends on the rate of change of the field. Therefore, thermal breakdown strength is generally lower for ac fields and decreases with increasing frequency. It is also affected by the

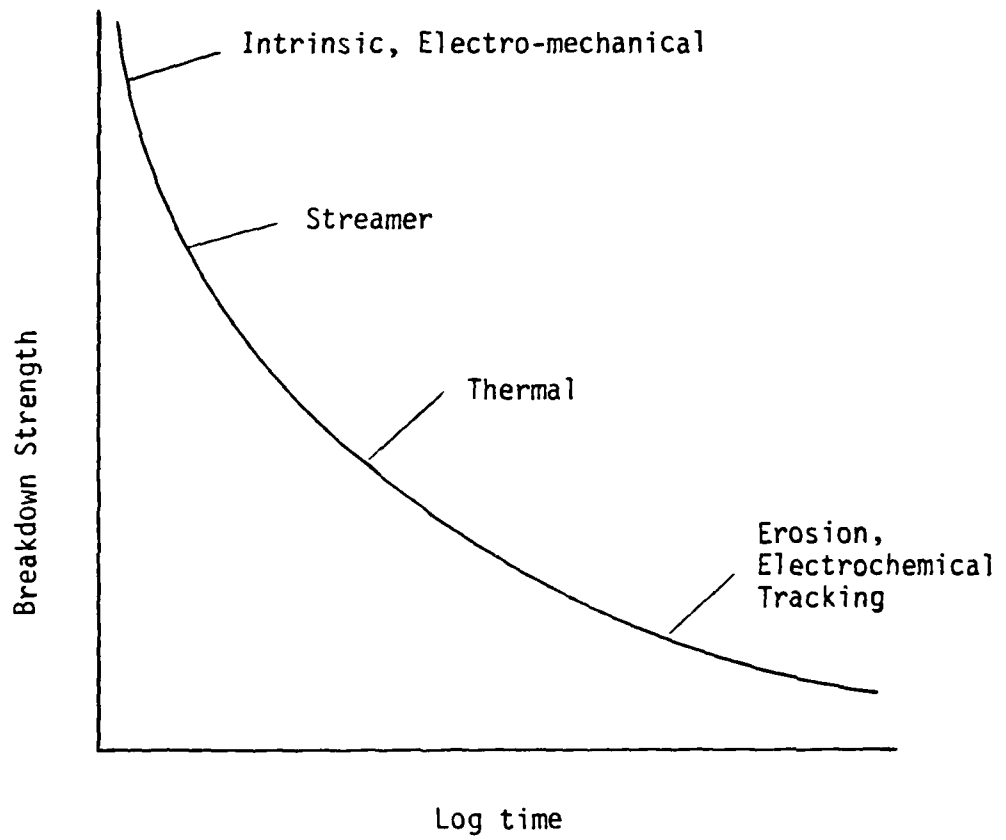


Figure 2.1 Variation of breakdown strength with time of stressing. [6]

to the breakdown depends on the duration of the applied stress and are summarized in Figure 2.1. [6]

Intrinsic breakdown occurs when the electric strength of a solid material increases rapidly and reaches its intrinsic electric strength under the influence of the applied voltage for a short period of time. The intrinsic strength of a material is reached when the electrons in the valence band gain sufficient energy to cross the forbidden gap to the conduction band. The stresses which cause that kind of electrical breakdown are usually well above 10^6 V/cm (2.5 kV/mil). [6]

Electromechanical failure occurs when the electrostatic pressure or the electrostrictive force resulting from the attraction between surface charges produced by the electric field exceeds the mechanical compressive strength of the material. Under an applied voltage V , the electrostatic compressive stress is in equilibrium if

$$\frac{\epsilon}{2} \left(\frac{V}{d_b} \right)^2 = Y \ln \left(\frac{d_0}{d_b} \right) \quad (2.1)$$

where ϵ is the permittivity of the dielectric, Y is its Young's Modulus, d_0 is its initial thickness, and d_b is the resulting thickness ($d_b < d_0$) due to the applied voltage V . [7]

Streamer breakdown occurs when an electron drifting from the cathode towards the anode (with electrodes embedded in the material to avoid external effects) under the influence of the applied field undergoes collision with other electrons or atoms gaining energy between collisions and losing it on collisions. Upon collision, an additional free electron is produced when the free path is long enough for the energy gain to ex-

Besides the basic physical, electrical, mechanical and chemical properties of a dielectric, some other factors also need to be considered, such as the availability to meet the demand required by the industry, cost and environment. All of these have to be examined carefully before coming to a decision as to which insulant is to be suitably employed in any particular application. This is reviewed and interpreted in detail in this section. All of this involves an understanding of the field-induced phenomena in electrical insulation.

2.2 Characteristic Properties of a Dielectric

The various sensitive factors that a material is characterized with, and are of importance to its behavior are, amongst other things, the dielectric strength, the dielectric constant, the loss factor, electrical conductivity, its resistance to partial discharges, thermal stability, viscosity and moisture content/chemical stability. All of these are discussed below under separate subheadings.

a. Dielectric Strength

The dielectric strength is the value of the voltage which causes the electric rupture (or breakdown) of an insulating material in a specified test configuration. Dielectric breakdown can result from high electric fields due to field enhancement at sharp points, presence of weak spots in the dielectric, or ionizing discharges in existing voids. The failure appears as a formation of a highly conductive path through the dielectric, a channel of molten material, gas evolution, cracks or blisters, a jagged hole, or a tree-like decomposition pattern of carbonized or metallic matter.^[4,5] The various mechanisms leading

difficult to be discussed under one topic. Electrical insulants could be found as one, or a combination, of these forms:

1. Vacuum
2. Gas
3. Liquid
4. Solid

The selection of a proper insulating material for a desired application depends a lot on the requirements and operating conditions of the device. For example, materials having low electrical conductivity are desired in power transmission lines and cable industry in order to reduce losses and to inhibit heating and other prebreakdown effects.^[1] In Extra-High Voltage (EHV) insulation, materials with high dielectric strength, low dielectric constant and particularly important, low dissipation factor are required.^[2] In capacitor design where high capacitance is desired, it is essential to use insulation of highest dielectric constant while on the other hand, for certain pulsed power applications, where it is required to generate very high current/voltage pulses of the smallest possible rise times, it will be desirable to use a capacitor containing a dielectric of the lowest dielectric constant and the highest dielectric strength. In other applications, such as high-energy-density capacitors, materials with high permittivities and dielectric strengths are employed to achieve maximum energy density.^[3]

From a mechanical point of view, flexibility of a dielectric may be required in cables, while, on the other hand, rigidity and good mechanical strength may be required in overhead transmission lines insulators.

Material	Thickness (μm)	Density (g/c.c.)	Air Permeability (Gurley sec/ 100 c.c.)	Tensile strength (kg/cm ²)	Elongation at break (%)	Tensile Modulus $\times 10^3$ (kg/cm ²)	Dielectric constant ASTM-D150 at 60 Hz except noted	Tan δ ASTM-D150 at 60 Hz except noted	Ac Breakdown strength ASTM-D149 (V/ μm)	Impulse Breakdown strength (V/ μm)	Water Absorption %	Ref.
Kraft Paper	127	0.67	1660	809	3.0	54	3.3 at 100 °C	0.00185 at 100 °C	9 (79)	23	-	34 (44)
PML	127	0.80	-	290 - 700	4.3 - 8.9	15	2.78 at 80 °C	0.00077	144	24	-	33
Tenax Paper	122	0.78	7130	350	3.8	16	2.4 100 °C	0.00036 at 100 °C	52	130	-	34
MPSP	52	0.46 - 0.58	>10,000	309 - 630	26 - 54	12 - 18	1.29 at 1kHz	-	-	-	-	31
Mica	101	2.6 - 3.3	-	-	-	-	5.5 - 7.0	0.0001 - 0.001	16	-	-	23
Polysulfone	-	1.24	-	717	100	25	3.14 at 60 Hz 3.13 at 10 ⁶ Hz 3.10 at 10 ⁹ Hz	0.0008 at 60 Hz 0.0034 at 10 ⁹ Hz	16 (315)	-	0.22	23,45 (44)
Polycarbonate	-	1.20	-	668	130	25	3.17 at 60 Hz 3.02 at 10 ⁶ Hz 2.93 at 10 ⁹ Hz	0.009 at 60 Hz 0.0021 at 10 ⁶ Hz 0.010 at 10 ⁹ Hz	15 (276)	-	0.18	23,45 (44)
Polystyrene	-	1.04 - 1.09	-	844	2	42	3.1 at 60 Hz 2.65 at 10 ⁶ Hz 2.7 at 10 ⁹ Hz	0.0006 at 60 Hz 0.0004 at 10 ⁶ Hz 0.0004 at 10 ⁹ Hz	24 (20)	-	0.1	23,45 (44)
LDPE	3	0.91 0.94	-	162	800	3	2.35	0.0005	28 (178)	-	0.01	23,45 (44)
HDPE	4	0.955	-	387	1300	13	2.35	0.0005	24 (178)	-	0.01	45,46 (44)
Teflon	50	2.14 - 2.28	-	352	400	4	2.1	0.0002	160 (60)	-	< 0.01	45,38 (44)
Nylar	25	1.395	-	1760	130	300	3.3	0.0025 at 25 °C 60 Hz	296 at 25 °C, 60 Hz (197)	-	< 0.8	12,41,21 (44)
Polypropylene- paper	150	0.65 - 0.75	200 - 800	141 - 210	5-6	2	1.7-1.9 at 60 Hz, 90 °C	0.0002-0.0004 at 60 Hz, 90 °C	52 with 500V/sec rise time 60 Hz, 25 °C	-	-	42
PP	5	0.65 0.75	200 - 800	387	700	16	1.7-2.6 60 Hz	0.0002 at 60 Hz	26 (296) (378)	-	0.3	45,42 (64) (44)

1. PML: Polymethyl Pentene Paper
2. MPSP: Micro Porous Synthetic Paper
3. LDPE: Low Density Polyethylene
4. HDPE: High Density Polyethylene
5. PP: Polypropylene

Table 2.1. Some solid dielectrics with their properties.

It is cost effective and has good electrical and mechanical properties. Its density ranges from $0.7 \cdot 10^3$ to $1.1 \cdot 10^3$ kg/m³ and it has suitable mechanical strength for easy winding in cable and capacitor sections. It is chemically inert in its purest form, has low inherent electrical conductivity^[32] and has a dielectric constant of about 6.5 when it is impregnated with a suitable liquid. However, it is relatively inhomogeneous in thickness over its width. The differences in thickness, on one hand, impart a rough surface to the paper which assists in its impregnation and, on the other hand, the existence of thin spots in the paper causes the voltage for breakdown to be less than that of the thicker parts of the paper. When impregnated in oil, it can withstand temperatures up to 110 °C.^[23] The dissipation factor changes with temperature and frequency and tends to increase sharply beyond 40 °C.^[28] In excess of 500 kV operation of oil-impregnated Kraft paper cable, the paper exhibits dielectric loss heating and excessive increases in insulation thickness. Therefore, due to its lack of thermal stability, Kraft paper is limited in the high temperature range.

Polymethylpentene paper (PML), a newly developed insulating paper, which consists of one layer of polymethylpentene and two layers of cellulose paper laminated, has shown good mechanical and electrical properties, such as low dielectric loss, high dielectric strength and excellent heat resistance;^[33] however, it swells and it is very resistant to oil. It has been reported that upon immersion in different oils, PML experiences a decrease in thickness up to about 15 hours of immersion time after which an increase in its thickness takes place. Compared to cellulose paper, PML has a lower dielectric loss and tends to be stable above 60 °C temperatures.

Tenax paper, a synthetic polymer paper, has been tested^[34] and found to have excellent thermal stability in dodecylbenzene (DDB) impregnant and may provide an EHV cable capable of operating at 25 kV/mm (0.63 kV/mil) and 120 °C. Also, it undergoes no significant changes in its thickness, modulus and degree of polymerization at elevated temperatures even up to 180 °C. Although it is not compatible with polybutene impregnants, it shows superiority over other dielectrics. For instance, its dielectric strength at power frequency is higher than that of Kraft paper but its impulse strength is lower because of its higher air impermeability.^[34] Tenax paper has a dissipation factor of about 2×10^{-4} and under aging test, it remains very low and stable for a period of 300 days at a stress of 22.5 kV/mm (0.57 kV/mil).

Another new synthetic paper, Micro Porous Synthetic Paper (MPSP), mainly comprises polypropylene containing small quantities of additives, for making pores with very little antioxidant, and is prepared using the conventional stretching process from polypropylene sheet.^[35] Its density ranges from $0.46 \cdot 10^3$ to $0.58 \cdot 10^3$ kg/m³ and it has a stable dielectric constant up to a frequency of 10^5 Hz. The dielectric constant has values of 1.29 and 2.2 in dry and mineral oil-impregnated cases, respectively; however, its $\tan \delta$ value changes with frequency, increasing with frequency from a minimum of about 0.0001 at a frequency of 1 KHz. Although MPSP is inferior to polypropylene in its impulse breakdown strength, it exhibits higher ac and impulse breakdown strengths and lower dielectric loss than cellulose paper does and it has superior mechanical properties after impregnation (with the exception of Young's Modulus). Also, MPSP exhibits less polarity effect than polypropylene films but more than that of cellulose paper.

Mica, which is formed from thin sheets of complex silicate structure, has a high dielectric constant and a low power factor. Although it is widely used in capacitors, the limited size of the individual mica sheets and the high cost of preparation limit its use to low capacitance values. It shows an excellent resistance to erosion by prolonged discharges and has a thermal stability up to about 600 °C. However, its loss tangent and conductivity increase rapidly at high temperatures and this, therefore, may limit its permissible operating temperature.

In recent years, plastic materials have been replacing paper in impregnated systems because of their low permittivities and far lower losses at higher stresses.^[32] However, when voids and air gaps are present, which is usually the case, partial discharges, which degrade the dielectric, occur at comparatively low voltages. The existence of these air gaps arise from the fact that plastic film is flat on its surface and thus it is difficult to impregnate with fluid between two adjacent films without creating some air pockets. Also, voids and microcavities in the polymer are usually formed during the polymer fabrication processes.

Polysulfone is one of the most expensive polymers used extensively in capacitors operating at high temperatures. It has good mechanical and thermal properties and could be used at temperatures from -50 to 150 °C. It is soluble in many organic solvents but resistant to acids and alkalis and less susceptible to hydrolysis than polyester films.

Polycarbonate is a clear, transparent material which could be obtained in either amorphous or crystalline form. It has a high tensile strength and a crystal point of 268 °C. Because of its strength and ability to form thin films, it is widely used in capacitors,^[36] however, it is resistant to mineral oil and partly soluble in aromatic fluids and other organic solvents. Unimpregnated polycarbonate tracks readily under damped conditions and its loss tangent varies greatly with frequency where it has been reported^[23] that a very sharp increase in $\tan \delta$ occurs beyond 10^4 Hz and, therefore, it may not be suitable for pulsed and high frequency applications.

Polystyrene is also one of the low loss synthetic materials used in capacitors which are limited to a temperature range of 70 to 75 °C.^[23] It has a crystal melting point of 80 °C above which, it becomes too soft to possess any mechanical strength. However, its mechanical properties can be improved by suitable stretching and heat treatment. It is compatible with paraffinic and silicone oils but it degrades when attacked by organic solvents or when exposed to radiation.

Polyethylene (PE) which has a wide application in high frequency cables, has not found wide application in power capacitors. It is easy to handle, available, and has low electrical losses and low moisture absorption. It is however subject to deterioration when exposed to ultraviolet causing degradation such as embrittlement and loss of electrical characteristics.^[19] Being a saturated polymer, it is resistant to chemical attacks and does not dissolve in warm paraffin oils. It is slightly soluble in vegetable and silicone oils. Depending on its

crystallinity, polyethylene could be obtained as a low-density or a high-density polymer. Low-density polyethylene (LDPE) is about 50 to 60% crystalline with a crystal melting point of 110 to 115 °C and softening temperature of about 90 °C, while high-density polyethylene (HDPE) is 90% crystalline with crystal melting point of about 135 °C which makes it stronger than the LDPE with better low temperature brittleness and higher mechanical stability at high temperatures.^[23] It has been shown that the dielectric breakdown of 1.5 micron PE film tends to decrease very sharply above room temperature.^[12] This behavior is especially found true under ac conditions.

Polytetrafluorethylene (PTFE), commercially known as Teflon, is one of the polymers that has a low electrical conductivity and exhibits a good stability in charge storage properties.^[37] It is widely used as capacitor dielectrics, wrap-on insulation for high performance wire and cable, and as phase and layer separators in transformer construction.^[38] It is chemically inert, nonflammable, has a low coefficient of friction and shows good thermal stability at higher temperatures where no cracking or embrittlement occurs. Experimental results have shown that the Teflon capacitor undergoes hardly any change in temperature when operated at a 1 KHz pulse repetition frequency and 100 ns discharge time as compared to the rapid rise in the temperature of a Mylar-paper capacitor.^[39]

The dielectric constant of Teflon is about 2.0 over a wide range of frequency but it changes with variation in the material density due to the thermal expansion or contraction. Its dissipation factor depends

on the frequency, temperature, crystallinity and void content. This dependence on the frequency was mentioned before in section 2.2, where it was reported that $\tan \delta$ changes considerably between $10^6 - 10^{10}$ Hz and reaches a maximum of about 0.00042 at 10^9 Hz. Although it displays good properties, Teflon applicability has some limitations because it creeps and exhibits deformation under load and its high melting point makes it difficult to process. It also has a high coefficient of expansion and is shown to increase, almost linearly, with temperature.^[12] Although it does not track, it is very susceptible to discharges and as a result, its dielectric strength degrades rapidly in the presence of ionization when the system operates above its corona-inception level.^[40]

Mylar, a polyester film made from polyethylene terephthalate (PETP), is very widely used as a capacitor dielectric because of the ease it could be handled and metallized, its strength and tear resistance. It has a good moisture resistance, has a crystal melting point of 265°C and can withstand temperatures from -70 to 150°C .^[41] Although Mylar is not affected by mineral or silicone oil, or by chlorinated biphenyls, it is subject to attack by strong acids and becomes brittle in contact with phenols and cresols. It does not track readily and its moisture absorption depends on crystallinity. Its dissipation factor and dielectric constant are frequency dependent. While its dielectric constant decreases with frequency, its $\tan \delta$ increases with frequencies up to 10^6 Hz where it reaches a maximum value of 0.018 and then declines afterwards. Data also shows that its resistivity decreases with temperature.^[12]

Non-woven polypropylene-paper (PP-P), consisting of either commercial grade or a special electrical grade polypropylene with ash contents of 0.10 and 0.0003 weight percent, respectively, has been reported by E. Forster, et. al.^[42] to have better dielectric properties than cellulose paper, and can, therefore, be used as a replacement for Kraft paper. It has a density between 0.89 and 0.91 g/c.c. with a dielectric constant of 1.7 to 1.9 at 60 Hz and 90 °C. Its dielectric loss ranges between 0.0002 and 0.0004 and decreases slightly when aged. When impregnated, the ready penetration of the oil represents a definite advantage over Kraft paper which requires extensive vacuum drying; however, polypropylene, like other plastic films, swells and dissolves to some extent in oil where this problem is not encountered with Kraft paper. The degree of dissolution depends on the molecular composition of the oil.

In applications where low loss and stable capacitance over a wide range of temperature are desired, such as high-voltage energy-storage capacitors, polypropylene has been widely used.^[3] In the early stages of its introduction, polypropylene was used in combination with paper dielectrics, as mentioned earlier, because the surface roughness of the paper provided a wick and thus good impregnation. But with some modification in the polypropylene surface, such as embossed foil and textured HAZY film, impregnation was improved without the additional dissipation factor that comes with the paper dielectric.^[26] Because of its high dielectric strength and low dissipation factor, polypropylene has shown superiority to Kraft paper and it is reported that the breakdown strength of polypropylene film, whether dry or impregnated, is much higher and its dielectric loss is much lower than those of paper

film.^[31] Besides being capable of withstanding higher stresses, a saving in production and operating costs could be achieved by using polypropylene instead of paper in the design of capacitor with a given power rating.^[32]

Polypropylene has a dielectric constant of about 2.0, largely independent of frequency up to at least 1 MHz, but temperature dependent as its density changes with temperature. It has a low dielectric loss with $\tan \delta$ values typically around 2×10^{-4} or less at room temperature. Its chemical stability greatly improves if its low molecular weight fractions are removed during manufacturing and thermally unstable additives are not present.

As mentioned before, polypropylene swells when impregnated with a liquid and that results in an increase in the thickness of the dielectric and a degradation in its properties. For instance, it has been shown that polypropylene exhibits a 10% increase in its weight when impregnated with Pyralene 1460,^[22] and its dielectric properties are degraded upon immersion in Diarylalkane.^[43] The amount of swelling, however, can be reduced by impregnating with liquids whose molecular size is larger than that of the solvent.

In order to minimize the amount of conductor used in low and medium voltage capacitors, an emerging high technology area was introduced as early as 1977 by employing metallized dielectrics. The metallized dielectric, which serves as an electrode and an insulant at the same time, is prepared by depositing a metal layer (Aluminum, for example), by evaporation on the dielectric film. Biaxially oriented PP with an

isotactic content of 95 to 97 percent is widely used in metallized films.^[3] The biaxial orientation of the film provides it with a very high dielectric strength which is almost double of that of paper foil. Besides their high operating dielectric stress (1.32 kV/mil), metallized-PP capacitors have low dielectric losses and high partial discharge inception voltage. However, they have some limitations because of their high current densities due to their extremely thin electrode, and they exhibit a capacitance loss due to electrode corrosion. To achieve higher dielectric stresses (1.8 kV/mil) and to reduce the loss in capacitance experienced by metallized - PP film, metallized paper-polypropylene film has been used. The difference in electrode base materials is believed to be the reason in eliminating such a loss in capacitance. Other advantages such as ease of impregnation and better partial discharge characteristics could be achieved as well by employing metallized paper-polypropylene.

2.4 Liquid Dielectrics

The functions of a liquid acting as an impregnants in high voltage apparatus differ from one application to another. Basically, they serve as an adhesive between layers to provide support and mechanical consolidation, act as the heat transfer medium and most important, they improve the dielectric strength by eliminating voids and replacing air or other gases which are the major elements in causing or continuation, of partial discharges. Also they absorb gases developed at high stress region especially in sealed equipments such as cables and capacitors where oils containing hydrogen-absorbing constituents are generally used to ensure that gas is not evolved. Some disadvantages, however, do arise upon using liquid impregnants, such as an increase in the overall cost, an

increase in size and weight of the assembly and a change in the temperature range of operability; however, with the selection of a suitable impregnant to be used in combination with the solid laminate, one could improve the overall performance of the system.

The choice of an impregnant depends on the purpose it is being used for and on the area of application. The major key points that should be looked into are: The dielectric strength, power factor, insulation resistance and dielectric constant, the gas absorption properties, the ability of penetration into the polymer to fill any voids and micro-gaps if they exist, chemical purity, inertness and stability (under discharges and high temperatures), viscosity and surface tension, heat transfer properties (such as heat and thermal conductivity) and non toxicity and non hazardness.

In this section, only those liquid dielectrics will be discussed that serve as impregnants in power capacitors and are listed along with some of their properties in Table 2.2. It is important, however, to realize that the data listed in this table is obtained from different sources where experimental and test conditions are not necessarily the same.

Polychlorinated biphenyl (PCB), the most widely used liquid impregnant till 1972, is a non inflammable liquid with high dielectric constant, high dielectric strength and considerably low loss tangent. Because of its high degree of stability under high stress and temperature and its good performance under corona conditions, this fluid had been the major impregnant for nearly fifty years and used in both paper and polypropylene film - paper capacitors.^[47] It was also shown that when PCB replaced

Liquid Impregnant (oil)	Dielectric constant	$\tan \delta \times 10^{-3}$	Dielectric Strength ($V/\mu m$)	Conductivity $\times 10^{-13}$ (S/cm)	Viscosity (Cs)	Absorption index ($\mu t/min$)	Specific gravity (g/c.c.)	Pour point ($^{\circ}C$)	Flash point ($^{\circ}C$)	Fire point ($^{\circ}C$)	Ref.
Polychlorinated biphenyl	5.4 at 20 $^{\circ}C$, 50Hz	5-9 at 20 $^{\circ}C$, 50Hz	-	-	86 at 40 $^{\circ}C$	-20 at 30 $^{\circ}C$	1.39 at 20 $^{\circ}C$	-	170	300	28,47
Askarel	4.8 at 25 $^{\circ}C$	1-3	12-14 at 25 $^{\circ}C$	0.1-1.0 at 25 $^{\circ}C$	-	-	-	-14 - -20	166 - 180	320	12,58
Silicone	2.8 at 25 $^{\circ}C$	0.1 - 0.3	10-12 at 25 $^{\circ}C$	0.1 at 25 $^{\circ}C$	50	-	0.959	-60	280 - 320	310 - 370	12,56,59
Mineral	2.2-2.3 at 25 $^{\circ}C$	0.2 - 1.0	11-12 at 25 $^{\circ}C$	0.001 - 0.1 at 25 $^{\circ}C$	11.2 at 30 $^{\circ}C$	-	0.879	-40 - -55	145 - 154	150 - 170	12,56,60
Castor	4.7 at 27 $^{\circ}C$, 100 $^{\circ}C$, 50 Hz	0.5 at 85 $^{\circ}C$, 3 at 27 $^{\circ}C$	12	3.9 at 30 $^{\circ}C$, 50Hz	81 at 40 $^{\circ}C$	-19 at 30 $^{\circ}C$	0.947	-45 - -52	150 - 220	240 - 260	12,28,58, 52
Di-2-ethyl-hexyl phthalate	5.33	1.4	11	210	81 at 20 $^{\circ}C$	-	-	-50	218	246	61
Di-isononyl phthalate	4.66	0.5	12	29	95 at 20 $^{\circ}C$	-	-	-48	221	257	61
Fluorocarbon Liquid	1.75 - 1.89	< 0.5	39-45 kV ASTM 0-877	10^{-4} - 10^{-2}	0.475 - 2.96 at 25 $^{\circ}C$	-	1.69 - 1.87 at 25 $^{\circ}C$	-100 - -50	69 - 178	-	53
UGILEC * 101	2.66	< 4	> 70 kV VDE elect-trodes 2 mm gap	< 1	2.8 at 50 $^{\circ}C$, 6.5 at 20 $^{\circ}C$, 100 at -30 $^{\circ}C$	-	1.006 at 20 $^{\circ}C$, 0.948 at 100 $^{\circ}C$	-	144	154	54

* A benzyltoluene-based liquid

Table 2.2. Some liquid dielectrics with their properties.

mineral oil as an impregnant in power capacitors, the reactive power density (proportional to ϵE^2) was at least doubled.^[48] Its usage, however, was banned by the EPA after it was found to be toxic and would create environmental hazards to land and aquatic life.^[49] Therefore, finding impregnants that can replace PCB with equally good properties, as well as the search for new polymers that are compatible with such impregnants are still of great importance for the design and reliability of high voltage equipment.

Askarel is the generic name of a number of synthetic chlorinated hydrocarbons. Pentachlorodiphenyl, one of the askarel products, has good properties and is commonly used. Its dielectric constant, however, is greatly affected by the temperature where its value drops from about 5.0 at 25 °C to about 3.2 at -30 °C and thus resulting in a lower capacitance at low temperatures.^[12] This low temperature effect could be minimized by adding stabilizers or by reducing the freezing point of the fluid. Chlorinated aromated-askarel liquids have been primarily used for fire-resistant capacitors because of their good thermal stability and they do not exhibit any decomposition up to 175 °C.^[32] They also do not react with oxygen and moisture. They are slightly sensitive to ultraviolet light and when subject to partial discharges, they produce hydrogen chloride and scavengers which accelerate the chemical degradation of the system. Also, they do not perform well under high field and high frequency conditions.^[45]

Silicone fluids, formed from Si-O chains with organic (usually methyl) side groups, are chemically inert and have been considered as an alternative to PCB in heat-resistant oil-filled transformers and high voltage capacitors.^[50] They have low surface tension, low temperature coefficient of viscosity, low dielectric losses and high dielectric strength. Silicone oils are remarkably stable with a temperature range from about -65 °C to 200 °C and some have short-time capability up to 300 °C;^[45] however, these fluids are not suitable for use under corona discharge or breakdown conditions because they evolve gas and have the tendency to form carbon tracks under high electric fields. Also they burn readily when ignited and are, therefore, probably explosive.

Mineral oil, typically called transformer oil, is one of the insulating oils whose permittivity is low because they are essentially non-polar. Its electrical behavior is very sensitive to contamination and moisture and it is oxidized easily under the exposure of oxygen producing peroxides, organic acids and sludge.^[12] The formation of those products could be reduced by changing the aromatic content of the oil by introducing oxidation inhibitors into it.

Ester fluids have high dielectric constant (4 to 7) but are slightly more conductive than other liquids. Their thermal stability is poor and in high temperature applications they must be kept dry because they are sensitive to moisture presence, under which acids and alcohols formation can take place.^[45]

The desired output voltage was obtained by operating the output variac manually while a digital stop-watch was used to record the time. The voltage was applied as follows: the voltage was raised at a rate of 500 V/sec for 2 seconds and held constant for some time t_s , defined as the steady state time and which is one of the parameters in these investigations, then raised again at the same rate (500 V/sec) for another 2 seconds and then held constant for the same time t_s . This sequence was repeated until breakdown occurred. The breakdown was detected by the visual disappearance of glowing partial discharges and the discontinuation of the hissing corona sounds (in case of samples tested in air). At the same time, a sudden current flow was displayed on the ammeter with a simultaneous reduction of the high voltage in all the tests. For each data point, an average of seven measurements was made. All voltages appearing in the figures are in RMS values, except where noted. The applied voltage as a function of t_s is shown in Figure 3.4.

Corona inception voltages (CIV) and corona extinction voltage (CEV) as well as ac breakdown strength were determined using a Biddle partial discharge analyzer (PDA). The analyzer consists of a variable motor-driven, high voltage power supply, partial discharge detection and amplification circuitry and a CRT display. Discharges were measured and displayed simultaneously on the PDA CRT and on a Tektronix 556 oscilloscope. The PDA was calibrated using a Biddle partial discharge amplifier calibrator, model 6617250, and was found to be accurate for discharges having magnitudes as small as 2 picocoulombs (pC) and as large as 60 pC. When used for breakdown studies, the high voltage supply had an overcurrent detector that was set to open-circuit the supply when currents in the sample exceeded 5 mA. The entire measurement system was placed in

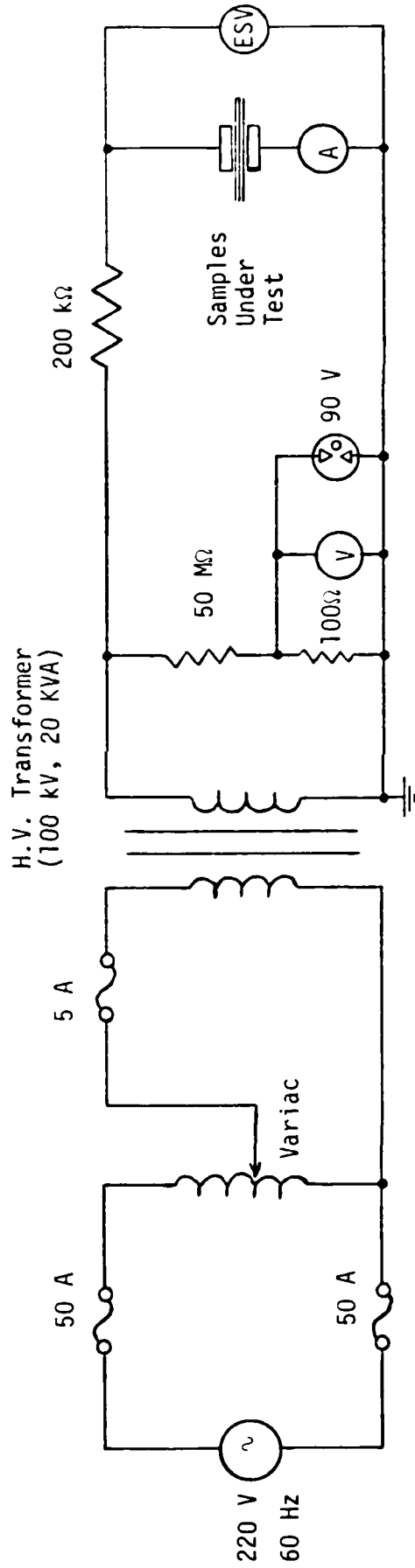


Figure 3.3. Circuit and test set up

In some samples, an artificial void was formed by using a small heated pin and piercing each sample individually. This void was made, in the middle layer of a 3-layer structure, and was about 4 mils in diameter. Care was taken to prevent the other two surrounding layers from coming in contact with each other.

The dielectrics used in the experiment and some of their properties are listed in Appendix A.

3.3 High Voltage Supplies and Measuring Systems

The alternating voltage power supply used was a Hipotronics ac Dielectric Test Set (Model 7100-20) which consisted of a controller connected to a High Voltage Transformer. The controller contained the on-and-off main power and control switches, high voltage-on push buttons, a voltmeter and an ammeter with a 2% accuracy, an adjustable overload protection (from 25 to 110% of rated current), and the output voltage variac. The unit required an input of 440 V ac with a maximum current of up to 50 A and was capable of supplying up to 100 kV at 200 mA. However, due to the limitations in the voltage available in the high voltage laboratory, 220 volts input was used, providing a maximum output voltage of 50 kV. A 200 k Ω current limiting resistor was placed in series with the high voltage (HV) output. The voltage across the test sample was measured by a Sensitive Research Electrostatic Voltmeter (ESV)-Model ESH-23X of $\pm 0.1\%$ accuracy. The circuit and test setup is shown in Figure 3.3.

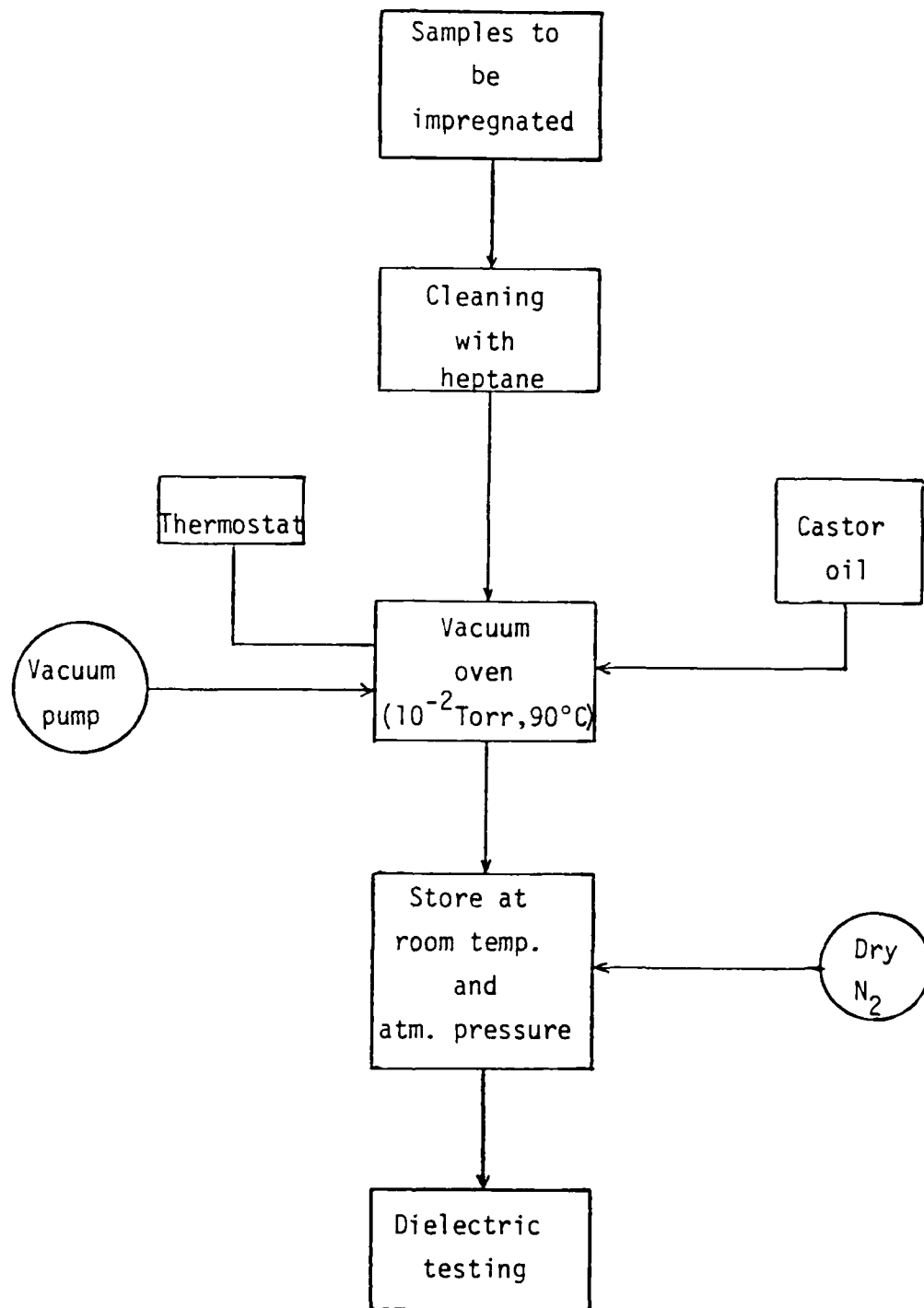


Figure 3.2 Block diagram of the impregnation cycle.

Before and during each test the electrodes were handled carefully with poly gloves in order to avoid getting any dirt or grease onto the polished electrode surface. The electrodes were cleaned by first polishing them with Brasso liquid using cheese cloth and then by washing them with heptane. Heptane was used as a cleanser because it proved to be more efficient than acetone and ethanol in removing moisture and any other contaminants.

3.2 Samples Preparation

The samples to be tested were cut by a sharp blade to the required size. The size of each sample was large enough to assure that breakdown occurred through the sample and no surface flashovers took place. The thickness of each sample was determined by using a sensitive micrometer, taking the average of five measurements. The dry samples were cleaned by wiping both surfaces with heptane just before use. The samples, which had to be impregnated with oil, were first dried in a glass vessel in a GCA Precision Vacuum Oven at a pressure of 10^{-2} Torr at 90 °C for 16 hours. The liquid impregnant was then slowly brought into the oven until the samples were completely immersed in the fluid. In order not to break the vacuum, a DUO SEAL vacuum pump Model 1397 was used. The samples were then allowed to soak in this fluid for 16 hours at 90 °C under vacuum. At the end of this period, the samples were allowed to cool slowly to room temperature, then dry nitrogen was bled into the oven to bring the pressure up to atmospheric. The glass vessel containing oil-covered samples was then removed from the oven to a dessicator and stored under nitrogen until needed. In carrying out the tests on impregnated samples, the samples and the electrodes had to remain covered by the test fluid to avoid corona discharges, surface trackings or air breakdown. A block diagram of the impregnation cycle is shown in Figure 3.2.

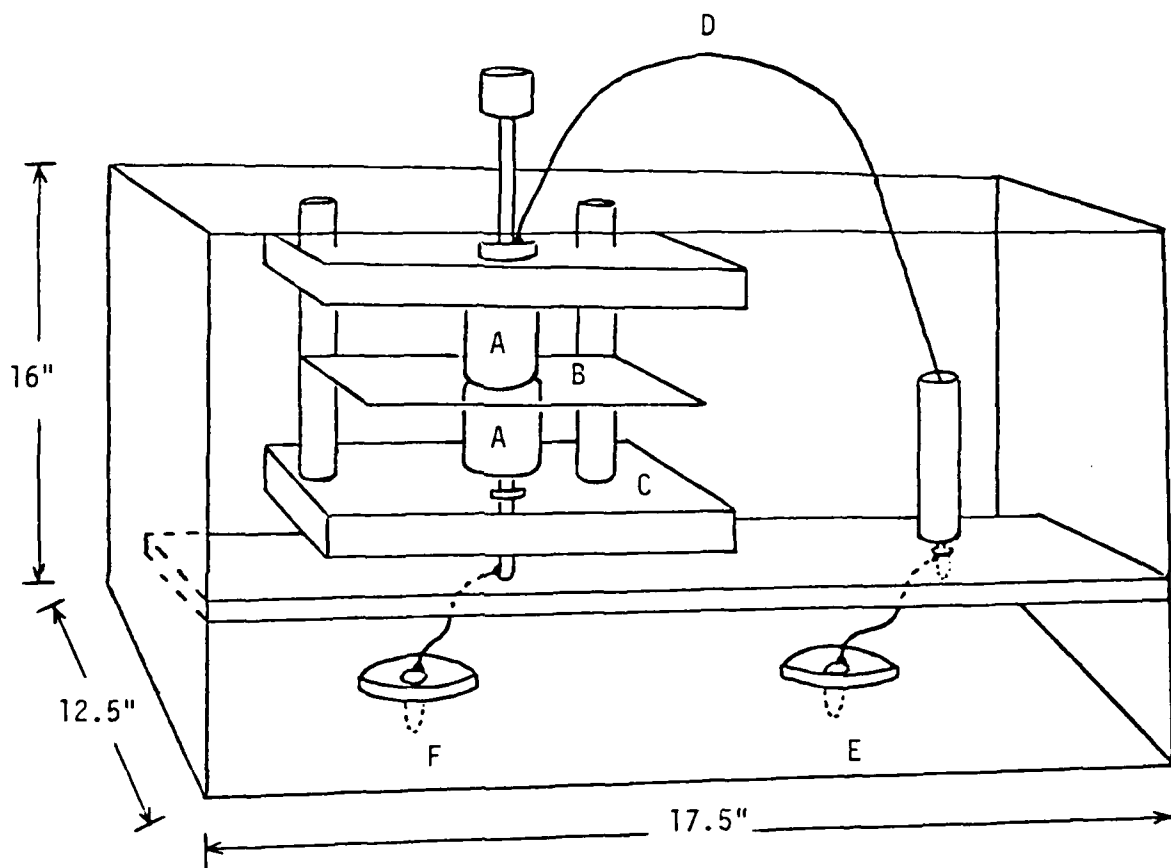


Figure 3.1 Test fixture and electrodes mounted in the test chamber (A: test electrodes, B: test sample, C: test fixture, D: high voltage lead, E: high voltage feed through (banana plug), F: ground connection (banana plug).

3. EXPERIMENTAL WORK

3.1 Test Cell and Electrodes Systems

The investigations were carried out in a test fixture designed to meet ASTM specifications D-149 for testing sheets, plates and tapes for electrical insulation. A test sample, inserted between the electrodes, may be tested either in a gas or in a liquid by inserting the test fixture in a test chamber which has dimensions of 0.32 m wide, 0.44 m long, and 0.41 m deep. The test chamber was made of clear plexiglass for full view of the test specimen and for the visual observation of the discharges. High-voltage and ground leads are connected to the bottom of the test compartment.

The brass electrodes used were in accordance with ASTM-D149. A one 1/4-inch (6.35 mm) diameter rod electrode having a 1/32 inch (0.79 mm) radius rounded edge and weighing 50 g, and two 2-inch (50.80 mm) diameter plane electrodes with 1/8 inch (3.18 mm) radius edges having a weight of 450 g each were used to produce a nonuniform and uniform field, respectively. The lower electrode had a swivel pad to assure full contact of both electrode surfaces on the material surface under test and was terminated in a banana plug on the bottom of the fixture assembly. The upper electrode assembly was connected through a flexible lead terminating in another banana plug on the bottom of the fixture assembly. To insert the specimen to be tested, the upper, or movable, electrode was lifted and the test sample was placed between the electrodes. The upper electrode was then replaced back on top of the specimen surface. The test fixture and the electrodes mounted in the test chamber are shown in Figure 3.1.

It is, therefore, highly desirable that in this initial stage investigations be carried out to determine the basic dielectric properties of composite laminate insulation structures under ac and pulsed voltages along the lines of the ongoing research activities of the high field materials research group at Buffalo. This data is required for some commonly used dielectrics under both uniform and non-uniform field configurations.

As the influence of partial discharges and aging effects is crucial in determining the withstand voltage of a system, it was also felt that there is a need to obtain data under both the 500 V/sec (ASTM standard D-149) and slower rate of rise of applied voltages. Under these conditions, occurrence of partial discharges within the laminate structure would be primarily responsible for dielectric breakdown. Lastly, the influence of an artificially created void on the dielectric strength, to further intensify such discharges, also needs to be determined.

Therefore, on the basis of the review presented within this section, the following research was undertaken: an experimental system was designed and developed (Section 3.1 to 3.3), tests were performed (Section 3.4) and some theoretical studies were carried out (Section 4) to get a better insight into the field-induced phenomena in electrical insulation.

where ϵ_0 is the dielectric constant of free space, A is the area of a plate electrode, and C is the capacitance.

The major key points that have to be examined carefully in order to have a good match between the laminates and the impregnants are: the dielectric strengths for use in high energy density capacitors, the dielectric constants, the different thicknesses to be employed of each material corresponding to the change in the dielectric constants (for example to minimize losses or to obtain required capacitance), the chemical stability between the different dielectrics, the temperature limit of each of the insulants, and the nature of the application to be used, especially in power capacitors. For example, when the application requires a high discharge inception voltage, the dielectrics must have as high a permittivity as possible consistent with maintaining a sufficiently low overall dielectric loss for the capacitor, while thermal runaway condition dictates the use of a dielectric combination with the lowest possible dielectric loss. [32]

2.6 Conclusion

To our knowledge, there seems to be scarce data available in the published literature on the dielectric properties and breakdown voltages of laminate insulation structures. Among other things, little information is available on the effects of rise time and pulsewidth of the applied voltage on breakdown behavior. Also, as can be seen from Tables 2.1 and 2.2, there is inconsistency in the available data even on the basic dielectric properties of insulating materials used in power capacitors. This could be attributed to the varying experimental techniques that each author has applied to suit his or her own needs.

$$E_1 = \frac{V}{d_1 + d_2 \left(\frac{\epsilon_1}{\epsilon_2}\right)} \quad (2.5)$$

$$E_2 = \frac{V}{d_1 \left(\frac{\epsilon_2}{\epsilon_1}\right) + d_2} \quad (2.6)$$

where V is the total voltage across the electrodes, E_1 and E_2 are the voltage stresses in materials 1 and 2, ϵ_1 and ϵ_2 are the dielectric constants of materials 1 and 2, d_1 and d_2 are the thicknesses of materials 1 and 2.

Also, it has been shown^[63] that for a three-layer system consisting of different dielectrics, such as oil, paper, and plastic film, the field in any layer is given by

$$E_i = \frac{V}{\epsilon_i} \div \left[\frac{d_i}{\epsilon_i} + \frac{d_j}{\epsilon_j} + \frac{d_k}{\epsilon_k} \right] \quad (2.7)$$

where V is the applied voltage, ϵ_i is the layer dielectric constant, and d_i is the layer thickness.

The over-all capacitance as well as the loss factor change by employing a composite structure. Those two parameters for a two dielectric system can be expressed as follows:^[45]

$$C = \frac{\epsilon_0 \epsilon_1 \epsilon_2 A}{\epsilon_1 d_2 + \epsilon_2 d_1} \quad (2.8)$$

$$\tan \delta = \frac{\left(\frac{d_1}{d_2}\right) \epsilon_2 \tan \delta_1 + \epsilon_1 \tan \delta_2}{\epsilon_1 + \epsilon_2 \left(\frac{d_1}{d_2}\right)} \quad (2.9)$$

2.5 Laminate Insulation Structures

As discussed previously, in power capacitors where the requirements call for high energy density, insulating films with high dielectric strengths are used. In these capacitors, the solid dielectric (paper, for example), consists usually of a number of thin layers, impregnated with a liquid insulant. The use of a laminate, which is a composite structure consisting of two or more layers of insulating material, ensures that a defect (e.g., a pin hole) in one layer does not result in a breakdown of the dielectric at that point.^[62] Some other benefits are gained by using the laminate structure such as the ability to use some solid dielectrics in the form of thin layers which are very hard, or might crack, in their application with a certain thickness, especially, in a roll-type capacitor. Most important of all is that better cooling can be achieved by having one of the layers to undergo a thermal runaway rather than the whole specimen as one part. Also, in case of a discharge initiation, this discharge has to propagate through many different media, including the impregnant in order to cause a complete deterioration and breakdown of the insulating material.

In utilizing composite dielectrics, various factors have to be examined carefully in order to ensure a good match between the laminate and the impregnant. Basically, the presence of a second (or third) insulation in series with the primary insulation upsets the voltage distribution across the insulation and under ac voltages, the electric stress is permanently distributed in a ratio inversely proportional to the dielectric constants of the materials present. In a two dielectric system, the stress distribution can be computed as follows:^[8]

Conduction currents in liquid dielectrics lead to instabilities that are characterized by violent fluctuations in magnitude when the applied stress exceeds a few hundred kilovolts per centimeter. These fluctuations or pulses increase rapidly with the applied voltage and ultimately lead to a complete breakdown. To overcome such a problem, gas-saturated liquids are being used extensively in power apparatus. Of those dissolved gases, oxygen, nitrogen and sulfur hexafluoride SF_6 are commonly employed. The introduction of gases into liquid impregnants seems to improve their characteristics and tends to have a little increase in the overall cost of the system. It is believed that the electron affinity (or electronegativity) of the gases enhances the dielectric strength of the liquids saturated with those gases. The degree of enhancement depends on the amount of the gas absorbed by the liquid, which in turn, is a function of the applied hydrostatic pressure. It has been shown that upon addition of oxygen into transformer oil, a decrease by an order of magnitude results in the conduction currents level in the liquid compared to that of the degassed oil.^[55]

In the case of n-hexane, minute quantities of dissolved oxygen results in an increase in the breakdown strength and a decrease in the conductivity at high electric fields, and with nitrogen dissolved in oil, conduction currents as well as current pulses are considerably reduced.^[56] Also, it has been found that the ac partial discharge inception voltage for an oil saturated with SF_6 gas at a high pressure of 10 atm and under a high hydrostatic pressure of 12 atm increases to a value of 1.4 times larger than that for a degassed oil at 5×10^{-5} Torr.^[57]

strength; however, when fluorine, like chlorine, replaces the hydrogen it seems to result in a lower impulse strength but a higher ac strength.^[23] Therefore, fluorine liquids tend to have some limitations under impulse conditions. They also have limited applications in apparatus in which arcing may take place, because, although they produce less carbon and less gas on arcing than petroleum oils, the gases produced may be quite corrosive.^[12]

Because of their low dielectric constants, fluorinated liquids have been favored in applications where interelectrode capacitance effects, which may be introduced by the liquid, need to be minimized. Also, it had been reported that the heat transfer efficiency increases from 50 to 300 percent when fluorinated liquids replace transformer oil in cooling power transformers and considerably more power can be put into the system.^[53]

A newly developed liquid from France, UGILEC 101, has been reported to play an important role as an impregnant in high voltage power capacitors.^[54] The impregnant which is manufactured from the cheapest aromatic hydrocarbon is economically as well as technically very attractive and it displays excellent performance in the low temperature range of operation (-40 °C). It has a dielectric constant of about 2.66, a dielectric loss of less than 0.004 and a very low viscosity, even at low temperatures. Because of its very low viscosity and very high aromaticity, the new liquid has shown outstanding partial discharge characteristics.

Castor oil, which is a polar dielectric and one of the ester fluid family, has been successfully used as an impregnant in power capacitors including the paper-type ones. It undergoes little decomposition under the influence of electric fields and that permits using higher operating voltages in the insulation and as a result, higher energy densities can be obtained. It is remarkably stable within the temperature range from -20 to +85 °C but its loss angle increases with frequency and temperature; however, it is possible to reduce its rate of rise of dissipation factor with temperature.^[51] An important characteristic of castor oil is that its relaxation frequency, which lies between 800 KHz and 1 MHz, makes it very desirable as an impregnant in high-frequency high voltage capacitors.^[50] Its gas absorption capability, which is relatively smaller than other liquids, might limit its usage. Although it is an inflammable fluid, it has been replacing the PCB due to its nontoxicity and since its vapors have no harmful effects on living organisms.^[49] The properties of castor oil as well as two other phthalate ester derivatives, namely Di-2-ethylhexyl and Di-isononyl, are also listed in Table 2.2.

Fluorinated liquids, used in electronic circuits for cooling and usually referred to as fluorocarbons or perfluorocarbons to emphasize the replacement of hydrogen by fluorine, are also used as impregnants in capacitors; however, many of them are very volatile. They are non-flammable liquids, inert and stable to temperatures above their boiling points (> 178 °C) which make them compatible with other materials used in capacitors for the long-term storage point of view. They have relative permittivities of 1.75 to 2.1 with low loss and good dielectric

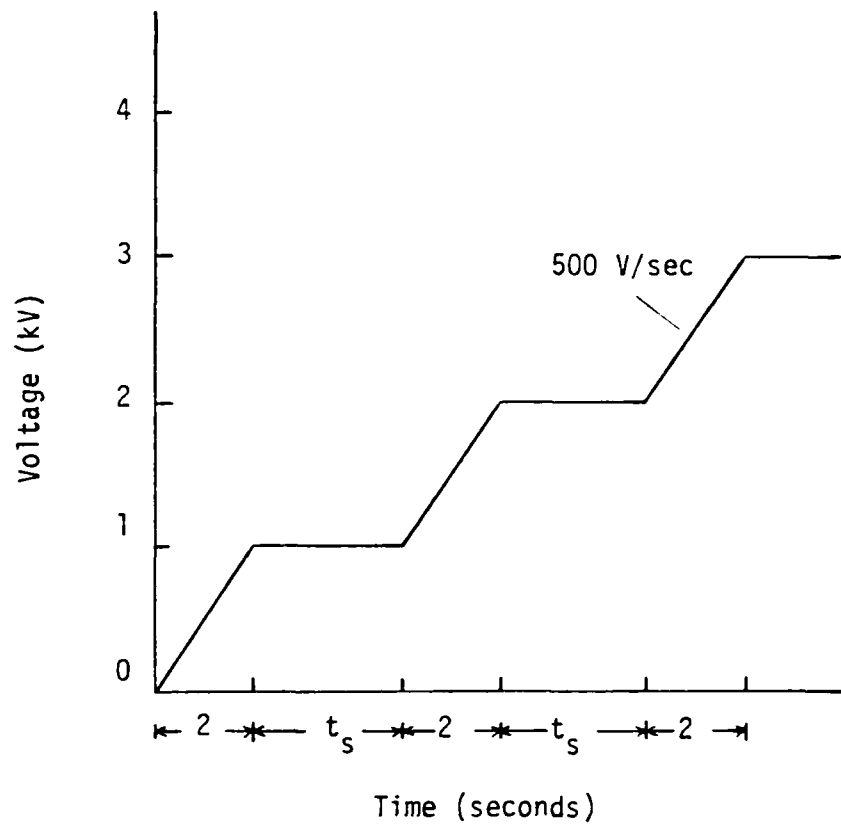


Figure 3.4 Rise of applied voltage as a function of time ($t_s = 0, 15, 30, 60, 90$ seconds).

a screen enclosure to prevent spurious rf signals from interfering with the measurement. The voltage was applied to the test cell and increased slowly until stable, repetitive discharges exceeding 5 pC were observed. The voltage, which was monitored by a digital voltmeter at which the 5 pC discharge level was reached was taken as the CIV. After raising the voltage 100 volts above this level, the voltage was reduced slowly until the discharges fell below the 5 pC level, and the voltage at which this occurred was taken as the CEV.

The Pulse breakdown voltages were determined by using an MIT Model 9 hard-tube pulser. The pulser, which was initially designed to drive a magnetron radar unit, produced pulses at rates up to 1700 pulses per second (pps). The pulses initially had peak voltages of up to 25 kV, a rise-time of 50 ns and pulse-widths of 800 ns. The pulser was, however, modified for the present work to provide pulses with continuously variable pulse widths between 10 ns and 5000 ns, and rise times between 50 and 5000 ns. A Tektronix P6015 high voltage probe was used to view the pulses applied to the test cell and the pulses were displayed on a Tektronix 556 oscilloscope. A digital counter was used to count the number of pulses to breakdown.

The dielectric constant and the dissipation factor of the specimen as a function of frequency were determined at room temperature by using a Capacitance Bridge Type 1615-A which requires an external generator and a detector. A General Radio type 1311-A audio oscillator and General Radio type 1232-A tuned amplifier and null detector were used. In order to avoid waveform distortion, the input to the bridge was adjusted in a way not to exceed 30 volts for every kilo hertz. Shielded patch cords were also used to reduce noise in connecting all of those instruments.

Some of the physical properties of a polymer such as, the dynamic modulus and the mechanical $\tan \delta_m$ of electrically stressed and unstressed samples, were also determined in a temperature range from 22.5 °C to 130 °C using a Rheovibron model DDV-II which is a direct reading type dynamic viscoelastometer. In the Rheovibron, a sinusoidal strain of 110 Hz frequency is applied to one end of the dielectric specimen with dimensions of 1.2" long, 0.1" wide, and 3 mils thick and the response or stress was measured at the other end by a transducer. The mechanical $\tan \delta_m$ could be directly read off on the meter. The complex modulus of elasticity could then be calculated from the amplitude of stress and strain and δ values.

3.4. Experimental Results

3.4.1 Dielectric Constant and Dissipation Factor

The dielectric constant and dissipation factor ($\tan \delta$) for a 1-mil film of polypropylene were determined at room temperature using the GCA capacitance bridge. The values obtained as a function of frequency are shown in Figure 3.5. While the dielectric constant exhibited no change as the frequency increased from 50 Hz to 10 KHz, $\tan \delta$ remained constant with a value of 0.0002 up to a frequency of 2 KHz above which a very little increase occurred. The obtained results agree with those reported in the literature. [32]

3.4.2 Complex Modulus and Mechanical $\tan \delta_m$

To examine the physical properties of an electrically stressed and unstressed polymer, investigations were performed on 3-mil samples of Polypropylene where the complex modulus of elasticity (E^*) and the mechanical $\tan \delta_m$, referred to as the damping factor, were determined as a function of temperature. The value of $\tan \delta_m$ is read directly and E^* can easily be calculated from instrument readings and sample dimensions as follows [65]

$$|E^*| = \frac{2 \times \ell \times 10^9}{A \times F \times S} \quad (4.1)$$

where $|E^*|$ is the dynamic complex modulus, ℓ is the sample length, A is the sample section area, F is the dynamic force, and S is a correction factor.

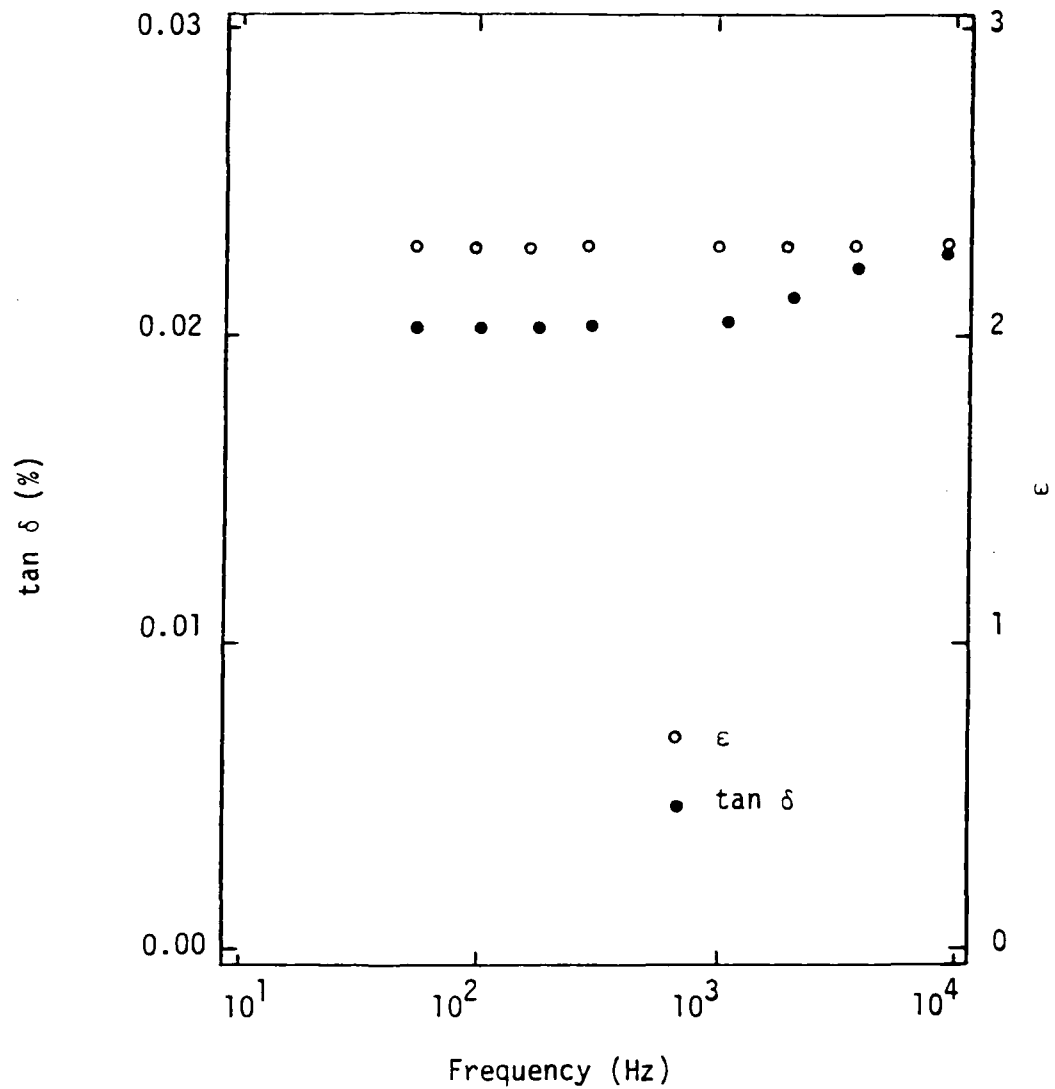


Figure 3.5 Dissipation factor ($\tan \delta$) and relative dielectric constant (ϵ) of 1-mil polypropylene film at 21 °C as a function of frequency.

Of the two samples tested, one was subject to breakdown ($t_s = 0$ sec.), while the second was a virgin sample. The temperature dispersion of complex modulus of elasticity E^* and $\tan \delta_m$ profile are shown in Figures 3.6 and 3.7, respectively, where it can be seen that an increase in temperature results, on one hand, in an increase in $\tan \delta_m$ and on the other hand, the increase in temperature results in a decrease in E^* . The reason for this behavior is due to the fact that the higher the temperature, the softer the polymer. Also, it is interesting to note that the variation that occurred in the values of $\tan \delta_m$ and E^* for both the electrical stressed sample and the original film was very minimal. That is because $\tan \delta_m$ as well as E^* are proportional to the sample size and are not affected by the breakdown which is a local event resulting in creating a very small hole in the specimen compared to its overall size.

3.4.3 Alternating Voltage

Breakdown voltages of certain dielectrics such as Mylar, Teflon and Polypropylene were determined under rod-plane electrodes configuration in air. Each dielectric was tested with a total thickness of 3 mils, where in one part of the tests, a one 3-mil film was used while for the other tests, 3 layers of 1-mil thickness each were employed. Different values of t_s were used in these tests. This was done in order to see if the rate of rise of the applied voltage had any effect on the dielectric breakdown. These results are shown in Figures 3.8 and 3.9, respectively.

It is interesting to note that the breakdown voltage of all dielectrics decreased, almost exponentially, as t_s increased. It is believed that partial discharges caused this reduction in the breakdown voltage.

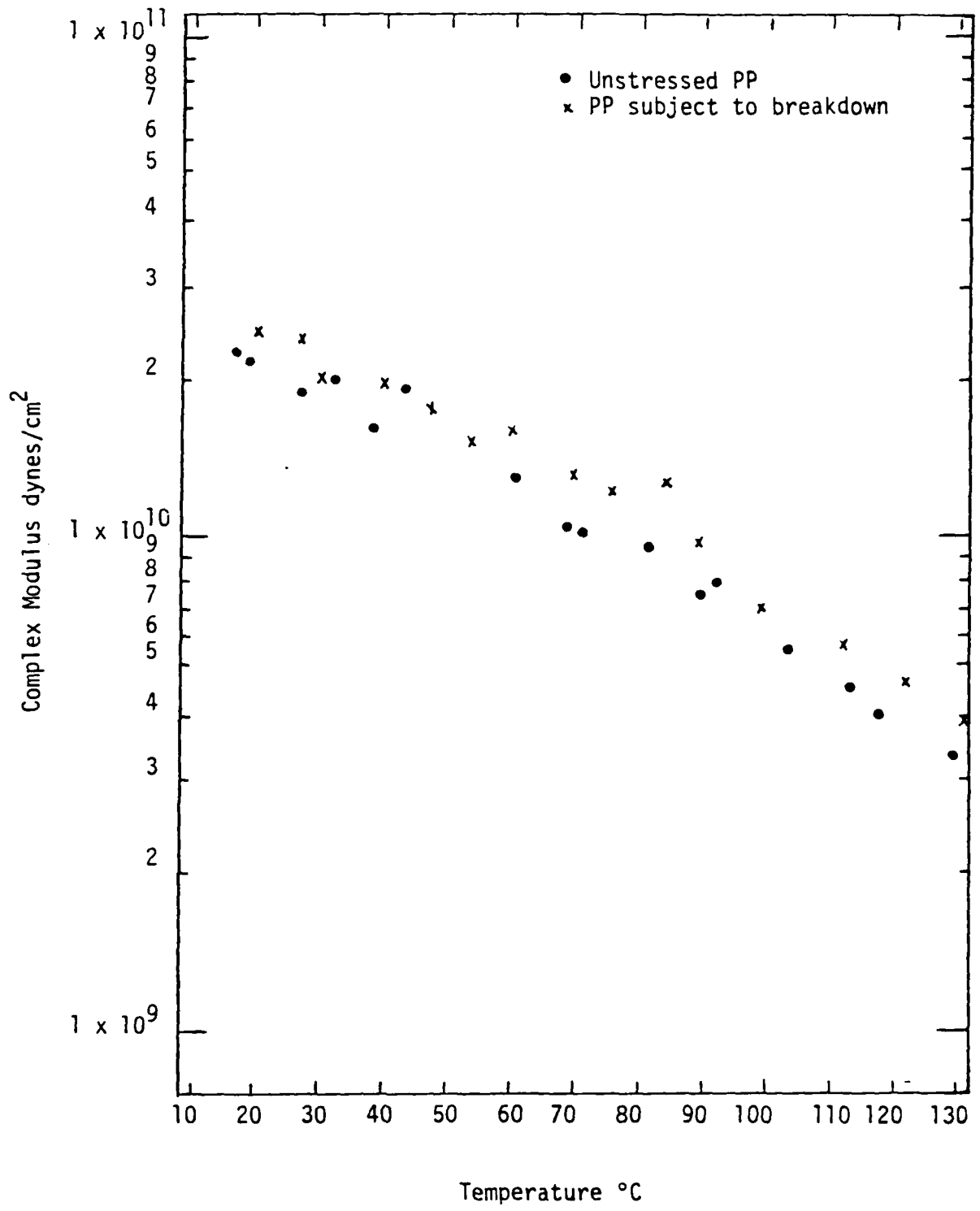


Figure 3.6 Complex Modulus of a 3-mil polypropylene film as a function of temperature at 110 Hz.

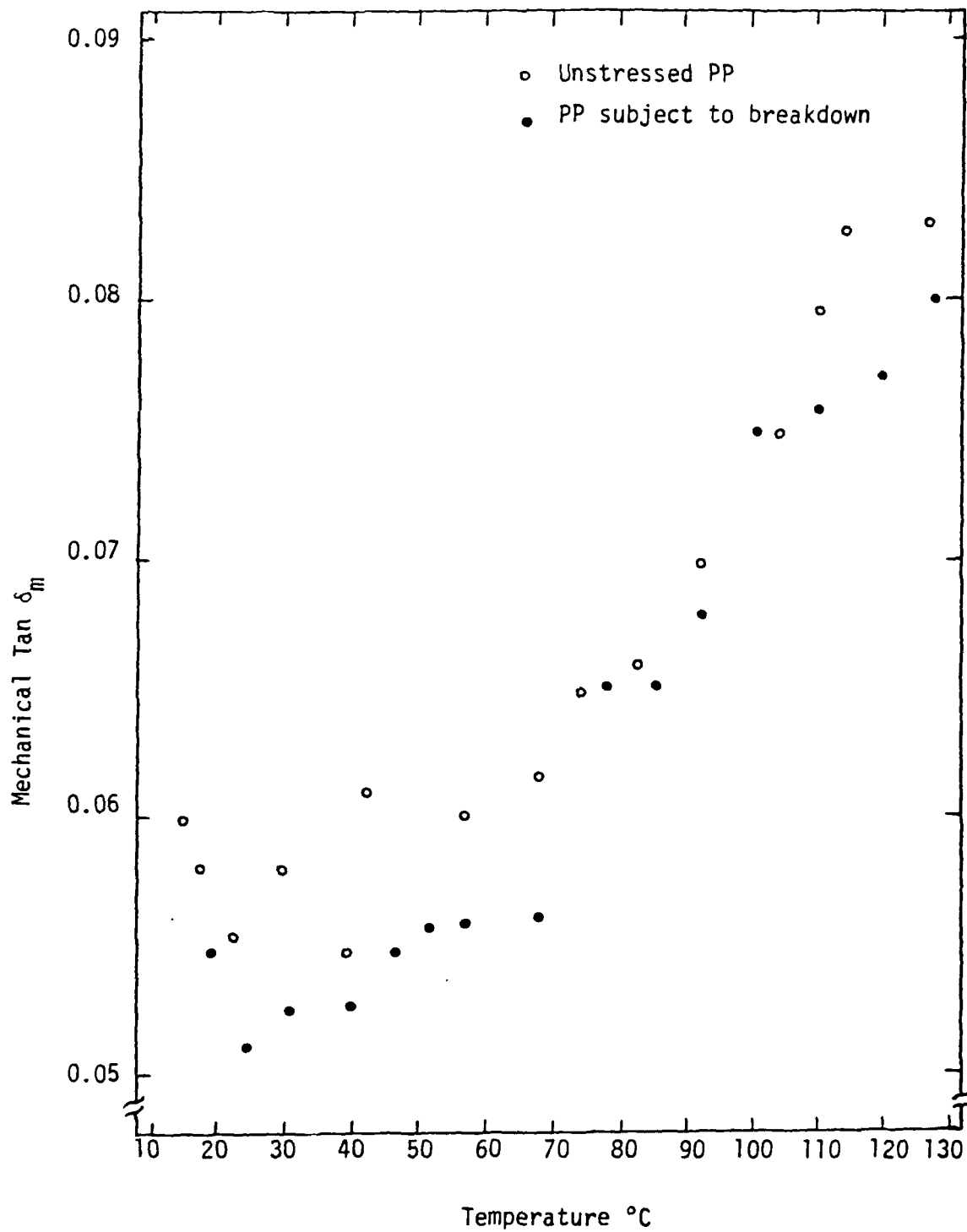


Figure 3.7 Mechanical $\tan \delta_m$ of a 3-mil polypropylene film as a function of temperature at 110 Hz.

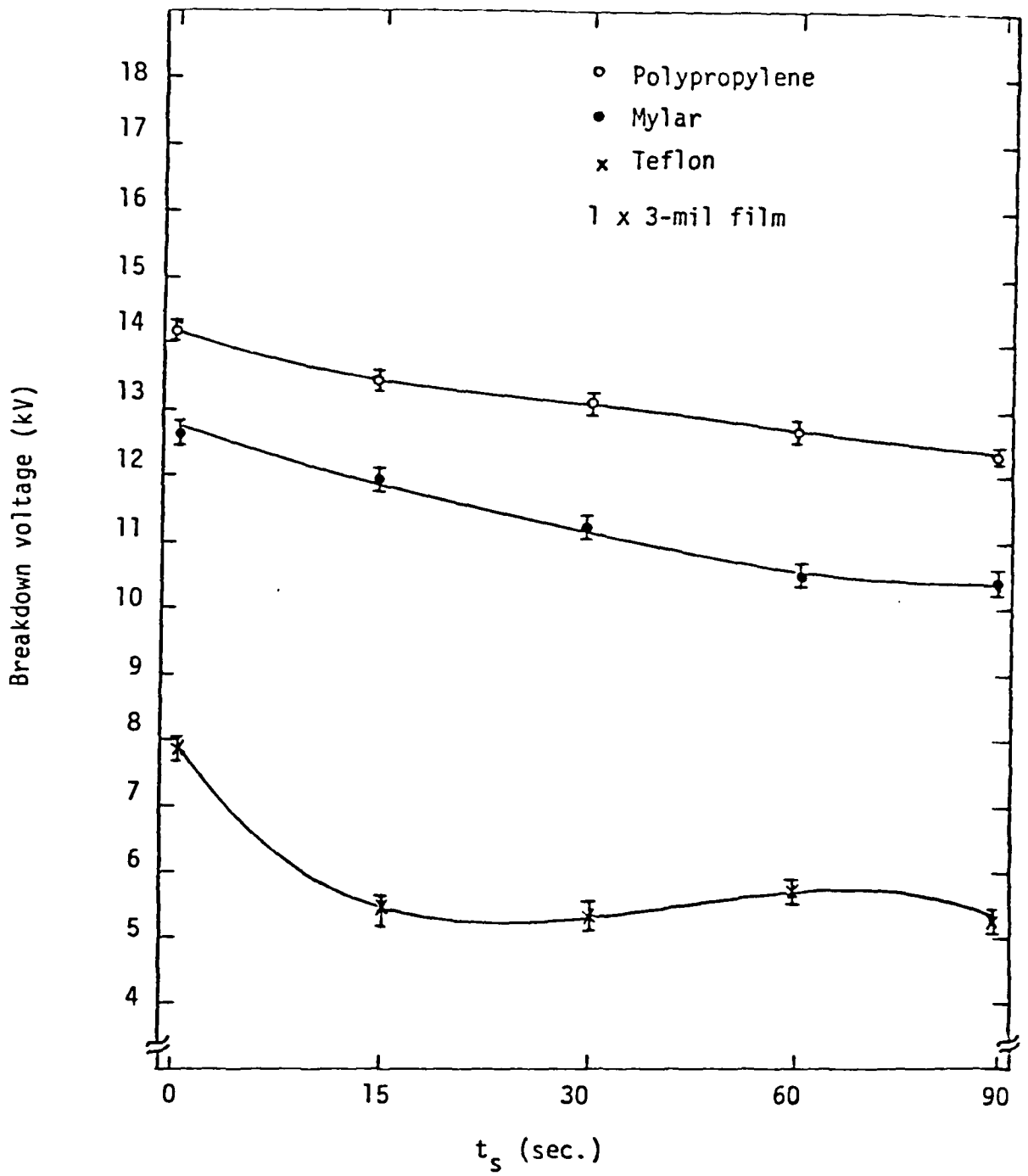


Figure 3.8 Breakdown voltage of Mylar, Teflon, and Polypropylene in a one layer structure in air under non-uniform field as a function of t_s .

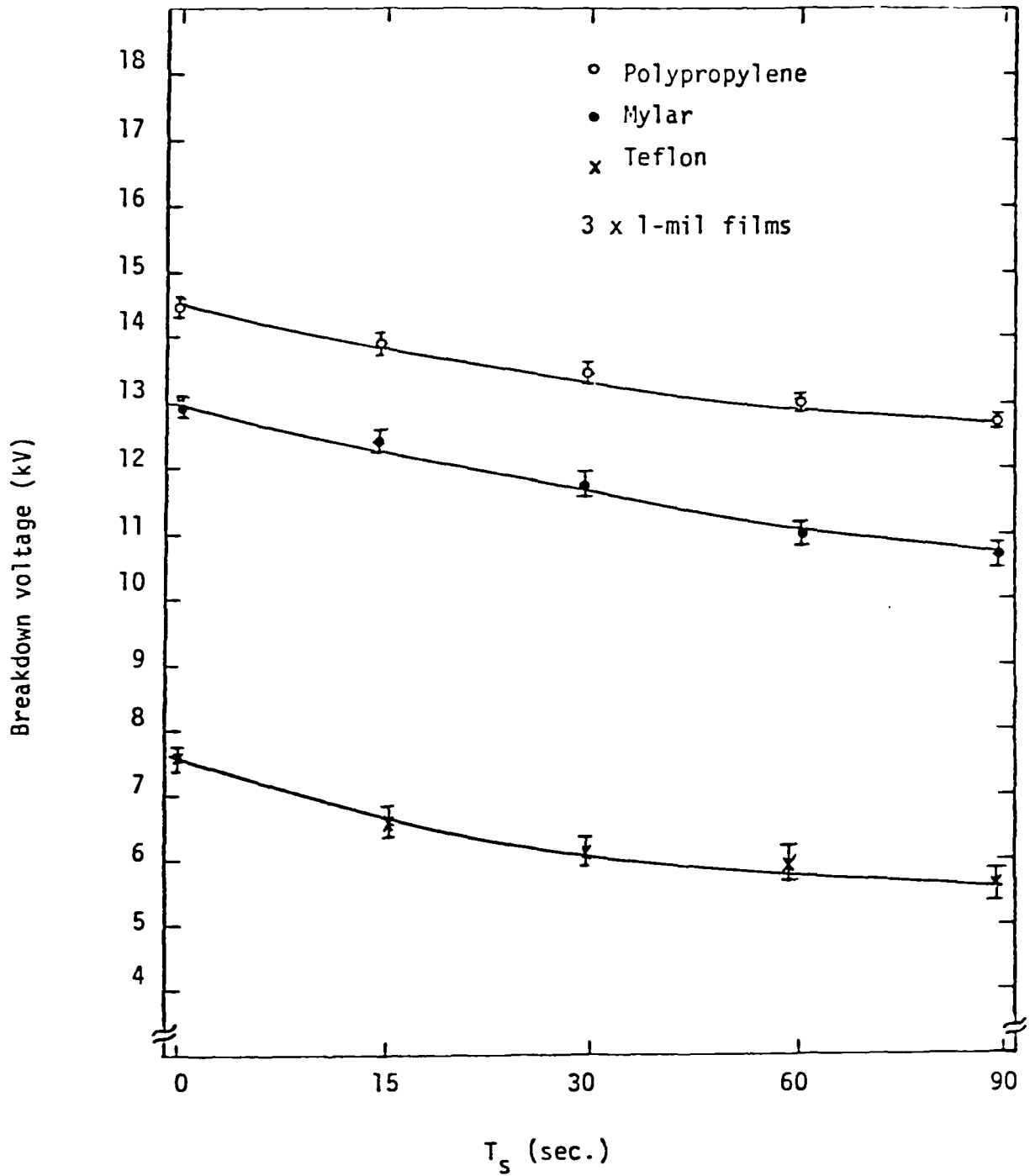


Figure 3.9 Breakdown voltage of Mylar, Teflon, and Polypropylene for a 3-layer structure in air under non-uniform field as a function of t_s .

As the voltage is raised, ionization in the surrounding air or in a gas pocket or void inside the dielectric takes place which, upon collisions with other molecules, creates more ions. When these traveling ions strike the dielectric surface, they start initiating erosion or degradation of the material until a complete deterioration occurs. As a result of this erosion, the dielectric strength of the specimen reduces thereby causing a breakdown at a lower voltage. As t_s is increased, these discharges are acting on the sample for a longer period of time, therefore, causing more damage and hence reducing the dielectric strength even further.

It can also be seen from comparing Figures 3.8 and 3.9 that the laminate structure has a higher dielectric strength as compared to a single layered structure. Also, it can be seen easily that polypropylene has superiority in its dielectric strength compared to the other two dielectrics. Also, the longer the time the electric stress is applied on any material, the lower is the dielectric strength. Some of this can also be attributed because of damage caused by space charge. [8]

It is interesting to note that the partial discharges, which appear in the gaseous phase, are found to originate from the rounded edge of the rod electrode (the high voltage electrode) and sweep radially along the surface of the dielectric above the plane electrode. The discharges initiated at the vicinity of the rod electrode seemed very intense and that is probably due to the large value of the electric field at this sharp edge. The intensity of these discharges seemed to reduce further

away from the edge of the rod electrode, and therefore the test specimen was subject to less damage there. This visual observation of the damage on the dielectric is shown in Figure 3.10 for a 3-mil thick film of polypropylene. Similar observations were made for Teflon and Mylar samples, however, the damage in the case of Teflon and Mylar was slightly more. Teflon had the most severe surface damage.

To further investigate the advantages of using laminate structure, tests were continued on polypropylene films in air under both uniform and non-uniform field conditions. The data obtained on breakdown for laminated structure consisting of 1 to 5 films of 1-mil thickness each is shown in Figure 3.11. This is compared with the data for a single layer for the same total thickness.^[64] It can be seen from the figure that under uniform field, the breakdown voltage for a laminate structure is much higher than that of a single layer with the same total thickness. For example, the breakdown voltage of a 3-mil layer is 12.5 kV, while it approaches 15 kV when 3 layers are employed with a thickness of 1-mil each. Also, for the same composite structure, the breakdown voltage under uniform field is found to be higher than that of the non-uniform field. The fact is that, although the area of the specimen subject to electric stress between the two plane electrodes is larger and hence the probability of existence of a defect in the material is higher, no field enhancement takes place at the plane-plane electrodes interface where no sharp points exist. Based on this result, plane-plane electrodes geometry was employed in the remainder of this work.

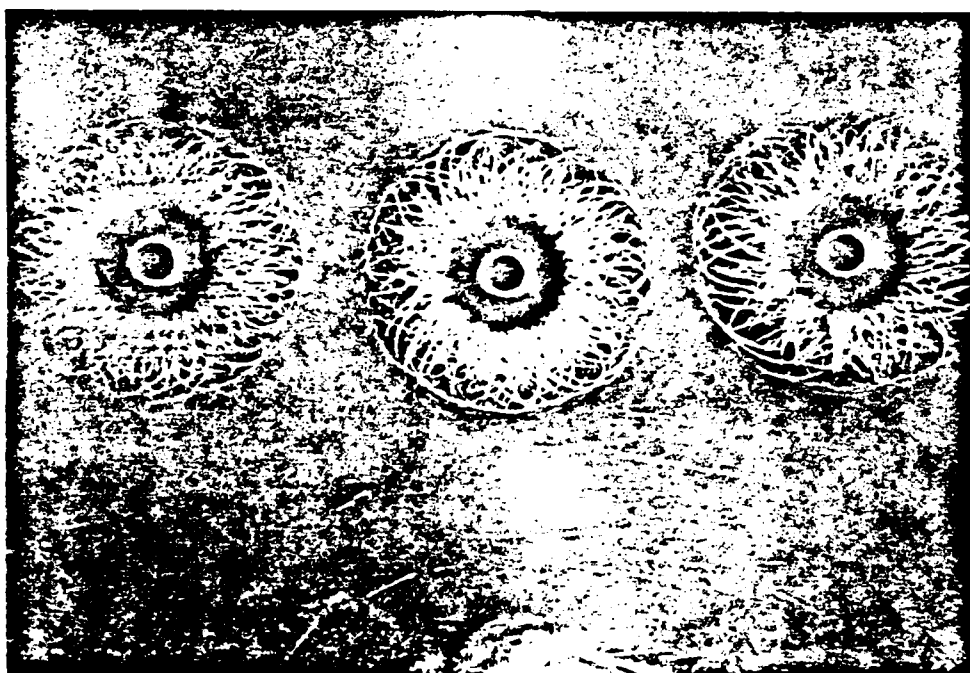


Figure 3.10 Damage on a 3-mil polypropylene film tested under non-uniform field in air.

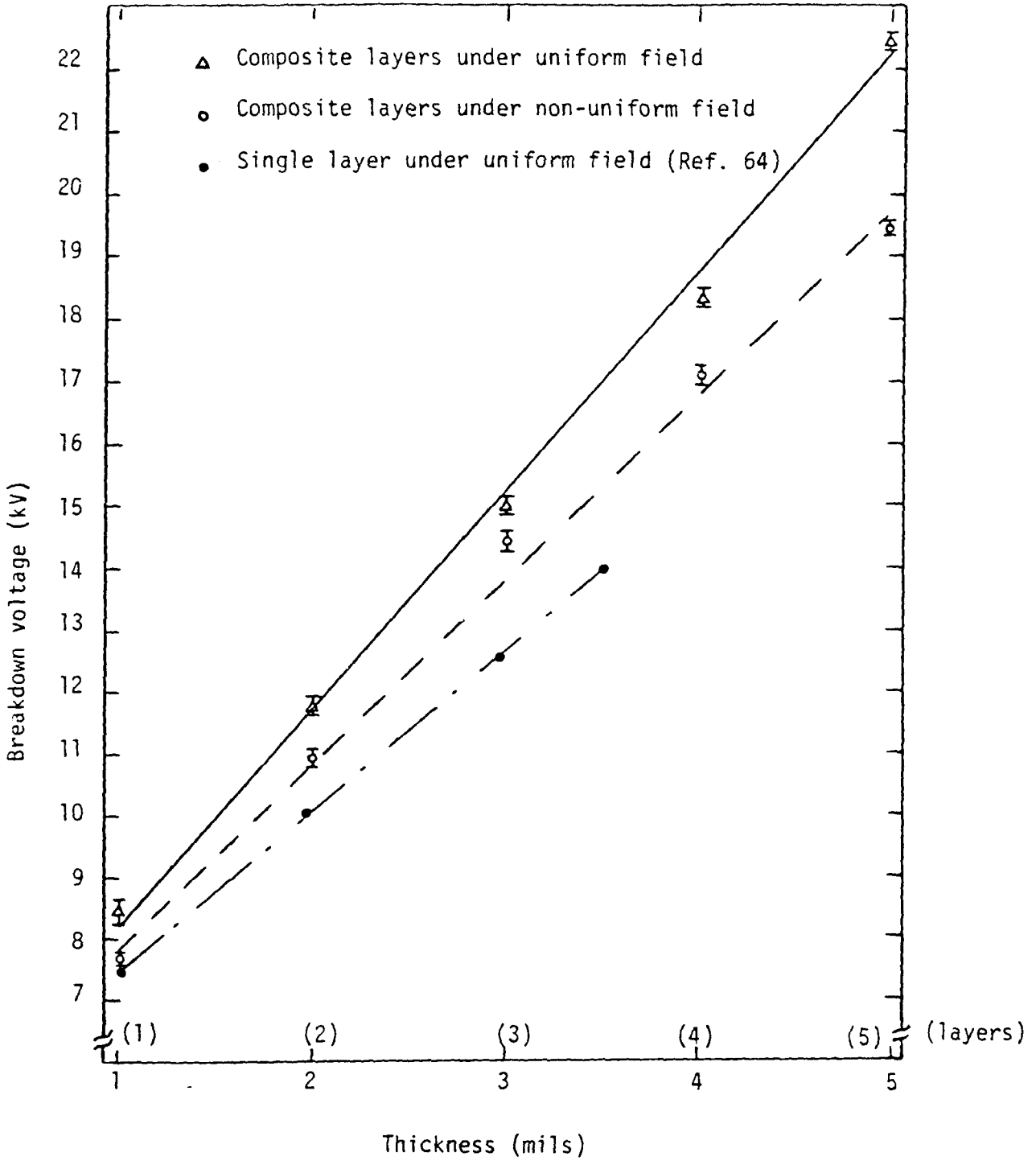


Figure 3.11 Breakdown voltage of polypropylene in air under uniform and non-uniform fields as a function of thickness.

as described earlier. A new sample or new sample area, depending on the sample shape, was placed between the electrodes to begin the testing. The ground was removed from the output bushing and the trigger was reconnected to the pulser. The dc voltage, V_a , was then raised at approximately 4 kV/s while the waveform was observed on the oscilloscope. The breakdown voltage was interpreted as the last voltage observed on the oscilloscope before the waveform collapsed. To permit a more accurate viewing of this breakdown voltage, it was necessary that it be above approximately 5 kV. If the breakdown voltage were below 5 kV then it would be reached within approximately one second. This was too short a time to permit an accurate observation of the magnitude of the breakdown voltage with the available instrumentation.

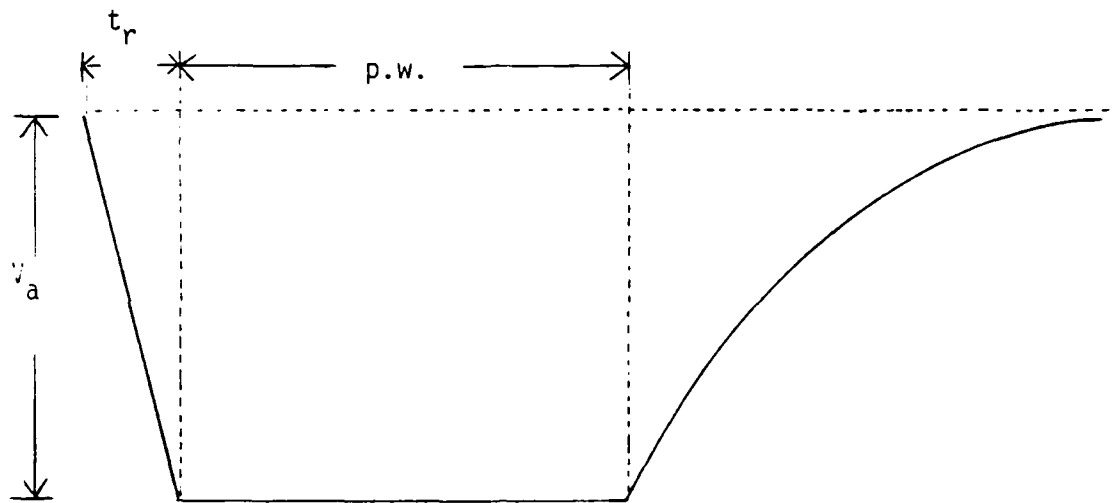
As indicated in Table 3.1, five of the nine tests measured the breakdown voltage as a function of pulsewidth. Five to twenty measurements were made for each data point, depending on the amount of fluctuation observed in the measurement. The results are graphed in Figures 3.18 through 3.22 on the following pages. The spread in the data is indicated, for each data point, by error bars which extend one standard deviation in either direction from the mean value. It may be noted that this procedure assumes a normal distribution for the data and not a Weibull distribution, which we would expect. The error bars, however, are included only to give an indication of the spread in the data. The measured parameters are indicated on each graph. A list of general observations follows.

TABLE 3.1 Summary of Experiment Descriptions

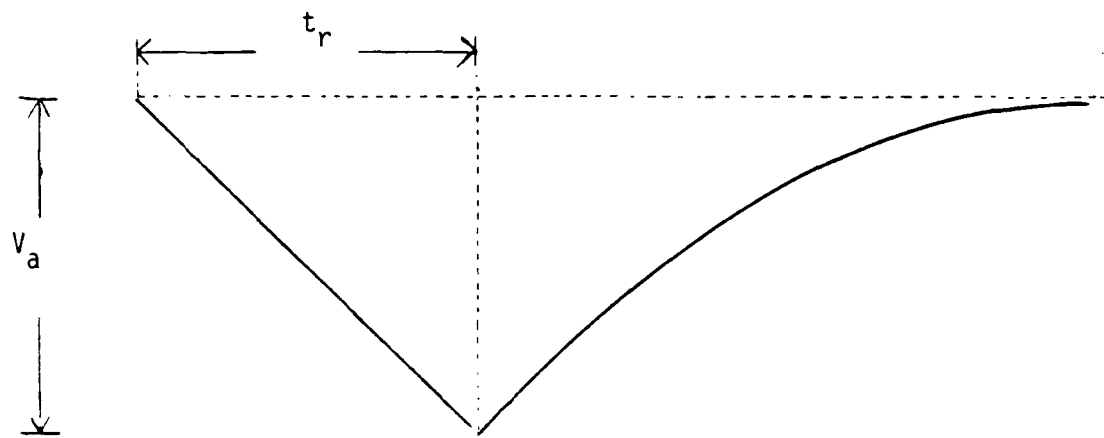
Fluid/Sample	2 layers of 1-mil Mylar				1 layer of 3-mil Mylar	1 layer of 1-mil Polypropylene Impregnated in Castor Oil
	1	2	3	4		
Air	1	2	3	4	-----	1
Fluorinert	-----	-----	-----	-----	1 2	-----
Transformer Oil	-----	-----	-----	-----	-----	1
Castor Oil	-----	-----	-----	-----	-----	1

The experiments performed were:

1. Breakdown voltage as a function of pulsewidth.
2. Breakdown voltage as a function of risetime of leading edge.
3. Number of pulses to breakdown at 10 kV as a function of pulsewidth.
4. Number of voltage applications to breakdown at 10 kV as a function of risetime of leading edge.



(a)



(b)

Figure 3.17 Typical waveforms for (a) pulsed and (b) ramped voltages. The parameters indicated are:

- t_r risetime
- p.w. pulsewidth
- V_a applied voltage (peak)

The applied voltage was either a pulsed or a ramped voltage, with typical waveforms appearing in Figure 3.17. This figure indicates that the voltage takes some time to decay back to zero. This time is required to discharge the parasitic capacitance in the system and can not be controlled. When the applied voltage was a pulse, the shape was varied by changing the pulsewidth. For ramped voltages, the risetime of the leading edge was varied. It should be noted here that the shortest pulsed-voltage pulsewidth was 0.1 μ sec and the fastest ramped-voltage risetime was 0.1 μ sec. These two waveforms looked virtually identical and, for graphing purposes, the same data were used when showing dependence on pulsewidth and dependence on risetime for the 0.2 μ sec value.

Table 3.1 summarizes the experiments performed on each sample type and in each of the available fluids, using the following procedure. In each case, the samples were either squares, 5 cm x 5 cm, or strips, 7 cm x 25 cm. The squares allowed one test per sample, while five tests were done on each strip, simply by moving the strip to an unaffected area.

At the beginning of each set of tests at a particular pulsewidth, a dummy sample was placed in the test cell. The pulser was turned on and the voltage was raised to approximately 5 kV. The pulsewidth was adjusted and the risetime measured. The trigger was removed to stop the pulsing. For safety while handling the electrodes, the pulser output was then grounded and the dc voltage was lowered. Mylar samples were cut into squares and polypropylene samples were cut into strips,

3.4.5 Pulse Voltages

A total of nine (9) tests were executed and corresponding data sets generated in these research experiments. The repetition rate of the applied pulsed voltage was kept at 500 Hz, while the pulse width and risetime of the leading edge were varied to assess the dependence of breakdown on these parameters. The repetition rate of 500 Hz was chosen because it was above the corona damage threshold observed by Rohwein and Sarjeant,^[8] so that the maximum damage per pulse was expected. The choice of sample thickness was guided by the experimental limitations. The pulser could not generate voltages above 25 kV and, for reasons which will be explained later, it was difficult to read voltages below 5 kV. Based upon preliminary testing it was decided that experiments would be performed using two sheets of 1-mil (25.4 μm) Mylar; 1 sheet of 3-mil (76.2 μm) Mylar; and 1 sheet of 1-mil (25.4 μm) Polypropylene which had been impregnated in castor oil.

During the tests, the samples were submerged in one of four fluids: Air, Fc-72, transformer oil or castor oil. The experiments were to designated determine (a) the breakdown voltage of the sample and, in selected cases, (b) the number of voltage applications necessary to break the sample as a function of the shape of the applied voltage pulse. When the number of voltage pulses applied was being counted, the peak values of the applied voltage was 10 kV.

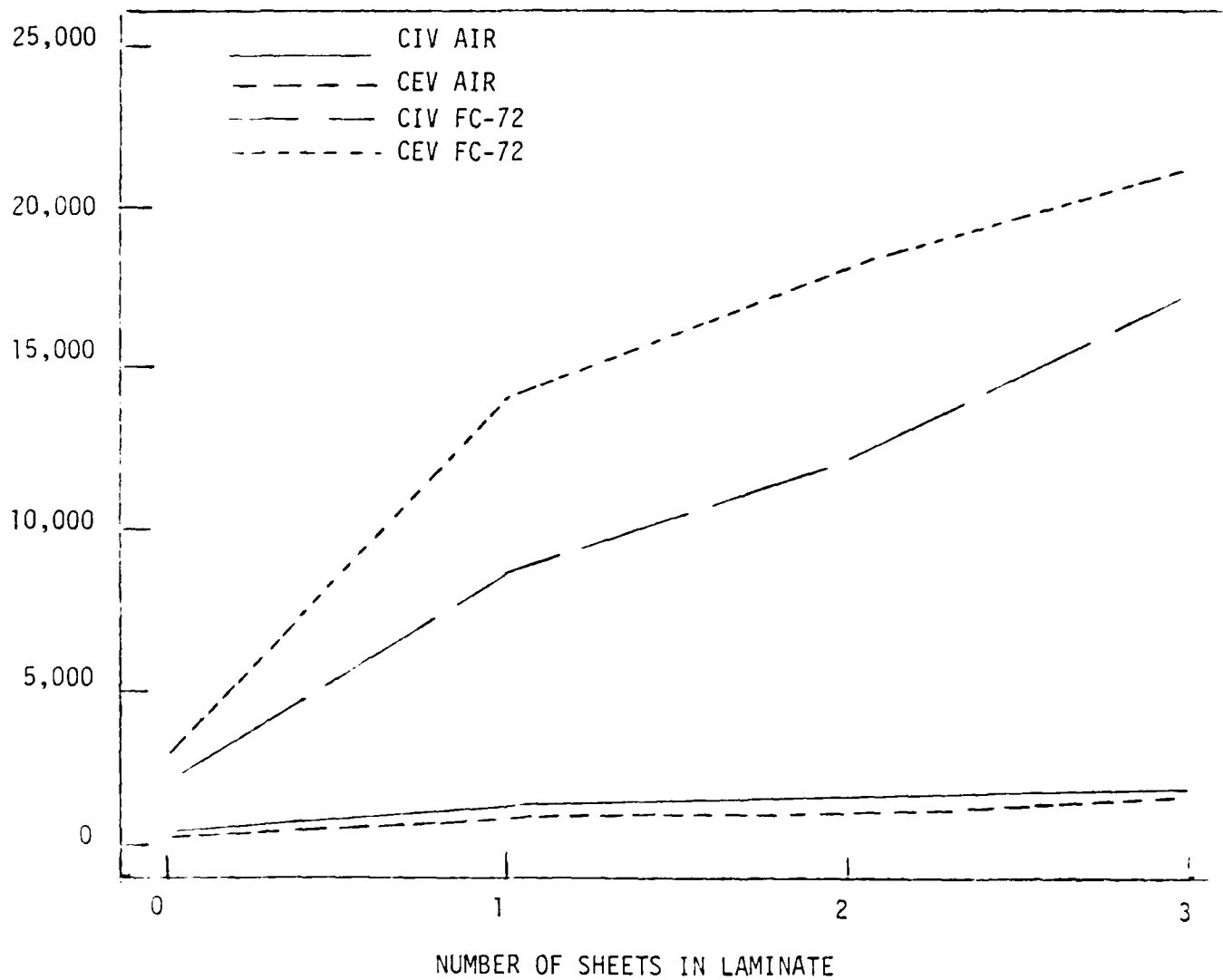


Figure 3.16. Corona Inception Voltage (CIV) and Corona Extinction Voltage (CEV), at 60 Hz ac, 1 kV/sec, as a function of number of Polyethylene sheets, each 2-mil thick.

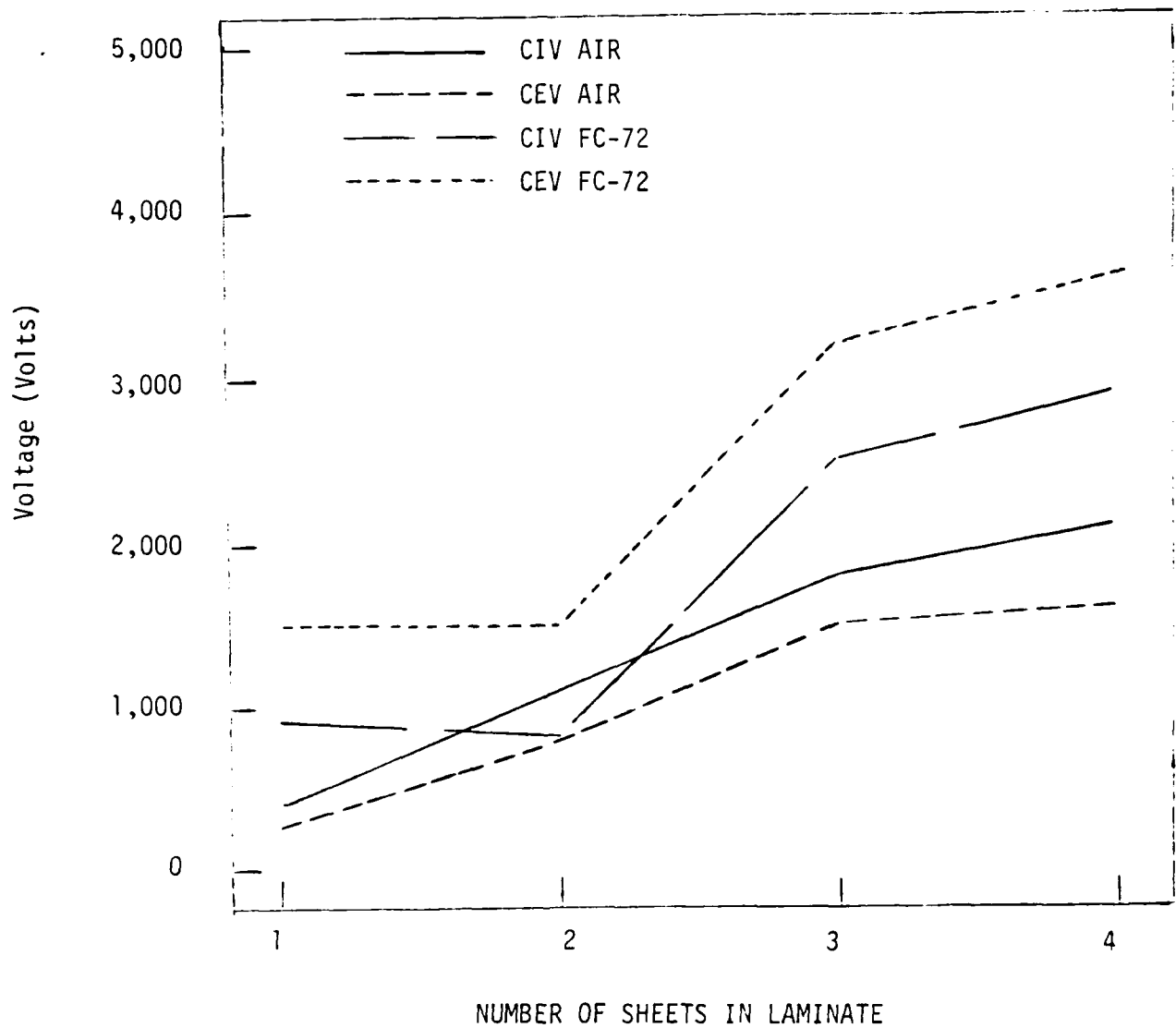


Figure 3.15. Corona Inception Voltage (CIV) and Corona Extinction Voltage (CEV), at 60 Hz ac, 1 kV/sec, as a function of number of Polypropylene paper sheets, each 2-mil thick.

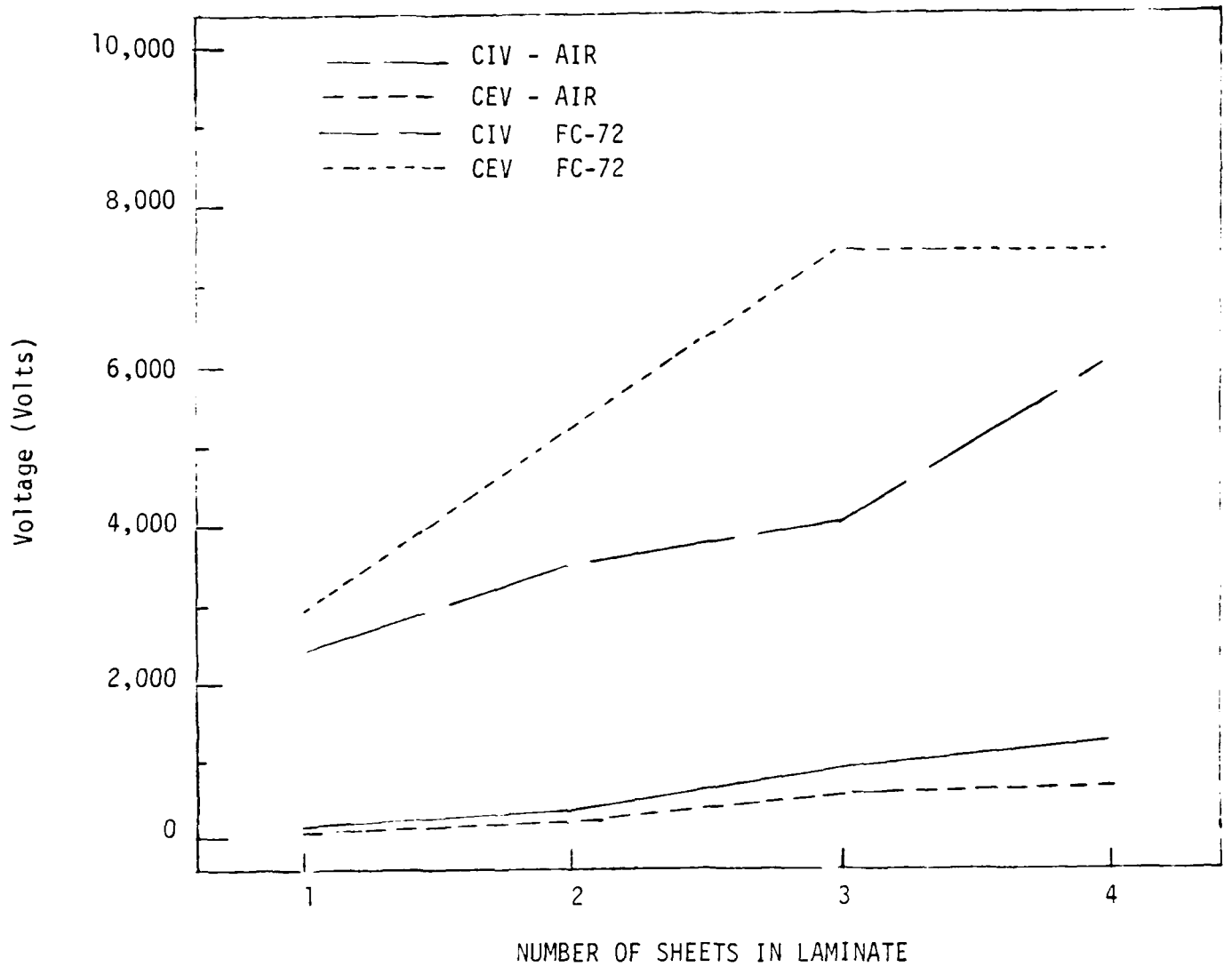


Figure 3.14. Corona Inception Voltage (CIV) and Corona Extinction Voltage (CEV), at 60 Hz ac, 1 kV/sec. as a function of number of Mylar sheets, each 3-mil thick.

3.4.4 Corona Inception/Extinction Voltage

Figures 3.14 to 3.16 show the corona inception voltages (CIV) and the corona extinction voltage (CEV) at 60 Hz ac, 1 kV/sec, as a function of Mylar, Polypropylene and Polyethylene sheets each 2 to 3 mil thick. The environments used were air and Fluorinert (FC-72).

Results show that the threshold voltage in the Fluorinert are much above those in air. Moreover, the threshold voltage for the more-layered laminated structure are significantly higher than those for the less-layered structure.

What is not surprising is that the extinction voltage levels are much below the inception voltage levels. This was found to be true for all the different laminate structures and impregnants.

This was the only initial warm-up activity made in this area. Experiments are presently in progress in obtaining corona-signatures on "aged" specimens. These will be reported in the progress report of the year-2 activity (1984-1985).

Based on the experimental work under alternating voltages, the following conclusions can be drawn.

Partial discharges, either within the dielectric or along its surface (surface discharges), greatly influence the behavior of the electrical breakdown of an insulating system by causing progressive deterioration and ultimate breakdown. The effect of the discharges is dependent on the time of the voltage applied where the longer the time of the voltage applied, the lower is the voltage needed to cause breakdown. Also, the uniformity of the electric field is found to affect the breakdown voltage, whereas partial discharges tends to be less severe under uniform field conditions than under non-uniform fields and therefore leading to higher breakdown voltages.

It has been also found that by the use of thin films in the form of laminate insulating structures, higher breakdown voltages are obtainable and by impregnating the system with a good impregnant, a further increase in the breakdown voltage can result. Therefore, it can be concluded that with the use of suitable solid laminated dielectric (containing more films per laminate), and by employing a matching impregnant, higher dielectric strengths and therefore higher energy densities can be achieved for a given system. Improvement in the methods of impregnation can also result in a more improved performance.

than those of the unimpregnated samples. The reason for this behavior is attributed to the fact described before, that is an air-filled void has lower dielectric constant than the dielectric itself and hence the field tends to be stronger in the void, and therefore, is a source of partial discharges, damage and subsequent failure. When it is filled with oil, as in case of the impregnated samples, discharges occur at a higher voltage level within the filled void, therefore, leading to an increased life time and dielectric strength of the dielectric.

The breakdown voltages for the 3-layer structure of polypropylene with and without void in air and in castor oil are compared in the same figure. It can be easily seen that the breakdown voltage in air with void occurring in the dielectric is much lower than that without a void. The system, therefore, could be said to be composed effectively of two layers rather than three layers. This assumption is strongly supported because of the fact that all the breakdowns that took place occurred where the void was made. On the other hand, the breakdown voltages of the impregnated samples with the artificial void are almost as high as those without the void. In this case, breakdown takes place mostly anywhere within the specimen surface.

Impregnation is therefore found to play an important role on the dielectric strength behavior of the insulating system. It is also worth mentioning that while the surface damage that occurred to the samples tested in air resulted from the partial discharges was evidently clear no trace of surface damage was found on the impregnated samples except for a very small hole, if seen, where breakdown occurred. This result, therefore, strongly supports the fact that impregnation reduces significantly, if not totally, partial discharges and hence more efficient and reliable systems can be developed.

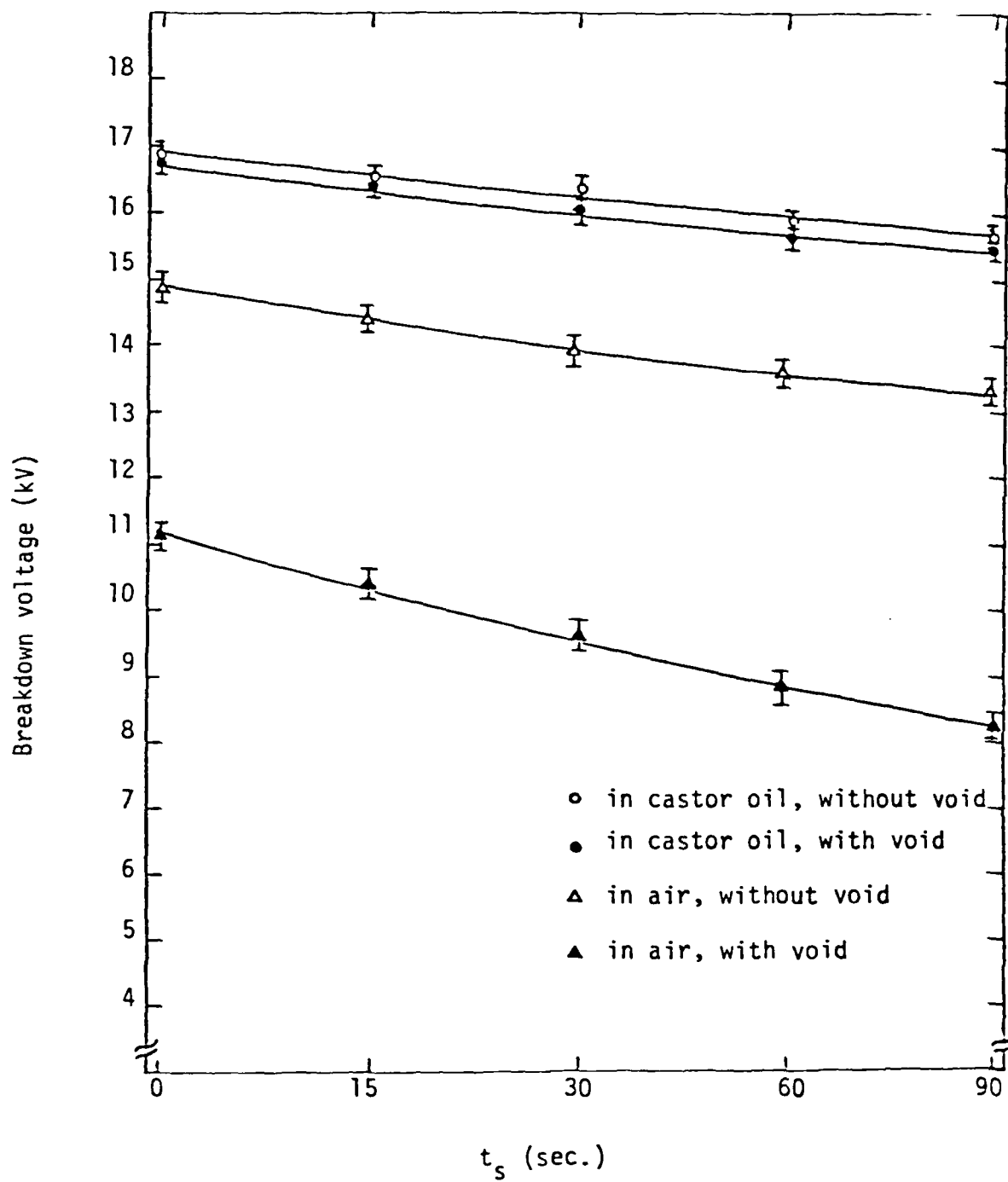


Figure 3.13 Breakdown voltage of polypropylene with and without a void in the center layer of a 3-layer structure under uniform field as a function of t_s .

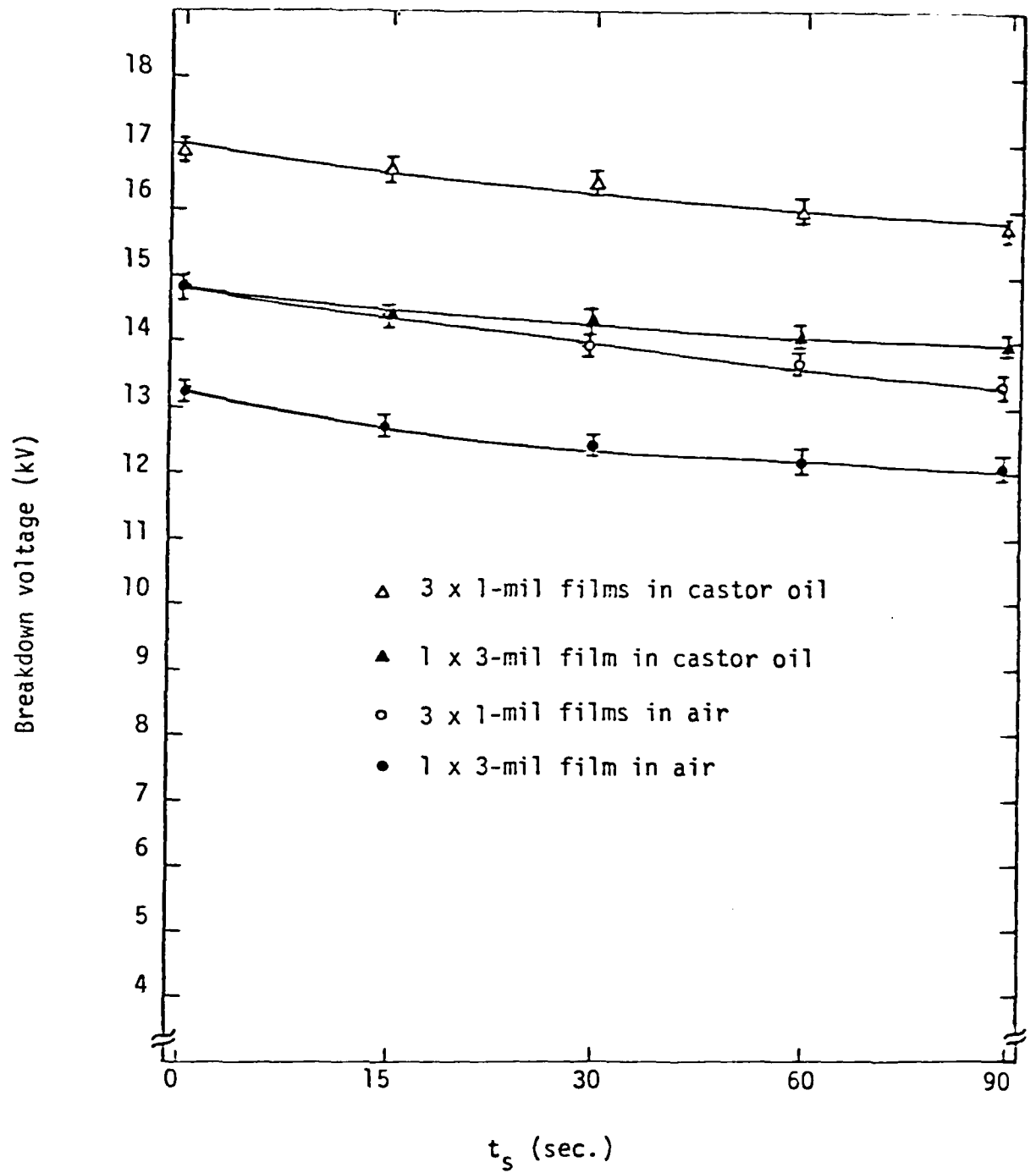


Figure 3.12 Breakdown voltage of polypropylene under uniform field as a function of t_s .

Castor oil-impregnated samples of polypropylene were also tested in castor oil using plane-plane electrodes for a single as well as for a 3-layer structure. The breakdown voltages for both structures were found also to decrease with an increase in t_s . Those results along with those obtained from the previous tests (under similar conditions but in air) are compared in Figure 3.12. It can be seen that the breakdown voltages of impregnated samples are much higher than those of the unimpregnated samples. Also, the decrease exhibited in the breakdown voltage of the dielectric in castor oil tends to be less severe than those in air as t_s is increased. The result indicates that impregnation improves the dielectric strength of the material by elimination any air pockets or voids existing in the dielectric and by suppressing any occurring partial discharges. This is not surprising because the impregnant, which is of a higher dielectric constant and dielectric strength than air, penetrates the polymer surface and fills up the voids and cavities which are the source of partial discharges. As the dielectric constant mismatching is now reduced, the stress tends to become evenly divided between the dielectric and the filled cavity, therefore, eliminating partial discharges and increasing the breakdown voltage.

To further elaborate on the above mentioned point, a 3-layer composite structure of polypropylene with an artificial void made in the center layer, as explained before, were tested under uniform field in castor oil as well as in air. These breakdown voltages as a function of t_s are plotted in Figure 3.13. It could be easily seen that the breakdown voltages, in the case of a void occurring in the solid dielectric, of impregnated samples for a certain t_s are at least 50% more

General Observations

The following observations were made during and after the tests.

- o For the tests done in air, the samples were cloudy, after the test, at the regions that were between or near the electrodes. The cloudiness was more severe near the edge of the electrodes.
- o The spread in the data was not significantly greater for tests done in air than for tests in which the sample was submerged in a fluid.
- o After breakdown, the visible damage of a sample tested in a fluid was only a small hole at the breakdown site. The size of the hole was determined by the length of time, after breakdown, the pulser was allowed to run.
- o Surface tracking of the discharge around the edge of the sample was noted for several of the tests done in air. Surface tracking was evidenced by a single line of melted plastic extending from the puncture site to the edge of the sheet.
- o The occurrence of surface tracking did not correlate with a lower breakdown voltage.
- o The polypropylene tests showed a lower breakdown voltage when the impregnant and fluid used for testing did not match.
- o In air, the electrodes generated a hissing noise before the breakdown voltage was reached.

As indicated in Table 3.1, the breakdown voltage as a function of risetime was measured for two cases: 2 sheets of 1-mil (25.4 μm) Mylar in air and 1 sheet of 3-mil (76.2 μm) Mylar in Fluorinert (type FC-72). The procedure for performing the tests follows: A dummy sample was placed between the electrodes. For both the 1-mil and 3-mil samples, squares were cut rather than strips. Using the dummy sample, the risetime was adjusted and the flatness of the linear ramp was checked. The risetime of the integrator was equal to the pulsewidth of the modulator. The values of R and C were chosen to produce a linear ramp with the breakdown voltage could be reached.

BREAKDOWN VOLTAGE VS PULSEWIDTH

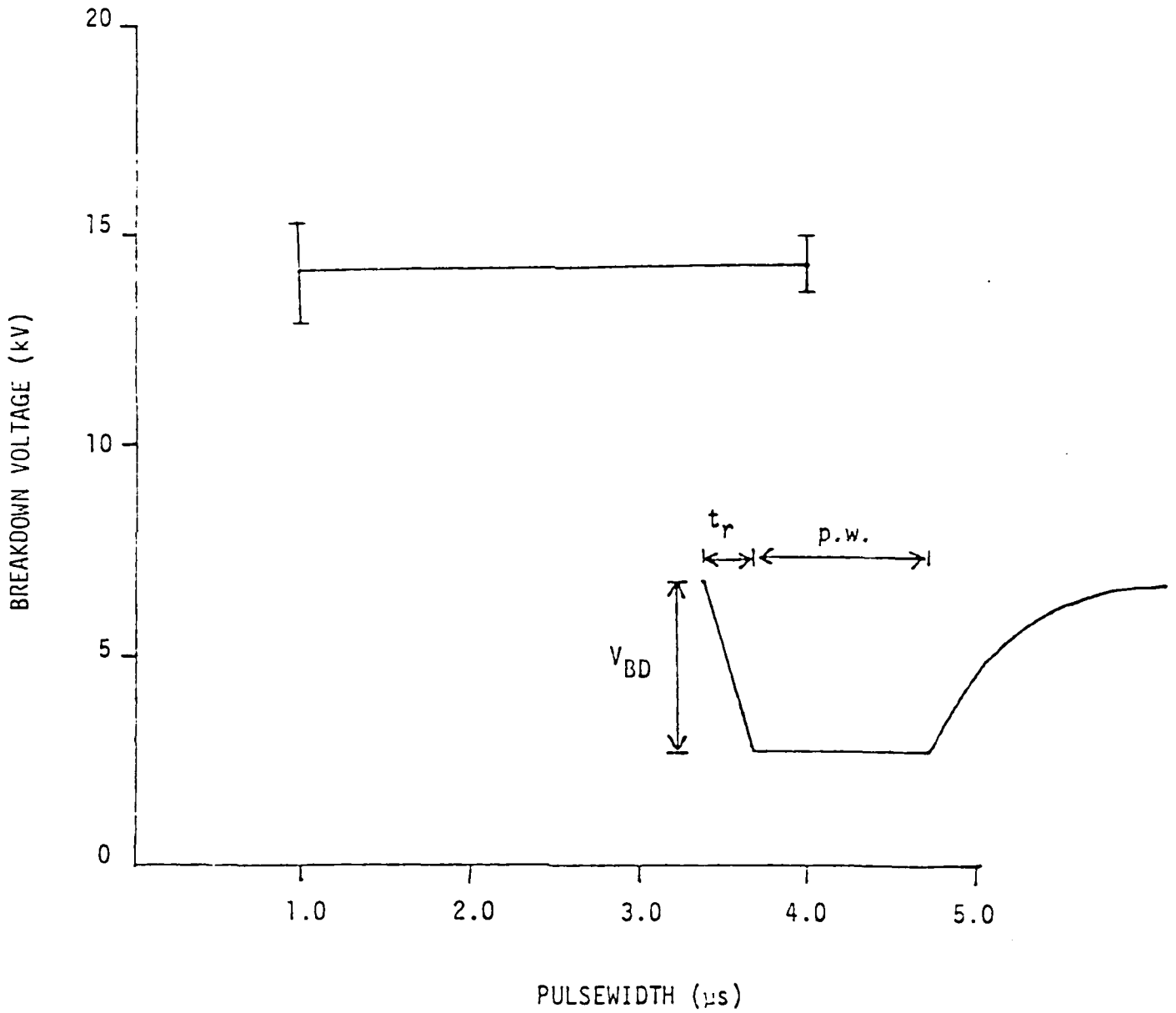


Figure 3.18 Breakdown Voltage vs. Pulsewidth for 1 sheet of 3-mil (76.2 μm) Mylar tested in Fluorinert. Risettime, t_r , is 0.1 μs. All parameters are indicated above.

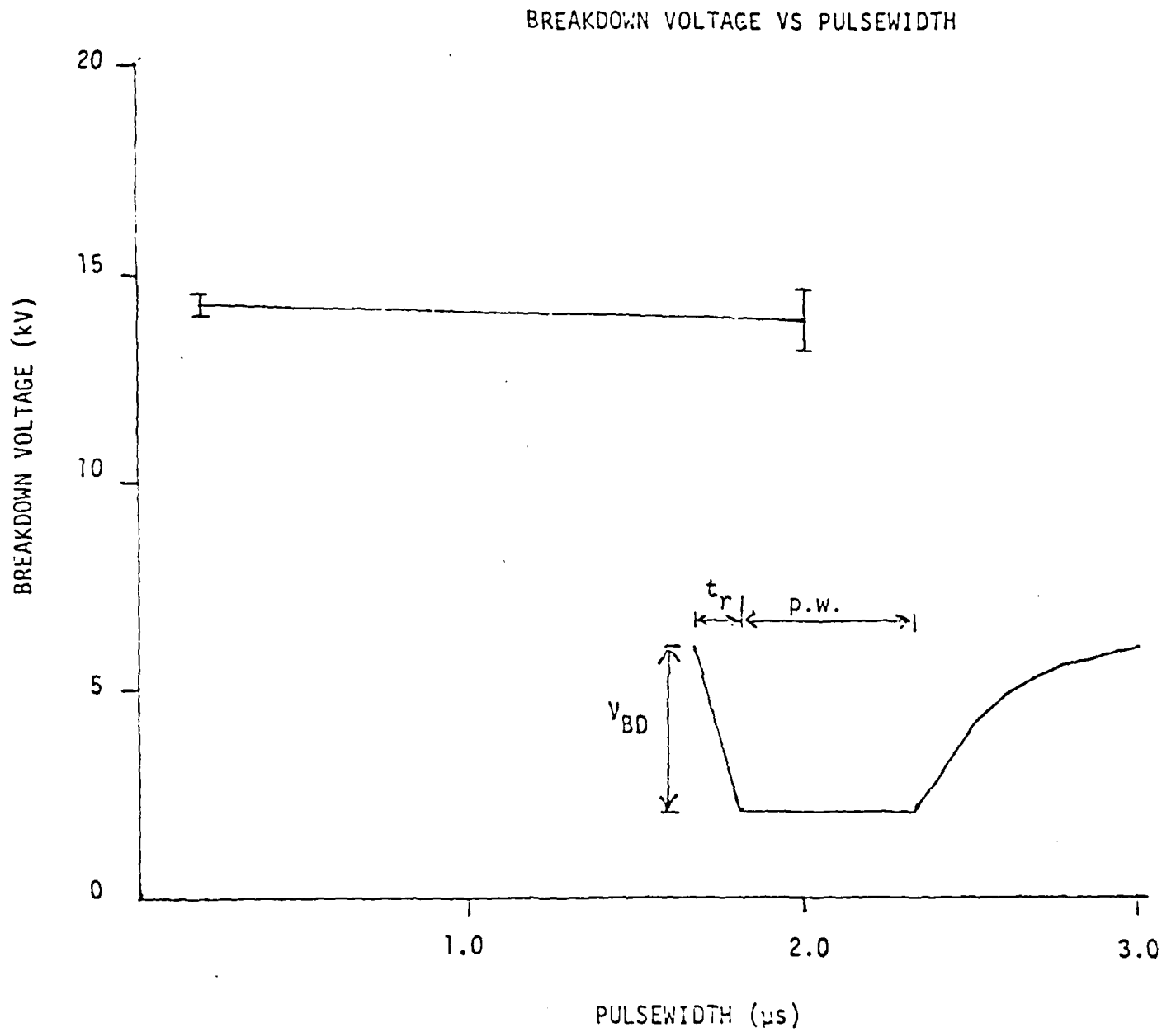


Figure 3.19 Breakdown Voltage vs. Pulsewidth for 2 sheets of 1-mil (25.4 μm) Mylar tested in air. Risettime, t_r , is 0.1 μs .

BREAKDOWN VOLTAGE VS PULSEWIDTH

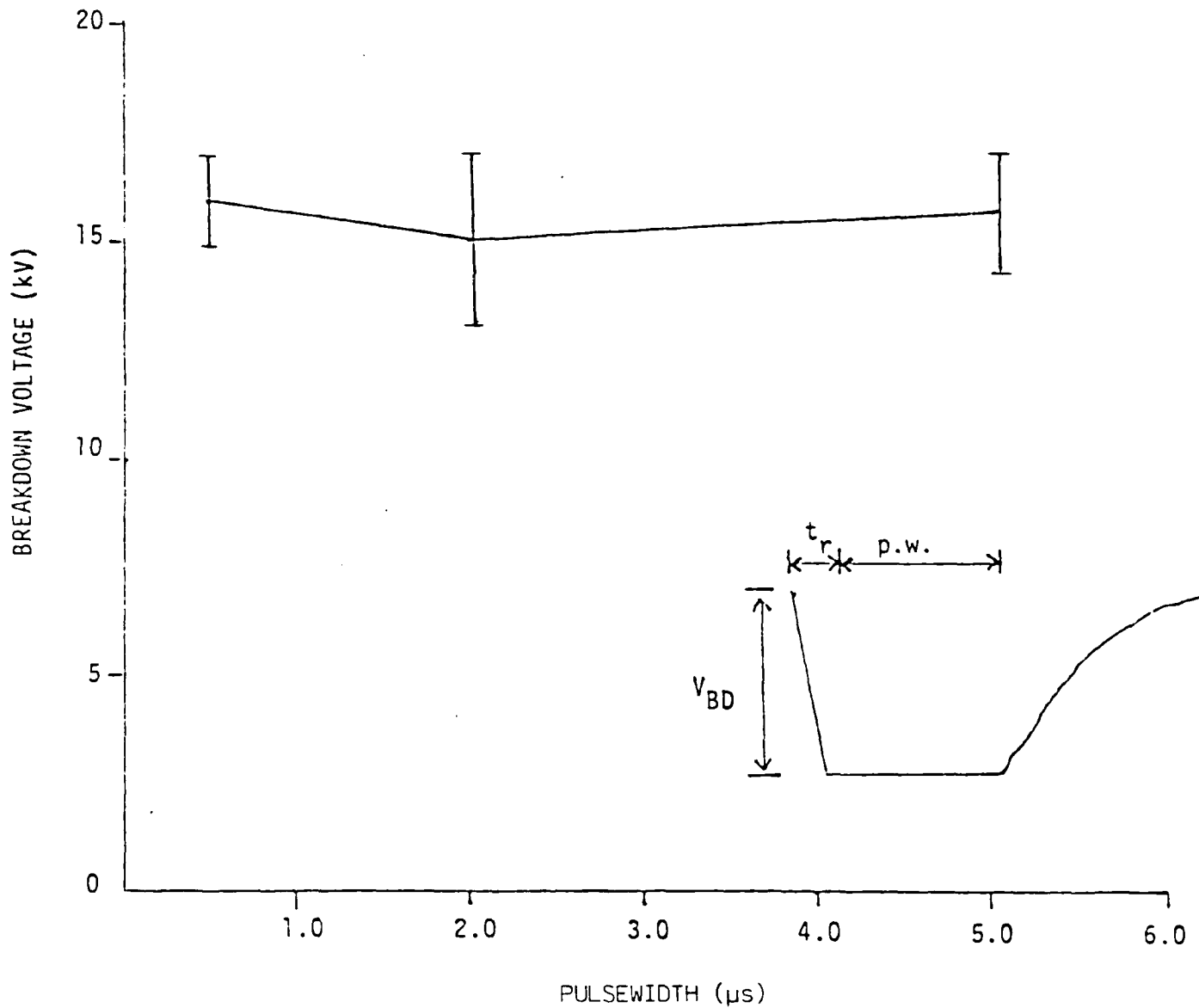


Figure 3.20 Breakdown Voltage vs. Pulsewidth for 1 sheet of 1-mil (25.4 μm) Polypropylene impregnated in Castor oil. Samples were submerged in Castor Oil during tests and t_r was 0.1 μs .

BREAKDOWN VOLTAGE VS PULSEWIDTH

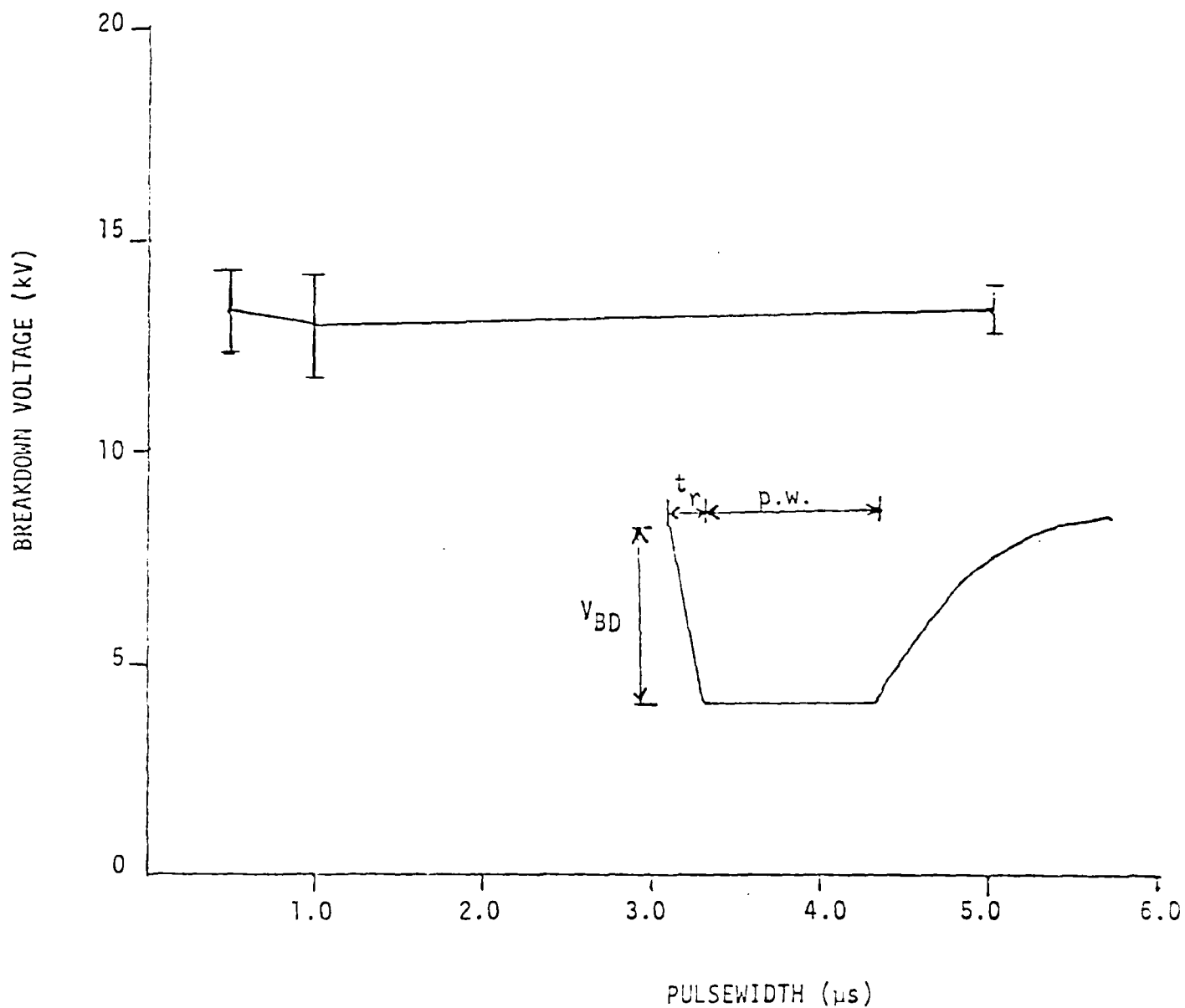


Figure 3.21 Breakdown Voltage vs. Pulsewidth for 1 sheet of 1-mil (25.4 μm) Polypropylene impregnated in Castor Oil. Samples were submerged in Transformer Oil during tests and t_r was 0.1 μs.

BREAKDOWN VOLTAGE VS PULSEWIDTH

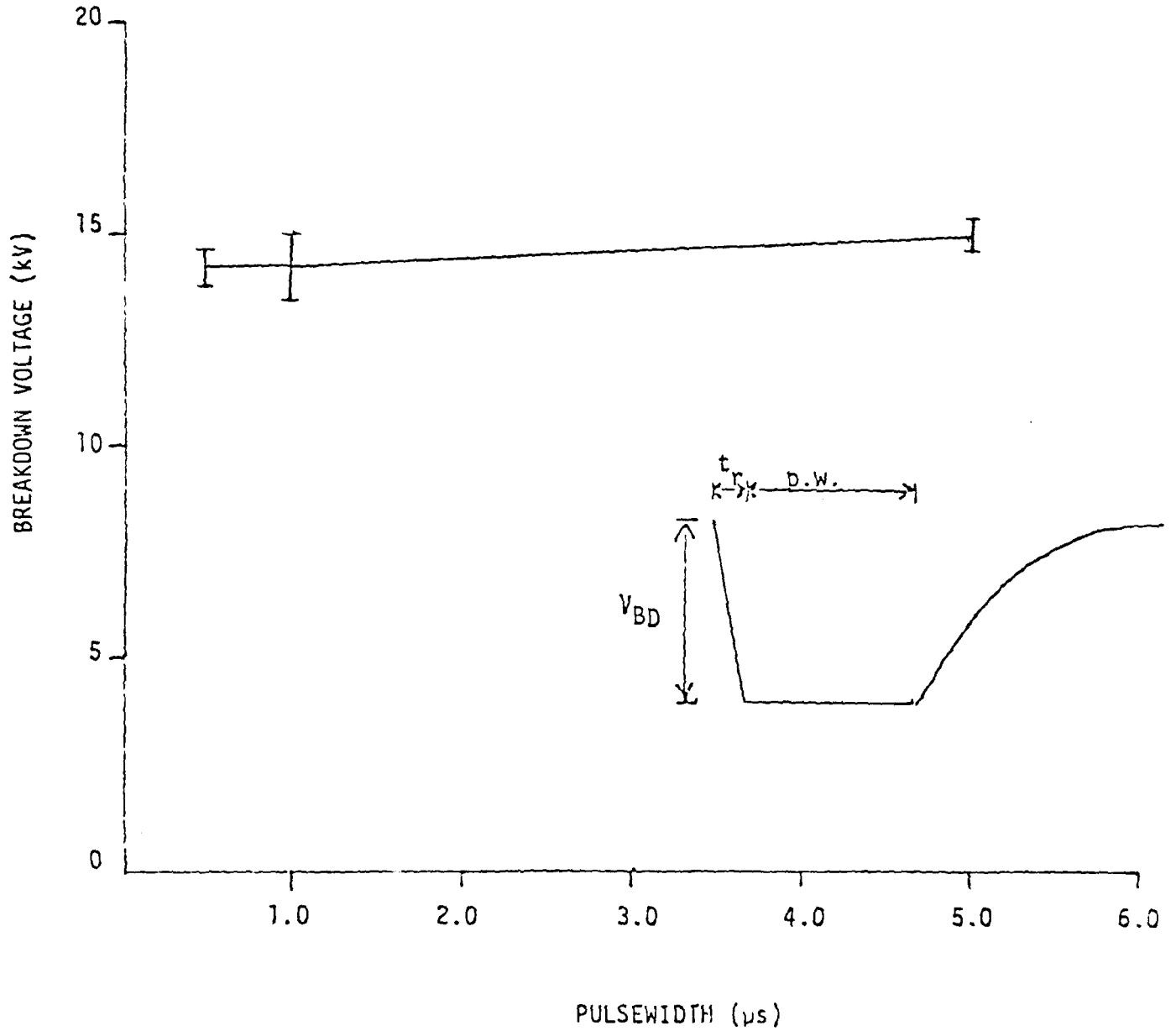


Figure 3.22 Breakdown Voltage vs. Pulsewidth for 1 sheet of 1-mil (25.4 μm) Polypropylene impregnated in Castor Oil. Samples were tested in air and t_r was 0.1 μs.

The dummy sample was then removed and the breakdown voltage of the Mylar was found for several ramped voltages. The test procedure was the same as that followed for pulsed voltages.

The results of these tests are summarized on Figures 3.23 and 3.24. Again, the spread in the data is indicated by error bars which extend one standard deviation above and below the average value measured at each particular risetime. The sample size for each data point was between 10 and 15 samples. Some general observations follow here. It should be noted that these results indicate the dependence of breakdown voltage on risetime and not the affect of the Fluorinert.

General Observations

- o Surface tracking occurred only during tests done in air, as before, particularly for the longer pulses.
- o A hissing noise was again generated in air before the breakdown voltage was reached.
- o For the tests done in Fluorinert, the breakdown point on the sample was a small hole with carbon around it.

These last two types of tests were done in air only. An outline of the procedure follows:

A dummy sample was placed between the electrodes and the output voltage of the pulser was raised to 10 kV. The trigger level on the oscilloscope was adjusted and a pulse counter was connected. The triggering pulse being sent to the modulator was turned off and the modulator output was grounded without lowering the output voltage of the dc power supply. The dummy sample was removed from the electrodes, a new sample inserted and the ground was removed.

BREAKDOWN VOLTAGE VS LEADING EDGE RISE TIME

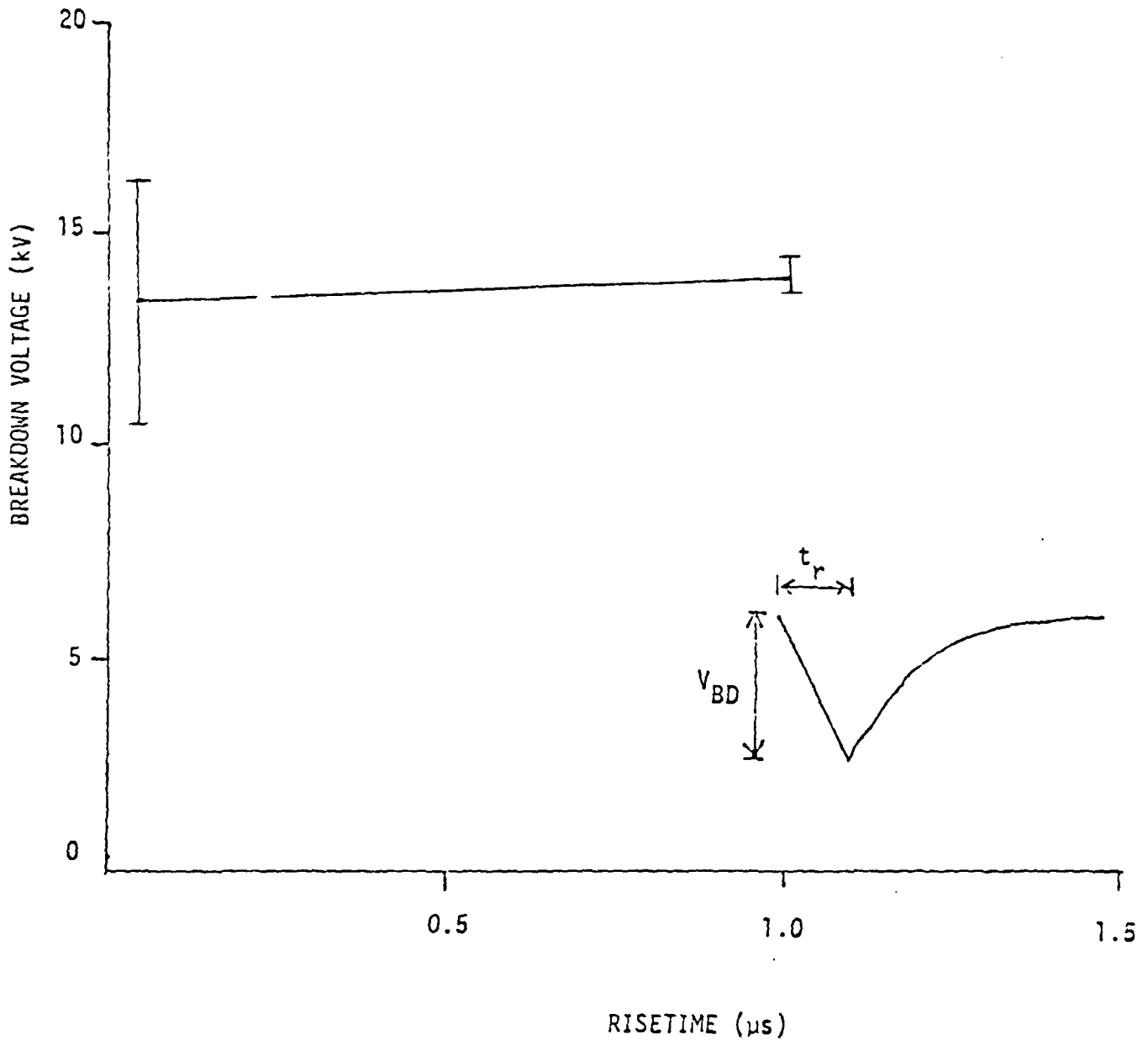


Figure 3.23 Breakdown Voltage vs. Leading-Edge Risetime for 1 sheet of 3-mil (76.2 μm) Mylar. Samples were submerged in Fluorinert during tests.

BREAKDOWN VOLTAGE VS LEADING EDGE RISE TIME

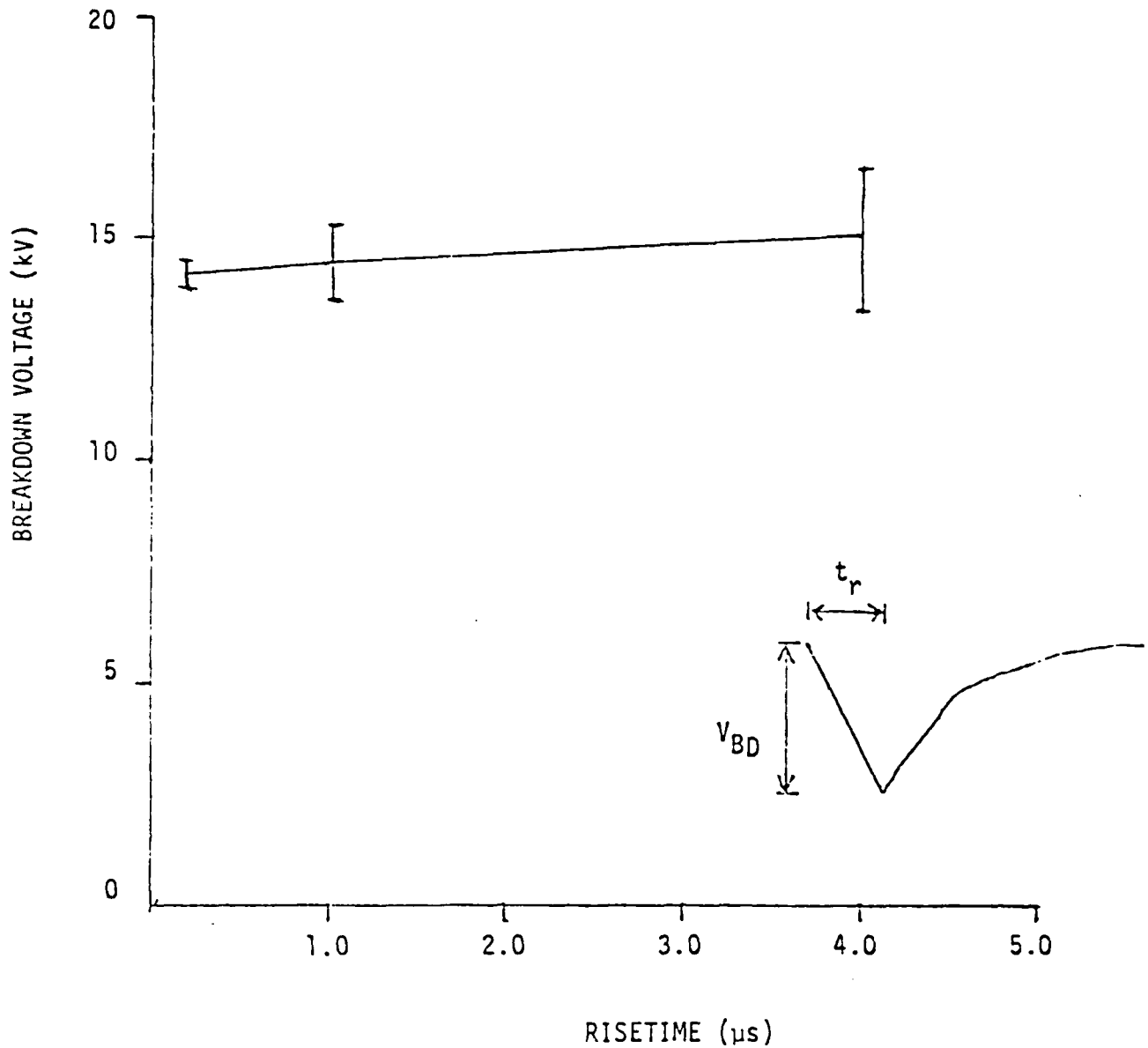


Figure 3.24 Breakdown Voltage vs Leaking-Edge Rise time for 2 sheets of 1-mil (25.4 μm) Mylar. Samples were tested in air.

The triggering pulse for the modulator was then turned back on. Pulses were counted until the sample punctured. The trigger was turned off and the output was grounded. The data was recorded, the old sample was removed and a new sample installed. The results of these tests are contained in Figures 3.25 and 3.26. The spread in the data, which turned out to be very large, is again indicated by the error bars. Some general observations follow here.

General Observations

- o It was found that in the fluorinert, a threshold breakdown voltage existed. If the applied voltage was below this threshold, the sample did not break for several million pulses. Above the threshold, the sample broke immediately (< 1000 pulses). This was not found in air.
- o A large spread in the data, was observed.
- o Surface tracking did occur in some instances.
- o The sample was very cloudy, after it was tested, in the areas which were between the electrodes and near the electrodes.

NUMBER OF PULSES TO BREAKDOWN VS LEADING EDGE RISETIME

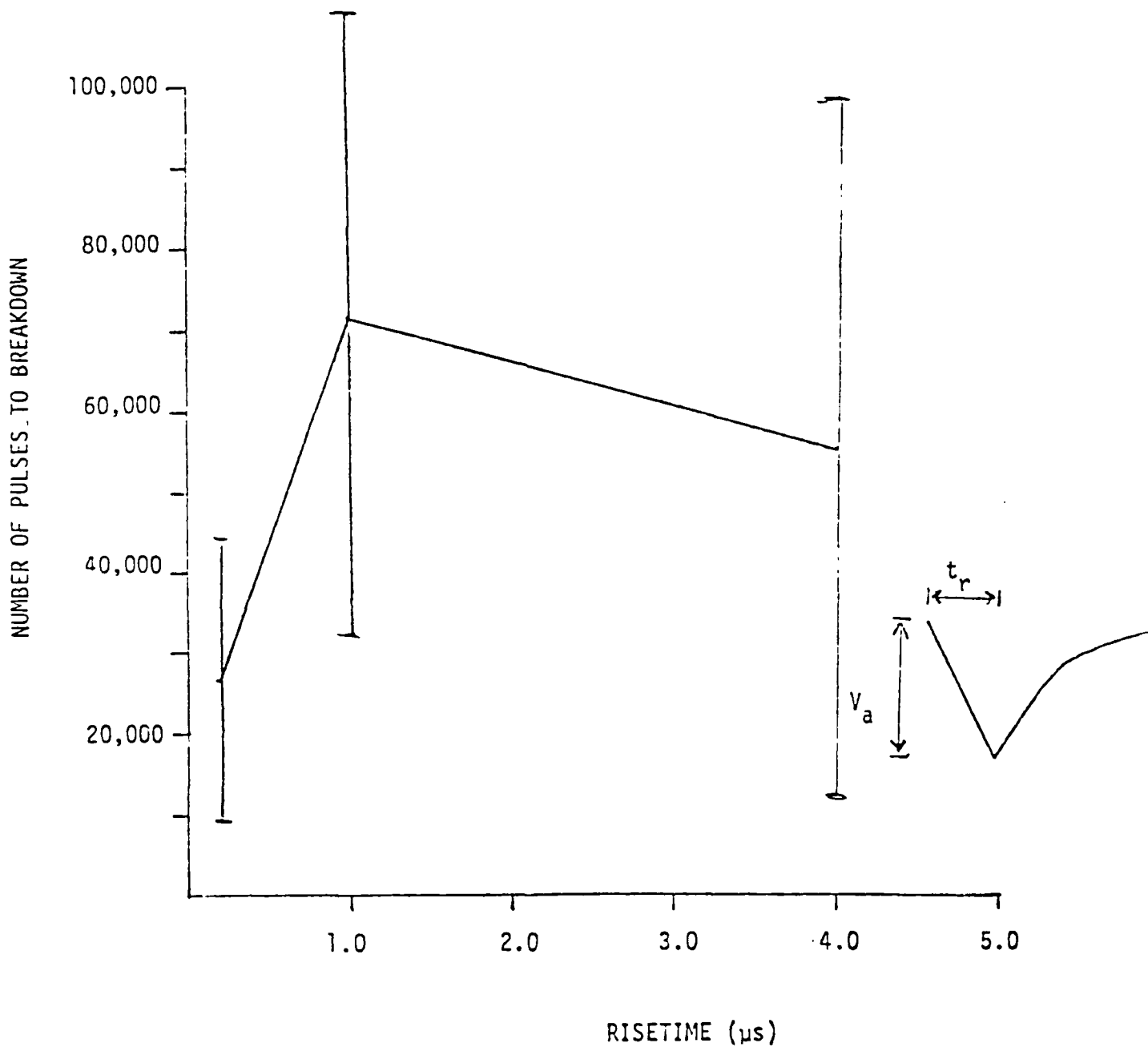


Figure 3.25 Number of Pulses to Breakdown vs. Leading-Edge Risetime for 2 sheets of 1-mil (25.4 μm) Mylar. Samples were tested in air and the applied voltage, V_a , was 10 kV.

NUMBER OF PULSES TO BREAKDOWN VS PULSEWIDTH

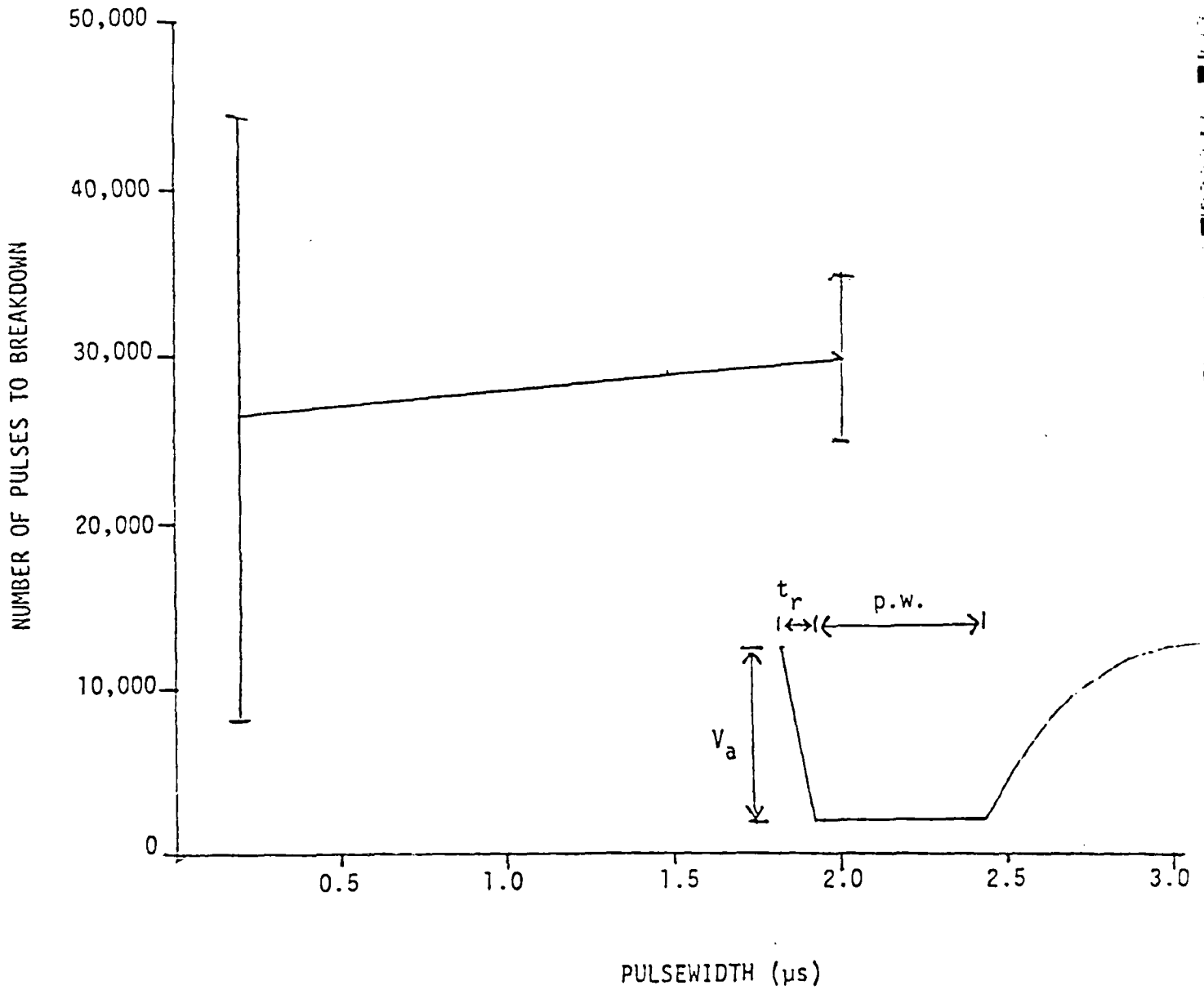


Figure 3.26 Number of Pulses to Breakdown vs. Pulsewidth for 2 sheets of 1-mil (25.4 μm) Mylar. Samples were tested in air and the risetime, t_r , was 0.1 μs . The applied voltage, V_a , was 10 kV.

4.0 THEORETICAL WORK

Theoretical studies were carried out in order to determine the temperature rise in laminate structures. Polymer insulation is subject to electric breakdown at high temperatures. This is generally known as thermal breakdown.^[66] Additionally, any rise in temperature due to dielectric losses within the polymer will tend to accelerate the process of breakdown by mechanisms other than the thermal mechanism if the temperature rise is not such as to cause breakdown by the thermal mechanism itself.

The work described here was undertaken in order to assess the steady state temperature rise in a laminate consisting of repeating layers of Aluminum, Fluorinert and Polypropylene. The heat generation term in the problem considered here could arise due to either mechanical or electrical dissipation of energy. This term would, of course, be related to the process conditions, but it is only the effect of this term that is considered here. As it turns out, the temperature rise at any point depends linearly on the amount of heat generated per unit mass per unit time. Consequently, the problem of relating the process conditions to the amount of heat generated can be uncoupled from the problem of calculating the temperature rise.

4.1 Problem Formulation

In a rectangular Cartesian coordinate system, the heat conduction equation, an equation which determines the variation of temperature in a solid through which heat is flowing, is given by.^[67]

$$k \left[\frac{\partial^2 T}{\partial x^2} + \frac{\partial^2 T}{\partial y^2} + \frac{\partial^2 T}{\partial z^2} \right] + \dot{Q} = \rho C_p \frac{\partial T}{\partial t} \quad (4.1)$$

where T = temperature, °C

x, y, z = spatial coordinates, m.

t = time, s

k = coefficient of thermal conductivity, J/(S-m-°C)

\dot{Q} = energy generated per unit time per unit volume, $\frac{J}{s-m^3}$

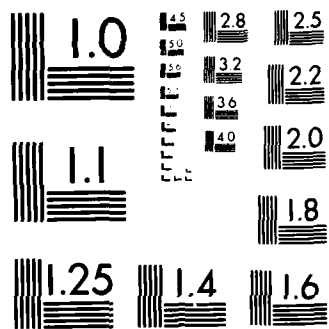
ρ = density, Kg/m³

C_p = specific heat, J/Kg-°C

Here it has been assumed that the physical properties of the solid do not depend on position or temperature, and that the heat generation term is a constant independent of time and position. For a composite material, Eq. (4.1) is assumed to hold in each layer of the composite.

4.2 Initial and Boundary Conditions

Before Eq. (4.1) can be solved, one needs to specify the initial and boundary conditions. For the case at hand, it is assumed that the structure is initially at room temperature and that the six faces are maintained at room temperature at all times. Thus, one seeks the temperature rise within the materials as a result of the generation term. Before proceeding further, though, we note that, without loss of generality, the room temperature may be set equal to zero. Thus, if $L, W,$ and H are respectively the length, width and height of the composite, the initial and boundary conditions take the form.



MICROCOPY RESOLUTION TEST CHART
NATIONAL BUREAU OF STANDARDS 1963 A

$$T(X, Y, Z, 0) = 0$$

$$T(0, Y, Z, t) = 0$$

$$T(L, Y, Z, t) = 0$$

$$T(X, 0, Z, t) = 0$$

$$T(X, W, Z, t) = 0$$

$$T(X, Y, 0, t) = 0$$

$$T(X, Y, H, t) = 0$$

The situation is shown graphically in Figure 4.1.

4.3 Steady State

At steady state the time dependent terms go to zero and Eq. (4.1) reduced to:

$$k \nabla^2 T + \dot{Q} = 0 \quad (4.2)$$

Equation (4.2) is recognized to be the Poisson equation, and its solution will yield the maximum possible temperature rise within the material.

4.4 Dimensionless Formulation

Before solving Eq. (4.2), it is useful to call \dot{Q}/k as Q and to make the spatial variables dimensionless according to:

$$X^* = \frac{X}{L} \quad (4.3)$$

$$Y^* = \frac{Y}{W} \quad (4.4)$$

$$Z^* = \frac{Z}{H} \quad (4.5)$$

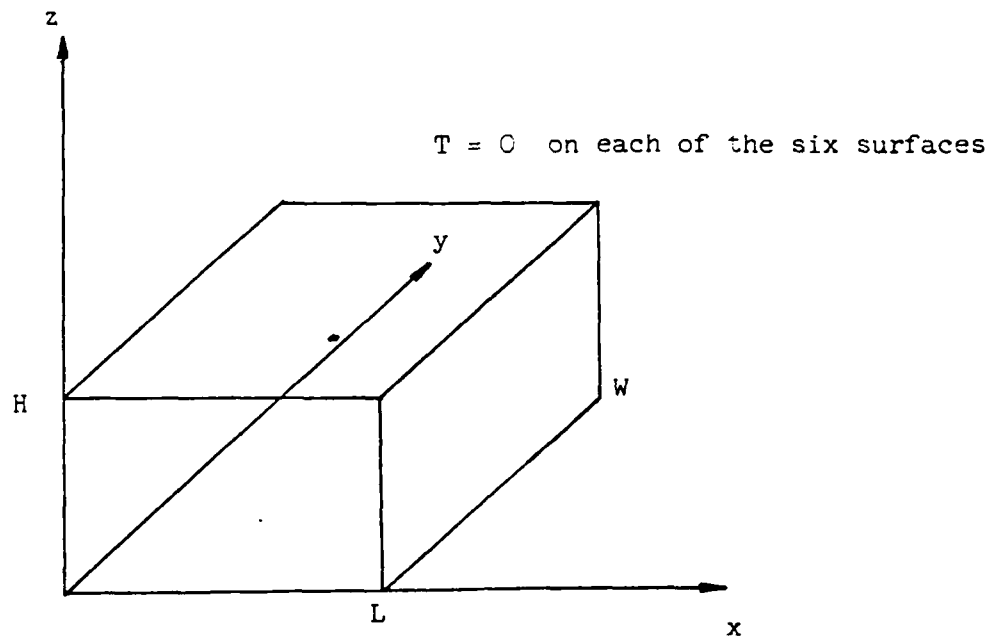


Figure 4.1 Geometry of the system.

With the help of Eqs. (4.3 to 4.5), Eq. (4.2) takes the form:

$$\left(\frac{\pi}{L}\right)^2 \frac{\partial^2 T}{\partial X^{*2}} + \left(\frac{\pi}{W}\right)^2 \frac{\partial^2 T}{\partial Y^{*2}} + \left(\frac{\pi}{H}\right)^2 \frac{\partial^2 T}{\partial Z^{*2}} + Q = 0 \quad (4.6)$$

Correspondingly, the boundary conditions take the form:

$$\begin{aligned} T(0, Y^*, Z^*, t) &= 0 \\ T(\pi, Y^*, Z^*, t) &= 0 \\ T(X^*, 0, Z^*, t) &= 0 \\ T(X^*, \pi, Z^*, t) &= 0 \\ T(X^*, Y^*, 0, t) &= 0 \\ T(X^*, Y^*, \pi, t) &= 0 \end{aligned} \quad (4.7)$$

4.5 Application to Composites

For a composite laminate structure, Eq. (4.6) will be valid within each layer, albeit with different values of the quantity Q . Furthermore, continuity of temperature and heat flux at the interface requires that

$$T_i = T_{i+1} \quad (4.8)$$

$$k_i \left. \frac{\partial T}{\partial Z^*} \right|_i = k_{i+1} \left. \frac{\partial T}{\partial Z^*} \right|_{i+1} \quad (4.9)$$

where i refers to the number of a given layer.

4.6 Method of Solution

As is evident from an examination of Eq. (4.6), the temperature depends on the three variables X , Y , and Z . If one uses a finite sine transform, [68] one can eliminate the X and Y dependencies.

Recall that the finite sine transform $\bar{T}(Y^*, Z^*)$ of $T(X^*, Y^*, Z^*)$ is:

$$\bar{T}(Y^*, Z^*) = \int_0^\pi T(X^*, Y^*, Z^*) \sin P_1 X^* dx^* \quad (4.10)$$

If one multiplies Eq. (4.6) by the kernel $\sin P_1 X^*$ and integrates from 0 to π with respect to X^* , one gets (with some help from the boundary conditions)

$$-\left(\frac{\pi}{L}\right)^2 P_1^2 \bar{T} + \left(\frac{\pi}{W}\right)^2 \frac{\partial^2 \bar{T}}{\partial y^{*2}} + \left(\frac{\pi}{H}\right)^2 \frac{\partial^2 \bar{T}}{\partial Z^{*2}} + \frac{Q}{P_1} (1 - (-1)^{P_1}) = 0 \quad (4.11)$$

along with

$$\begin{aligned} \bar{T}(0, Z^*) &= 0 \\ \bar{T}(\pi, Z^*) &= 0 \\ \bar{T}(Y^*, 0) &= 0 \\ \bar{T}(Y^*, \pi) &= 0 \end{aligned} \quad (4.12)$$

and

$$\begin{aligned} \bar{T}_i &= \bar{T}_{i+1} \\ k_i \left. \frac{\partial \bar{T}}{\partial Z^*} \right|_i &= k_{i+1} \left. \frac{\partial \bar{T}}{\partial Z^*} \right|_{i+1} \end{aligned} \quad (4.13)$$

To eliminate the y dependence, one now multiplies each of Eqs. (4.11 to 4.13) by $\sin p_2 y^*$ and integrates from 0 to π with respect to y^* . The result is

$$-\left(\frac{\pi}{L}\right)^2 P_1^2 \bar{T} - \left(\frac{\pi}{W}\right)^2 P_2^2 \bar{T} + \left(\frac{\pi}{H}\right)^2 \frac{\partial^2 \bar{T}}{\partial Z^{*2}} + \frac{Q}{P_1 P_2} (1 - (-1)^{P_1})(1 - (-1)^{P_2}) = 0 \quad (4.14)$$

$$\bar{T}(0) = 0 \quad (4.15)$$

$$\bar{T}(\pi) = 0$$

$$\bar{T}_i = \bar{T}_{i+1} \quad (4.16)$$

$$k_i \left. \frac{\partial \bar{T}}{\partial Z^*} \right|_i = k_{i+1} \left. \frac{\partial \bar{T}}{\partial Z^*} \right|_{i+1}$$

Note that Eq. (4.14) is a second order, non-homogeneous linear ordinary differential equation with constant coefficients. It admits an analytical solution (of course $P_1, P_2 > 0$). However, before writing this down, it is convenient to rewrite Eq. (4.14) as:

$$\frac{d^2 \bar{T}}{dZ^{*2}} - H^2 \left[\frac{P_1^2}{L^2} + \frac{P_2^2}{W^2} \right] \bar{T} + \frac{H^2}{\pi} \frac{Q}{P_1 P_2} [1 - (-1)^{P_1}] [1 - (-1)^{P_2}] = 0 \quad (4.17)$$

or

$$\frac{d^2 \bar{T}}{dZ^{*2}} - P_3^2 \bar{T} + q = 0 \quad (4.18)$$

where

$$P_3^2 = H^2 \left[\frac{P_1^2}{L^2} + \frac{P_2^2}{W^2} \right]$$

and

$$q = \frac{H^2}{\pi} \frac{Q}{P_1 P_2} [1 - (-1)^{P_1}] [1 - (-1)^{P_2}]$$

The general solution of Eq. (4.18) is

$$\bar{T} = a e^{P_3 Z^*} + b e^{-P_3 Z^*} + \frac{q}{P_3^2} \quad (4.19)$$

Since this is valid in each layer, and since each layer has a different value of q , one has to write

$$T_i = a_i e^{P_3 Z_i^*} + b_i e^{-P_3 Z_i^*} + \frac{q_i}{P_3^2} \quad i = 1, 2, \dots, n \quad (4.20)$$

The $2n$ constants a_i, b_i are evaluated with the help of the $2(n-1)$ conditions at the $(n-1)$ interfaces and the two conditions given by Eq. (4.15).

For example, for the layers i and $i+1$:

$$a_i e^{P_3 Z_i^*} + b_i e^{-P_3 Z_i^*} + \frac{q_i}{P_3^2} = a_{i+1} e^{P_3 Z_i^*} + b_{i+1} e^{-P_3 Z_i^*} + \frac{q_{i+1}}{P_3^2} \quad (4.21)$$

$$k_i [a_i e^{P_3 Z_i^*} - b_i e^{-P_3 Z_i^*}] = k_{i+1} [a_{i+1} e^{P_3 Z_i^*} - b_{i+1} e^{-P_3 Z_i^*}] \quad (4.22)$$

where Z_i^* gives the location of the interface.

Also, equation (4.15) result in

$$a_1 + b_1 + \frac{q_1}{P_3^2} = 0 \quad (4.23)$$

and

$$a_n e^{P_3 \pi} + b_n e^{-P_3 \pi} + \frac{q_n}{P_3^2} = 0 \quad (4.24)$$

Equations (4.21 to 4.25) represent a 5-diagonal matrix which can be inverted to yield the $2n$ constants a_i and b_i . Note that this has to be done for each value of P_1 and P_2 .

Finally then, taking the inverse transform of Eq. (4.20):

$$T(X^*, Y^*, Z^*) = \frac{4}{\pi^2} \sum_{P_1=1}^{\alpha} \sum_{P_2=1}^{\alpha} T(Z^*) \sin P_1 X^* \sin P_2 Y^* \quad (4.25)$$

4.7 Material Properties Used

It is assumed that the repeat unit in the composite laminate is a sandwich consisting of layers of Aluminum, Fluorinert and Polypropylene. It is further assumed that there is no heat generation in the Aluminum layer and that the heat generation per unit mass is the same in the polypropylene and fluorinert layers. The coefficient of thermal conductivity is taken to be 0.056 watts/m°C for fluorinert and 0.117 watts/m-°C for polypropylene. The density of fluorinert and polypropylene is 1630 kg/m³ and 910 kg/m³, respectively.

Note that $Q = \left(\frac{\text{heat generated}}{\text{mass-time}} \right) \cdot \frac{L}{k}$

Thus if the heat generated per unit mass of polypropylene or fluorinert is 200 watts/kg, $Q = 5.82 \times 10^6 \frac{^\circ\text{C}}{\text{m}^2}$ for fluorinert and $Q = 1.55 \times 10^6 \frac{^\circ\text{C}}{\text{m}^2}$ for polypropylene.

4.8 Method of Solution

Once the temperature at any point (X^* , Y^* , Z^*) is known using Eq. (4.25), the temperature at the corresponding point (X , Y , Z) is obtained through the transformation described by Eqs. (4.3 to 4.5). A computer program was written to evaluate the sums in Eq. (4.25) and the logic is explained in the flow chart presented in Figure 4.2.

It might be mentioned that the variables that need to be considered are (i) the variables which enter the solution scheme itself, namely the upper limits of P_1 and P_2 . (ii) the process variables, namely values of Q (iii) the system dimensions-- L , W and H and also the number of layers at fixed values of L , W and H (keeping the total amounts of Aluminum, Fluorinert and Polypropylene constant).

START

READ: N
N=Number of single
layers

READ: T0
(surrounding Temperature)

READ: L,W
L - Length in m
W - Width in m

READ: DL1, DL2, DL3

DL1, DL2, DL3 =
Thickness of
Polypropylene,
fluorinert and
aluminum layers

CALCULATION OF THE
COORDINATES ZL OF
THE LAYER JUNCTIONS

READ: P1MAX, P2MAX

P1MAX, P2MAX=
maximum number of
terms in the sums
(eq. 25)

READ: K1, K2, K3

K1, K2, K3 = Thermal
Conductivity of
Polypropylene,
fluorinert and
aluminum

READ: Q1, Q2, Q3

Q1, Q2, Q3 = Heat
generation in the
Polypropylene,
fluorinert and
aluminum layers

READ: XP, YP, ZP
(Coordinates of the
point where temperature
is evaluated)

Transformation of the
coordinates

P2 = 1

P1 = 1

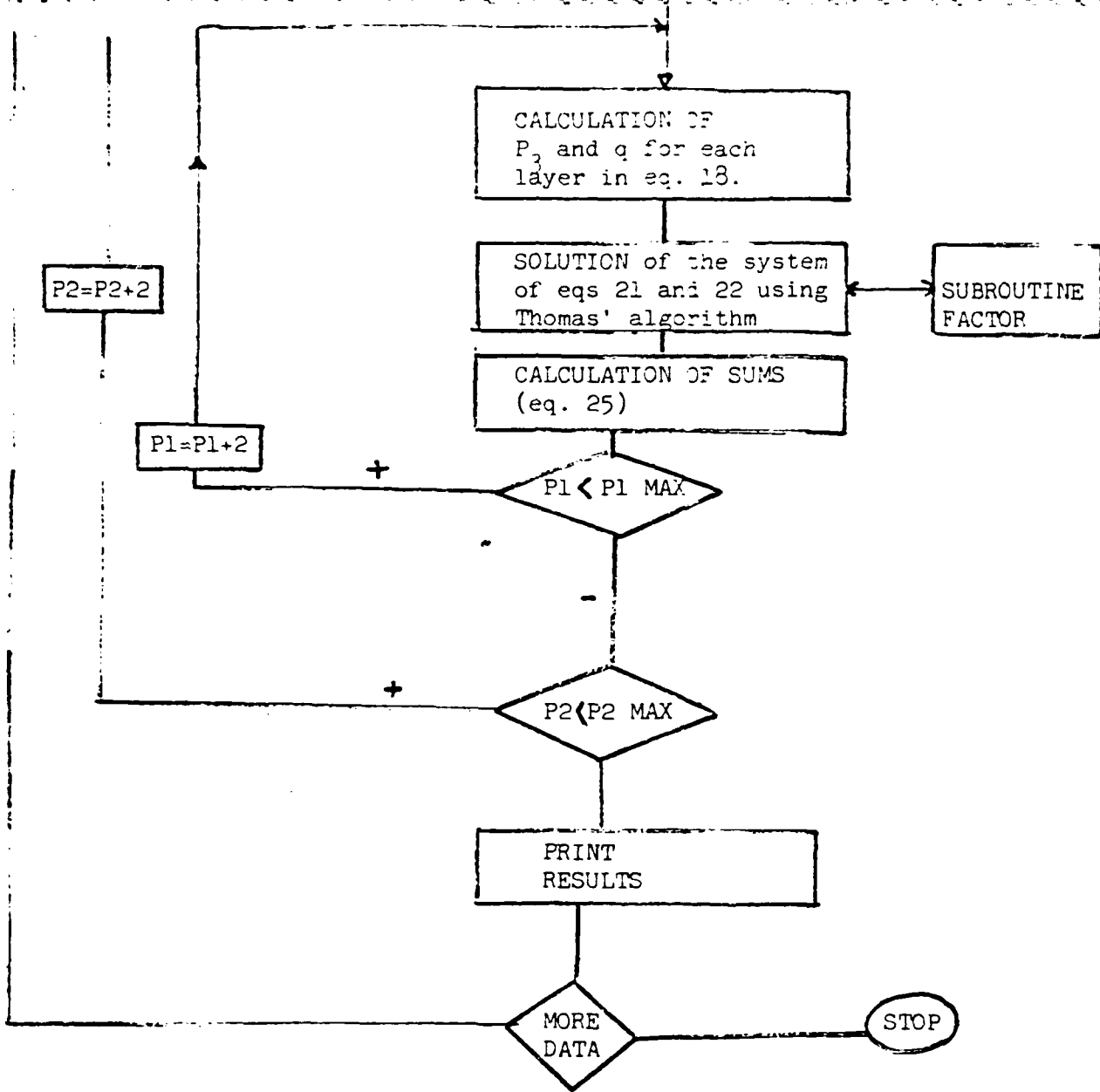


Figure 4.2 The flowchart of the Fortran program for the calculation of the steady state temperature profiles in the multilayer systems with heat generation.

4.9 Effect of Maximum Values of P_1 and P_2

Figure 4.3 shows the effect on the temperature at a particular point in the composite of varying the upper limits of P_1 and P_2 in Eq. (4.25). It is seen that the temperature stabilizes fairly quickly. Consequently, $P_{1 \max}$ and $P_{2 \max}$ were both taken to be eleven in the rest of this work.

4.10 Check of the Solution Scheme

In order to check the solution scheme, the temperature rise was calculated in a block of material having uniform properties. (i.e., Q was assumed independent of position). It was found that for a block of dimensions $L = W = 0.1$ m and $H = 0.0342$ m, the temperature at the center was

$$T_{\max} = 7.375 \times 10^{-4} Q$$

The number of layers, n , was 597.

Since obtaining an analytical solution for three dimensional heat conduction is not as easy task, it was assumed that the block was insulated at the top and bottom and the centerline temperature calculated. The solution is given in Appendix C and the final result is

$$T_{\max} = 7.366 \times 10^{-4} Q.$$

It would be intuitively expected that the centerline temperature in the insulated block would be close to the maximum temperature in the un-insulated block. Consequently the agreement between the two values is quite pleasing. Indeed one finds that for fixed values of L and W , the maximum temperature tends to an asymptotic value as H increases. So the

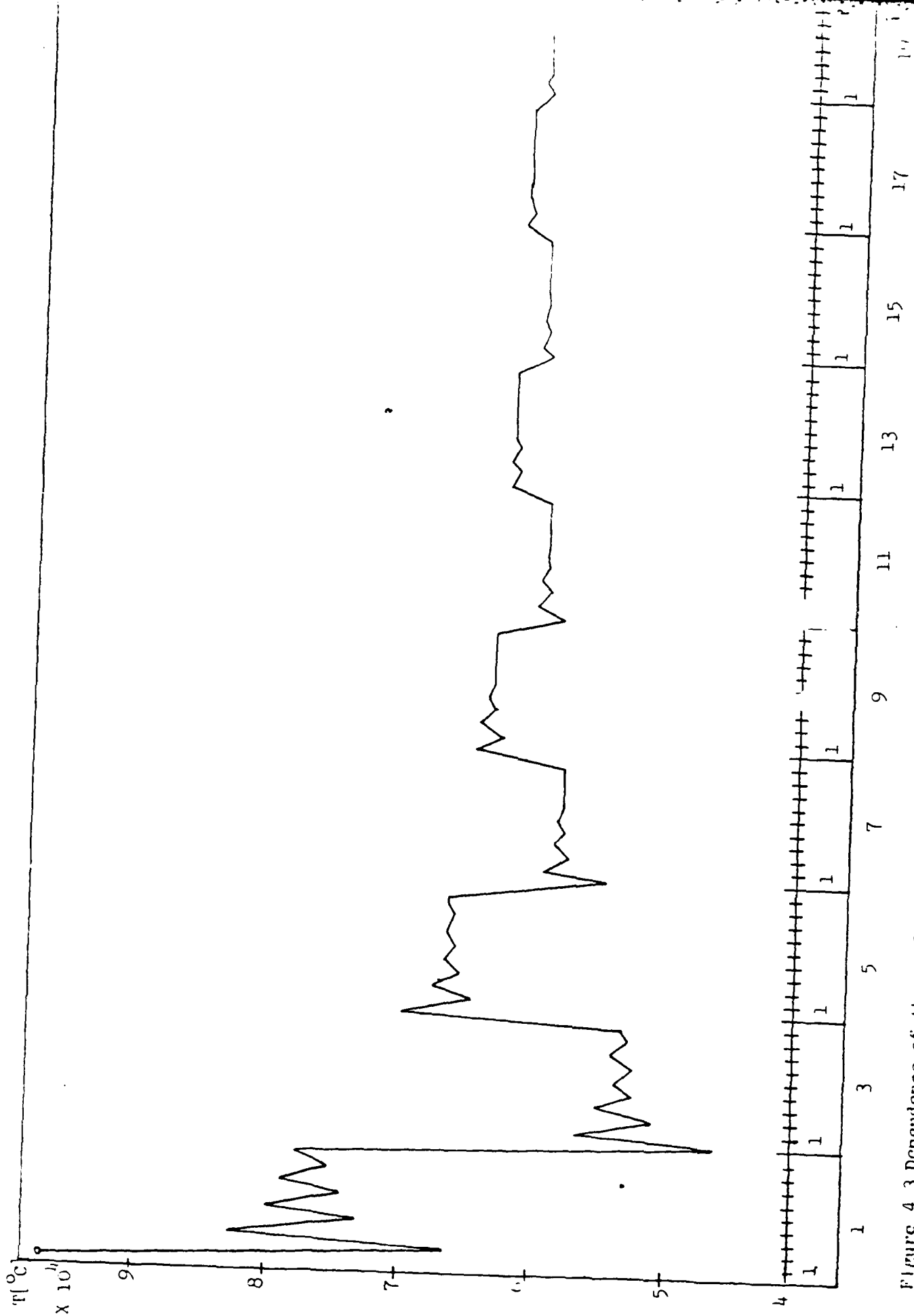


Figure 4.3 Dependence of the evaluated temperature vs. numbers of the terms in the summations in Equation (4).

agreement would be expected if one could anticipate the results in the following sections.

Before proceeding further, it is worth remarking that in this case, T_{\max} scales with Q . It was found that even in the case of a composite block, the temperature at any point scaled approximately with Q . Therefore, it was necessary to calculate the temperature rise for a single value of Q only.

4.11 Effect of Number of Layers at Fixed Values of L, W and H

In a typical capacitor, the thicknesses of the Aluminum, Fluorinert and Polypropylene layers may be 0.1 mil, 0.1 mil and 0.5 mil, respectively. The total number of layers in a block of reasonable thickness would, therefore, become very large. We, therefore, investigated the effect of decreasing the number of layers while simultaneously increasing their thickness when L , W and H were kept fixed.

Figures 4.4 and 4.5 show typical temperature profiles which reveal that it is permissible to "thicken" the layer as long as the total number of layers is still reasonably large. The calculations shown in Figures 4.4 and 4.5 were for a block having $L = W = 0.05$ m and $H = 0.01$ m. In all the cases to be discussed, the heat generated per unit mass was taken to be 200 watts/kg for both Fluorinert and Polypropylene. No generation was assumed in the Aluminum layer.

In Figure 4.4, the dimensions of the layers of the three different materials are -- Polypropylene, 0.635×10^{-4} m; Fluorinert, 0.127×10^{-4} m; Aluminum 0.102×10^{-4} m. In Figure 4.5, the number of layers has been

58. D. Miller, "Tests and Standards to Evaluate the Fire Safety of Electrical Insulating Fluids," IEEE Trans. on Elect. Insul. Vol. EI-13, No. 5, 1978, pp. 378-381.
59. R. Hakim, et. al., "The Dielectric Properties of Silicone Fluids," IEEE Trans. on Elect. Insul., Vol. EI-12, No. 5, 1977, pp. 360-370.
60. S. Yasufuku, et. al., "Dielectric Properties of Oil-Impregnated All PP Film, Power Capacitor Insulation System," IEEE Trans. on Elect. Insul., Vol. EI-13, No. 6, 1978, pp. 403-410.
61. S. Ross and G. Shirn, "Phthalate Ester Insulating Oils," IEEE Trans. on Elect. Insul., Vol. EI-13, No. 5, 1978, pp. 381-383.
62. R. Sillars, Electrical Insulating Materials, Peter Peregrinus Ltd., London, England, 1973, pp. 120-122.
63. R. Parker, "Design and Failure Mechanisms of High-Energy Density Capacitors Operating at High Repetition Rates," Conf. on Elect. Insul. and Dielectric Phenomena, 1980, pp. 150-154.
64. Hercules Inc., Technical information bulletin FN-30.
65. E. Collins, J. Bares and F. Billmeyer, Jr., Experiments in Polymer Science, Wiley-Interscience Publication, New York, 1973, pp. 468-469.
66. J. M. Schultz, Polymer Material Science, Prentice Hall, Englewood Cliffs, New Jersey, 1984
67. H. S. Carslaw and J. C. Jaeger, Conduction of Heat in Solids, 2nd Edition, Clarendon Press, Oxford, 1959.
68. C. J. Tranter, Integral Transforms in Mathematical Physics, John Wiley & Sons, New York, 1951.

48. B. Stenerhag and A. Danemar, "Partial Discharge Characteristics of Some Liquid Impregnated Insulating Systems," 3rd Int'l Conf. on Dielectric Materials, Measurements and Applications, 1979, pp. 26-29.
49. T. S. Ramu and Y. Narayana Rao, "Electrical Behavior of Castor Oil Impregnated Paper PP Systems," 3rd Int'l Conf. on Dielectric Materials, Measurements and Applications, 1979, pp. 37-40.
50. S. Yasufuku, et. al., "Phenyl Methyl Silicone Fluid and its Application to High Voltage Stationary Apparatus," IEEE Trans. on Elect. Insul., Vol. EI-12, No. 6, 1977, pp. 402-410.
51. K. P. Mommooty, "An Assessment of the Dielectric Behavior of Some Liquid Impregnated Systems," Ph.D. Thesis, IISC., Bangalore, India, 1982.
52. K. Mommooty and T. Ramu, "Analysis of the Dielectric Behavior of Castor Oil Impregnated All-Paper Capacitors," IEEE Trans. on Elect. Insul., Vol. EI-16, No. 5, 1981, pp. 417-422.
53. N. M. Bashara, "Some Fluorinated Liquid Dielectrics," Am. Inst. of Elect. Eng. Trans. on Comm. and Electronics, Vol. 72, Pt. 1, 1953, pp. 79-84.
54. N. Berger and P. Jay, "UGILEC-101 A New Impregnant for High Voltage Power Capacitors," IEEE Insul. Symp., Montreal, June 1984, pp. 319-322.
55. I. Y. Megahed and A. A. Zaky, "Influence of Temperature and Pressure on Conduction Currents in Transformer Oil," IEEE Trans. on Elect. Insul., Vol. EI-4, No. 4, 1969, pp. 99-103.
56. A. R. Nosseir, "Effects of Dissolved Gases, Stress, and Gap Spacing on High Field Conductivity in Liquid Insulants," IEEE Trans. on Elect. Insul., Vol. EI-10, No. 2, 1975, pp. 58-61.
57. T. Hirano, "Effects of High-Pressure SF₆ Gas Dissolved in an Insulating Oil on DC Conduction Currents and AC Partial Discharges," Jour. of App. Phys., Vol. 55, No. 1, 1984, pp. 9-14.

35. A. Tomago and T. Suzuki, "A New Synthetic Paper-MPSP for Insulation," IEEE Trans. on Elect. Insul., Vol. EI-12, No. 4, 1977, pp. 301-309.
36. L. T. Apps: Electronics and Power, 1970, pp. 369-372.
37. R. L. Remke and H. Von Seggern, "Modeling of Thermally Stimulated Currents in Polytetrafluoroethylene," Journal of App. Phys., Vol. 54, No. 9, 1983, pp. 5262-5267.
38. Chemplast Inc., Chemfluor Tapes Product Bulletin No. 8.
39. J. R. Laghari, et. al., "Partial Discharges in Polymer Insulation," Annual Report, Conf. on Elect. Insul. and Dielectric Phenomena, Amherst, Massachusetts, 1982, pp. 541-548.
40. J. C. Reed, et. al., "Effects of High Voltage Stresses on TFE and FEP Fluorocarbon Plastics," Insulation Magazine, 1964.
41. DuPont Company, Technical Information on Mylar Polyester Film, Bulletin No. M-1J.
42. E. Forster, et. al., "A Study of the Electrical Insulation Characteristics of Oil-Impregnated PP Paper," IEEE Trans. on Elect. Insul., Vol. EI-7, No. 4, 1972, pp. 162-169.
43. S. Yasufuku, et. al., "Maxwell-Wagner Dielectric Polarization in PP Film-Aromatic Dielectric Fluid System for High Voltage Capacitor Use," IEEE Trans. on Elect. Insul., Vol. EI-14, No. 6, 1979, pp. 334-341.
44. W. J. Sarjeant, High Voltage Engineering, State Univ. of New York at Buffalo, 1979.
45. D. Fink and H. Beaty, Standard Handbook for Electrical Engineers, McGraw Hill, New York, 1978.
46. R. Kaneko, et. al., "Dielectric Stability of Gas Pressurized HDPE Tape Insulation Under Conditions of Overvoltage," IEEE Trans. on Power App. and Sys., Vol. PAS-89, No. 3, 1970, pp. 478-483.
47. D. G. Shaw, "Ester Fluids for Liquid-Filled Capacitors," 1977 Annual Report, Conf. on Elect. Insul. and Dielectric Phenomena, Washington, D.C., 1979, pp. 151-161.

25. F. Ahmed and A. Ahmed, "Breakdown of Solid Insulating Films by Partial Discharges Using Sinusoidal and Pulse Voltages," IEEE Trans. on Elect. Insul., Vol. EI-13, No. 5, 1978, pp. 337-343.
26. D. Shaw, et. al., "A Changing Capacitor Technology - Failure Mechanisms and Design Innovations," IEEE Trans. on Elect. Insul., Vol. EI-16, No. 5, 1981, pp. 399-413.
27. J. R. Laghari and W. J. Sarjeant, "Partial Discharges and Breakdown in Laminate Insulation Structure," First Int'l. Conf. on Conduction and Breakdown in Solid Dielectrics, France, July 1983, pp. 282-285.
28. K. Mammotty and T. Ramu, "Properties of Castor Oil Impregnated All-PP and PP-paper Capacitors," IEEE Trans on Elect. Insul., Vol. EI-18, No. 5, 1983, pp. 541-550.
29. B. Ganger and G. Maier, "On Electrical Aging of Oil-Impregnated High-Voltage Dielectrics," IEEE Trans on Elect. Insul., Vol. EI-9, No. 3, 1974, pp. 92-97.
30. B. M. Weedy, et. al., "Partial Discharges in Lapped Polymer Taped Insulation Impregnated with Supercritical Helium," IEE PROC., Vol. 129, pt. A, No. 3, 1982, pp. 176-182.
31. A. Tomago, et. al., "Development of Oil-Impregnated, All-PP-Film Power Capacitor," IEEE Trans. on Elect. Insul., Vol. EI-12, No. 4, 1977, pp. 293-300.
32. N. Parkman, "Some Properties of Solid-Liquid Composite Dielectric Systems," IEEE Trans. on Elect. Insul., Vol. EI-13, No. 4, 1978, pp. 289-307.
33. T. Sakurai, et. al., "275 kV Self-Contained Oil-Filled Cable Insulated with Polymethylpentene Laminated Paper," IEEE Trans. on Power App. and Sys., Vol. PAS-100, No. 5, 1981, pp. 2575-2580.
34. H. Fujita and H. Itch, "Synthetic Polymer Papers Suitable for Use in EHV Underground Cable Insulation," IEEE Trans. on Power App. and Sys., Vol. PAS-95, No. 1, 1976, pp. 130-137.

12. A. R. Von Hippel, Dielectric Materials and Applications, The Technology Press of M.I.T. and J. Wiley and Sons, Inc., New York, 1954.
13. J. Artbauer and J. Griac, "Some Factors Preventing the Attainment of Intrinsic Electric Strength in Polymeric Insulations," IEEE Trans. on Elect. Insul., Vol. EI-5, No. 4, 1970, pp. 104-113.
14. M. Ieda, "Dielectric Breakdown Process of Polymers," IEEE Trans. on Elect. Insul., Vol. EI-15, No. 3, 1980, pp. 206-224.
15. A. M. Bueche, "Electrical Technology and Polymer Science," IEE Proc., Vol. 126, No. 4, 1979, pp. 351-356.
16. DuPont Company, Teflon FEP Fluorocarbon Film, Bulletin No. T-4E.
17. G. R. Johnson, "Dielectric Properties of Polytetrafluoroethylene," 1966 Annual Report, Conf. on Elect. Insul. and Dielectric Phenomena, Washington, D.C., 1967, pp. 78-83.
18. K. Sato, et. al., "Characteristics of Film and Oil for All-PP-Film Power Capacitors," IEEE Trans. on Power App. and Sys., Vol. PAS-99, No. 5, 1980, pp. 1937-1942.
19. R. Von Olshansen, et. al., "AC Loss and DC Conduction Mechanisms in Polyethylene Under High Electric Fields," IEE PROC., Vol. 128, Pt. A, No. 3, 1981, pp. 183-191.
20. DuPont Company, Design Data for Teflon Notes.
21. R. Bartnikas, "Electrical Conduction in Medium Viscosity Oil-Paper Films-Part 1," IEEE Trans. on Elect. Insul., Vol. EI-9, No. 2, 1974, pp. 85-92.
22. B. Gosse, et. al., "Ion Conduction Through Paper and PP Foils Impregnated with Liquid Dielectric," IEE PROC., Vol. 128, Pt. A, No. 3, 1981, pp. 165-173.
23. R. W. Sillars, Electrical Insulating Materials and Their Applications, Billing and Sons, Ltd., Guildford and London, 1973.
24. D. B. Watson, "Dielectric Breakdown in Perspex," IEEE Trans. on Elect. Insul., Vol. EI-8, No. 3, 1973, pp. 73-79.

8.0 REFERENCES

1. H. J. Wintle, "Photoelectric Effects in Insulating Polymers and Their Relation to Conduction Processes," IEEE Trans. on Elect. Insul., Vol. EI-12, No. 2, 1977, pp. 97-102.
2. E. J. McMahon and J. O. Punderson, "Dissipation Factor of Composite Polymer-and Oil-Insulating Structures on Extended Exposure to Simultaneous Thermal and Voltage Stress," IEEE Trans. on Elect. Insul., Vol. EI-8, No. 3, 1977, pp. 92-97.
3. C. W. Reed, "Proceedings of a Symposium on High-Energy-Density Capacitors and Dielectric Materials," National Academy Press, Washington, D.C., 1981, pp. 1-14.
4. F. Clark, Insulating Materials for Design and Engineering Practice, John Wiley and Sons, Inc., New York, 1962.
5. A. R. Von Hippel, Dielectrics and Waves, John Wiley and Sons, Inc., London, 1962.
6. E. Kuffel and M. Abdullah, High Voltage Engineering, Pergamon Press, Hungary, 1970.
7. C. H. Park, et. al., "Effect of Heat Treatment on Dielectric Strength of Polyethylene Terephthalate Under Compressive Stress," IEEE Trans. on Elect. Insul., Vol. EI-18, No. 4, 1983, pp. 380-389.
8. W. J. Sarjeant, "Polymer Laminate Structure," Applied Physics Communications, Vol. 3, No. 1 & 2, 1983, pp. 83-167.
9. J. J. O'Dwyer, "Breakdown in Solid Dielectrics," IEEE Trans. on Elect. Insul., Vol. EI-17, No. 6, 1982, pp. 484-489.
10. P. P. Budenstein, "On the Mechanism of Dielectric Breakdown of Solids," IEEE Trans. on Elect. Insul., Vol. EI-15, No. 3, 1980, pp. 225-235.
11. N. Yoshimura and F. Nato, "Dielectric Breakdown of Polyparabanic Acid Film Under Square Pulse Conditions," IEEE Trans. on Elect. Insul., Vol. EI-18, No. 1, 1983, pp. 48-52.

7.0 OTHER SUPPORTING INFORMATION

7.1 Papers Presented

None so far.

7.2 Personnel Supported

Faculty

W. J. Sarjeant Electrical and Computer Engineering	10% academic 1983 - 1984 2 months, Summer 1984
J. R. Laghari Electrical and Computer Engineering	10% academic 1983 - 1984 2 months, Summer 1984
R. K. Gupta Chemical Engineering	10% academic 1983 - 1984 1 month, Summer 1984

Personal Donation

R. E. Dollinger Electrical and Computer Engineering	1 month, Summer 1984
---	----------------------

Clerical

Joan Bennett	10% calendar
--------------	--------------

Technician

Willi Schulze	10% calendar
---------------	--------------

Students/Research Personnel

B. Pyszynski (1)	Research	Chemical Engineering
M. Treanor (2)	Graduate	Electrical Engineering
T. Bilodeau (3)	Graduate	Electrical Engineering
A. Hammoud (4)	Graduate	Electrical Engineering
K. Kumar (5)	Graduate	Chemical Engineering

- (1) -- Theoretical and Computer modeling
- (2) -- Pulsed voltage
- (3) -- Corona inception/extinction voltages
- (4) -- Alternative voltage
- (5) -- Impregnation, mechanical testing.

6.0 EXPERIMENTS IN PROGRESS

Experiments are presently in progress to determine

- o The influence of thermo-electrical ageing on the electrical and mechanical properties (such as permittivity, dielectric loss, pulse breakdown, corona signatures, tensile strength, etc.) of impregnated laminate insulation structures.
- o The influence of injected electronic space charge on the dielectric strength and dielectric properties of insulating materials.
- o The measurement of temperature increase in an around voids/defects under long-term ac and pulsed stresses and its correlation to the dielectric strength and dielectric breakdown.

5.0 CONCLUSIONS (Year-1 Activity)

A summary of conclusions that can be drawn from the work performed in the first year is as follows.

- o Composite laminate structures give better electrical properties versus single film structures.
- o Partial discharges greatly reduces dielectric strength and life.
- o Certain impregnants such as Fluorinerts, give better corona performance of insulating materials.
- o A threshold voltage is found in Fluorinert below which breakdown will not occur, irrespective of the number of pulses. This is not found in air.
- o Pulse-width has very little effect on dielectric strength under existing experimental conditions.
- o Pulse rise time may influence time-to-break of insulation in certain cases.
- o A theoretical model was established to calculate the temperature increase in each layer of a composite laminate structures.

4.14 Concluding Remarks

Using a finite sine transform method, the steady state temperature rises have been calculated in a block consisting of alternating layers of Aluminum, Fluorinert and Polypropylene. It was found that the maximum temperature rise was about 5.5 °C (at the center of the block) when the block dimensions were 0.1 m x 0.1 m x 0.05 m. In these calculations, it was assumed that there was no heat generation in the Aluminum layer and that the rate of heat generation was 200 watts/kg in both Fluorinert and Polypropylene. This would represent the lower limit of the rise in temperature since it has been assumed that the six faces are kept at room temperature and that the Aluminum layers, which provide a low resistance path, are all in contact with the outside of the block. In practice, both these assumptions may not hold if a capacitor is made into the shape of a cylinder by rolling a three-layered sandwich. To calculate the maximum temperature rise, we can assume that the shape of the composite is a cylinder with insulated ends and that it contains no Aluminum. In this case the centerline temperature is given by. [67]

$$T_{\max} = \frac{Q}{4} r^2$$

where r is the radius. If Q is about 10^6 °C/m² and if r is about 0.05 m, this yields $T_{\max} = 625$ °C. This is an enormous number and it is clear that the actual temperature rise will depend critically on the physical design of the composite.

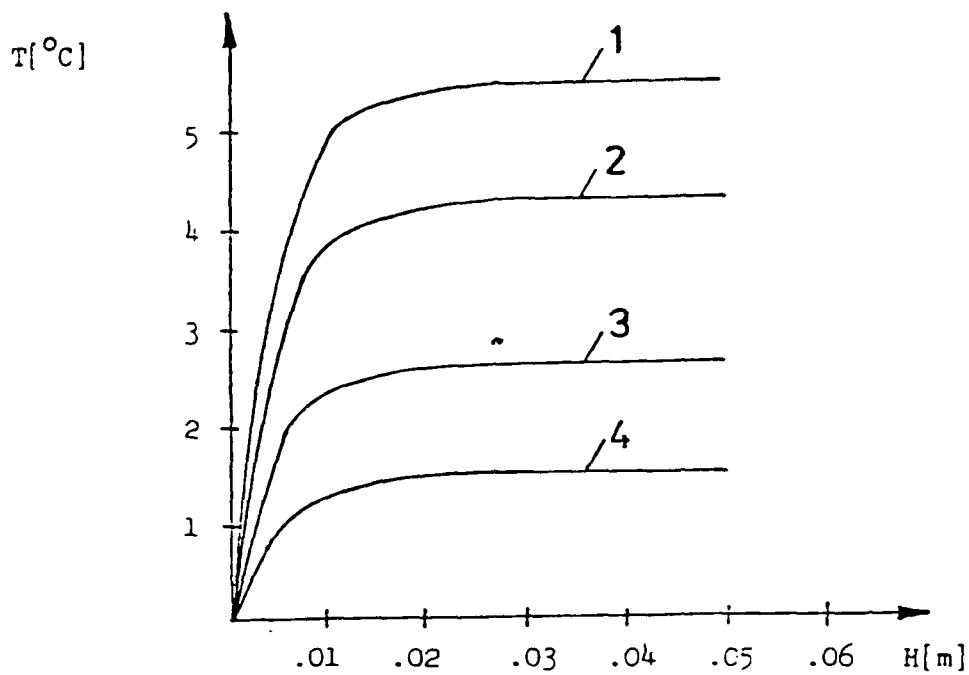


Fig. 4.7 Dependence of the temperature on height ($L = 0.1$ m, $W = 0.1$ m) for different X - positions (scheme 2).

$$1 - x = 0.05\text{m}, \quad y = 0.05, \quad z = H/2$$

$$2 - x = 0.025\text{m}, \quad y = 0.05, \quad z = H/2$$

$$3 - x = 0.0125\text{m}, \quad y = 0.05, \quad z = H/2$$

$$4 - x = 0.00625\text{m}, \quad y = 0.05, \quad z = H/2$$

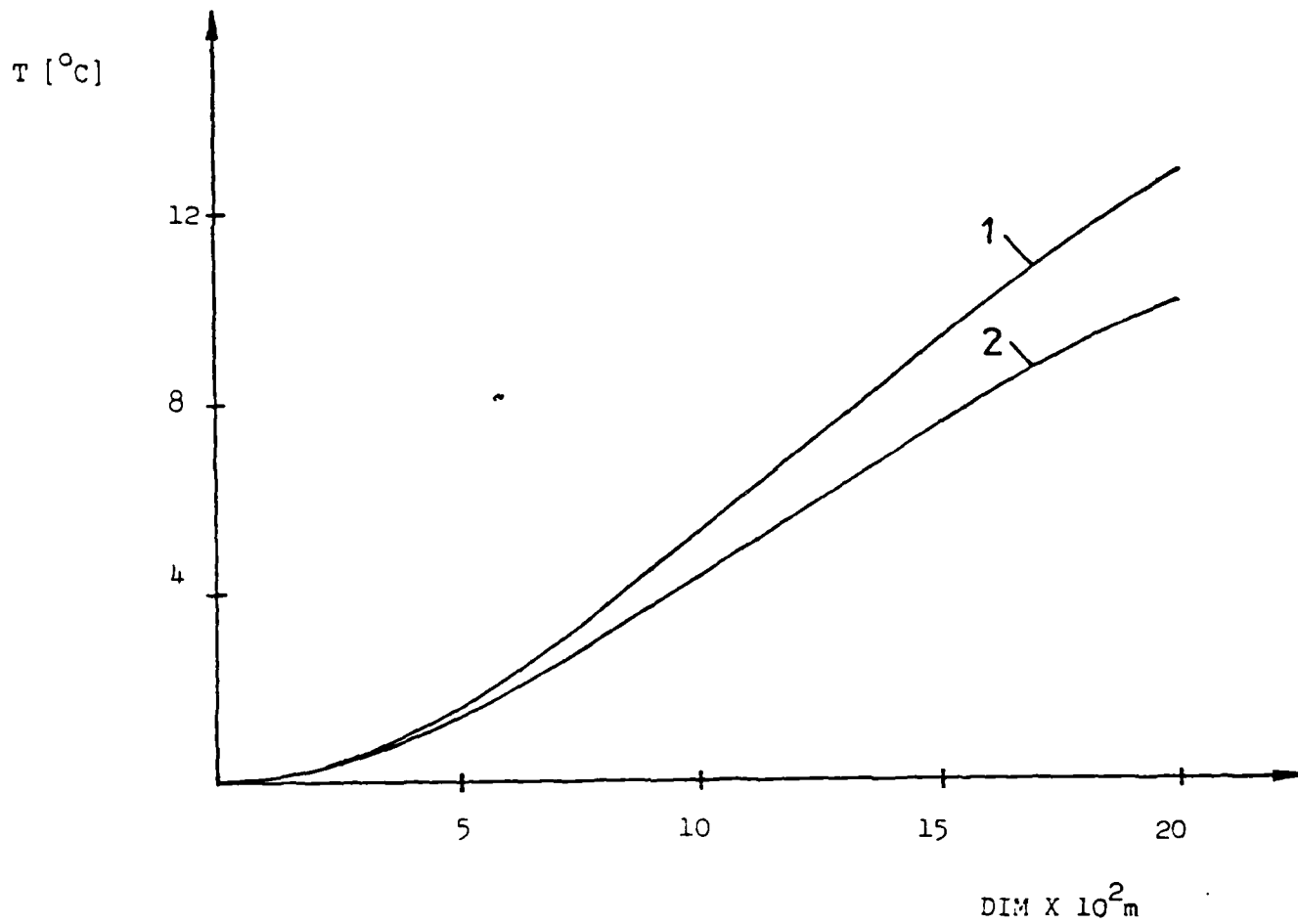


Fig. 4.6 Dependence of the temperature on the dimensions of the system ($L=W=DIM$, $H=1. \cdot 10^{-2}$ m) (scheme 2)

1 - $Z = 5.0 \cdot 10^{-3}$ m

2 - $Z = 2.5 \cdot 10^{-3}$ m

halved without affecting the results. The maximum temperature rise is seen to be about 1.4 °C. Of course, if Q is doubled, this figure will also double. The reason for this low figure is availability of a low resistance conduction path through the Aluminum.

4.12 Effect of L and W Keeping H Constant

If one keeps everything else constant, but changes L along ($L = W$) the temperature at a fixed point seems to increase almost quadratically with L . This is illustrated in Figure 4.6 and is consistent with the analytic solution derived for two dimensional heat conduction in a homogeneous material. Changing L from 0.5 m to 0.1 m results in the maximum temperature rise going from 1.4 °C to 5.2 °C.

4.13 Effect of Changing H

Finally, we investigated the effect of increasing H , keeping everything else constant. If L and W were each 0.1 m, it was found that increasing H beyond 0.01 m had little effect on the temperatures. All this can be rationalized if we realize that increasing H indefinitely would result in a slender bar of square cross section and insulated ends; for this case, the temperature should be independent of H . This is shown graphically in Figure 4.7.

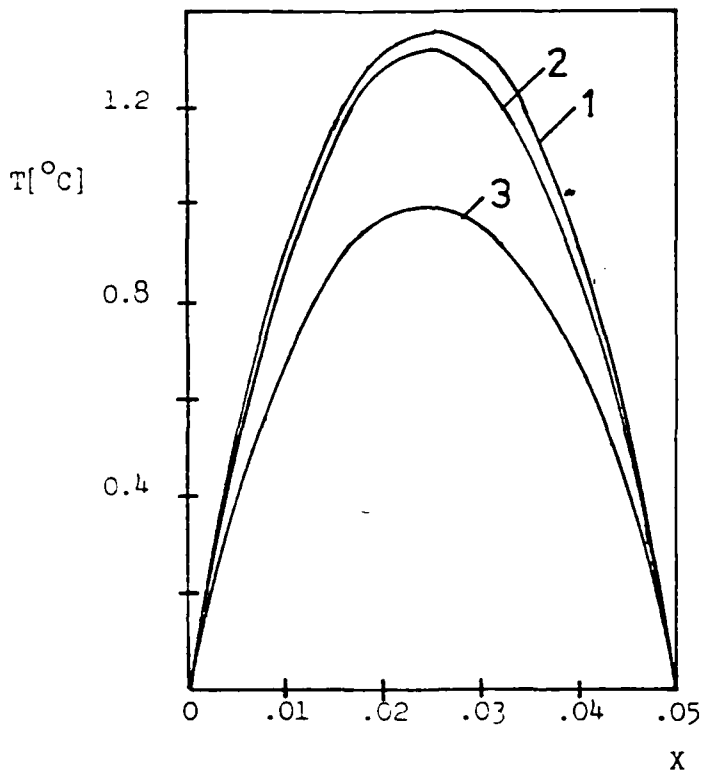


Figure 4.4 Scheme 1

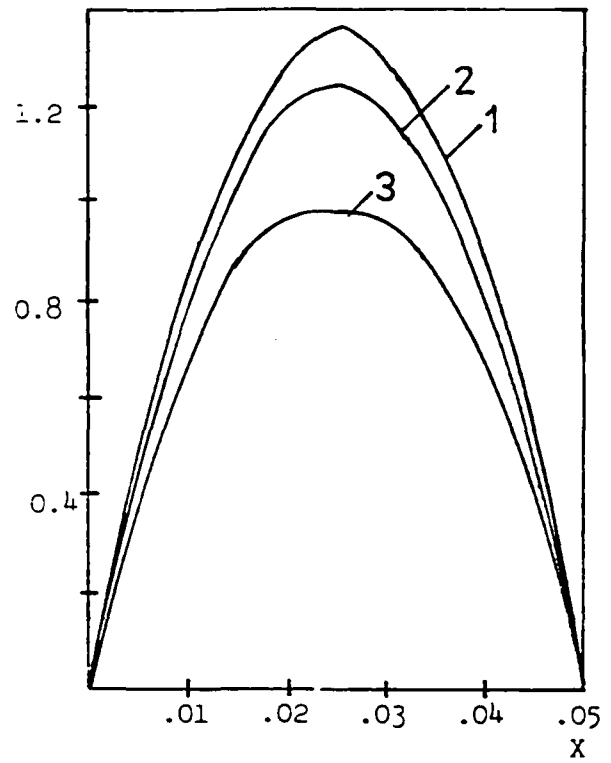


Figure 4.5 Scheme 2.

Temperature profiles vs. X direction for different Z positions
 ($y = 0.025\text{m}$) ($L=0.05\text{m}$, $W=0.05\text{m}$, $H = 0.01\text{m}$)

1 - $Z = 5.0 * 10^{-3}\text{m}$

2 - $Z = 2.5 * 10^{-3}\text{m}$

3 - $Z = 1.0 * 10^{-3}\text{m}$

9.0 APPENDICES

APPENDIX A

PROPERTIES OF DIELECTRICS USED [12,41,45,64]

	Mylar	Teflon	Polypropylene	Castor Oil
ϵ (21 °C, 60 Hz)	3.3	2.1	2.2	4.7
$\tan \delta$ (21 °C, 60 Hz)	0.0025	0.0002	0.0002	0.003
ac V_{bd} (V/mil)	5000	4000	7500	305
ρ (g/c.c.)	1.395	2.20	0.65	0.947

ϵ : dielectric constant

$\tan \delta$: dielectric loss

V_{bd} : ac breakdown voltage

ρ : density

APPENDIX B

STANDARD DEVIATIONS (\bar{X}) AND BREAKDOWN VOLTAGES (V_{bd})

Rod-Plane Electrodes

In Air

t_s (sec)	Mylar				Teflon				Polypropylene			
	3-mil film		3x1-mil films		3-mil film		3x1-mil films		3-mil film		3x1-mil films	
	V_{bd} (kV)	\bar{X}										
0	12.58	0.4930	12.70	0.6708	7.92	0.7610	7.34	0.3505	14.02	0.2913	14.42	0.4376
15	12.07	0.1729	12.36	0.4922	5.44	0.8243	6.72	0.5872	13.50	0.5000	14.0	0.0000
30	11.35	1.0049	11.91	0.3237	5.39	1.2571	6.15	0.9314	13.32	0.4724	13.38	0.4337
60	10.75	0.2700	11.08	0.2268	5.78	1.0416	5.91	0.3472	13.11	0.5398	13.17	0.2138
90	10.64	0.4504	10.65	0.4995	5.37	0.8280	5.60	0.3651	12.14	0.3779	12.22	0.1762

APPENDIX B (Continued)

BREAKDOWN VOLTAGES (V_{bd}) AND STANDARD DEVIATIONS (X)

Plane-Plane Electrodes

with void

in castor oil

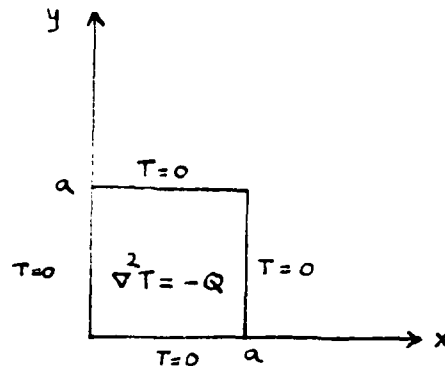
in air

t_s (sec)	Polypropylene			Polypropylene			Polypropylene								
	3x1-mil films			3x1-mil films			3x1-mil films								
	3-mil film	V_{bd} (kV)	\bar{X}	3-mil film	V_{bd} (kV)	\bar{X}	3x1-mil film	V_{bd} (kV)	\bar{X}	3x1-mil films in castor oil	V_{bd} (kV)	\bar{X}	3x1-mil films in air	V_{bd} (kV)	\bar{X}
0	13.21	0.6362	14.92	0.5155	14.71	0.2193	16.90	0.1914	16.85	0.2440	11.24	0.2760			
15	12.77	0.9050	14.48	0.1346	14.55	0.1274	16.68	0.3761	16.58	0.1574	10.68	0.5273			
30	12.58	1.0621	14.07	0.2497	14.38	0.1346	16.40	0.2236	16.30	0.1290	9.78	0.1865			
60	12.17	0.1380	13.78	0.1865	14.14	0.1322	15.91	0.1952	15.71	0.2268	9.0	0.2309			
90	11.94	0.1512	13.20	0.2828	13.97	0.1380	15.58	0.3024	15.38	0.1865	8.27	0.2288			

APPENDIX C

Solution of two dimensional Poisson equation

Consider the situation shown in the figure.



We can represent any function in terms of a complete set of linearly independent functions, such as sine functions.

$$\text{i.e., } f(y) = \sum_1^{\infty} C_n \sin\left(\frac{n\pi y}{a}\right)$$

where

$$c_n = \frac{2}{a} \int_0^a f(y) \sin\left(\frac{n\pi y}{a}\right) dy$$

Specifically if $f(y) = Q$

$$\text{then } c_n = \begin{cases} \frac{4Q}{n\pi} & n \text{ odd} \\ 0 & n \text{ even} \end{cases}$$

$$\text{so that } Q = \frac{4Q}{\pi} \sum_1^{\infty} \frac{1}{n} \sin\left(\frac{n\pi y}{a}\right) \text{ where } n \text{ is odd.}$$

To solve the Poisson equation, seek

$$T(x, y) = \sum_1^{\infty} f_n(x) \sin \frac{n\pi y}{a}$$

$$\text{with } f_n(0) = f_n(a) = 0$$

Plugging the expressions for Q and T into the differential equation, one has

$$\sum_1^{\infty} (f_n'' - \frac{n^2 \pi^2}{a^2} f_n) \sin \frac{n\pi y}{a} = - \sum_1^{\infty} \frac{4Q}{n\pi} \sin(\frac{n\pi y}{a})$$

So that

$$f_n'' - \frac{n^2 \pi^2}{a^2} f_n = - \frac{4Q}{n\pi} \quad n = \text{odd}$$

$$= 0 \quad n = \text{even}$$

The f_n 's can be obtained in a straight forward manner with the result

$$T(x,y) = \sum_{n=1}^{\infty} f_n(x) \sin \frac{n\pi y}{a} \quad n = 1, 3, 5, 7, \dots$$

where

$$f_n(x) = c_1(n) e^{n\pi x/a} + c_2(n) e^{-n\pi x/a} + \frac{4Qa^2}{n^3 \pi^3}$$

with

$$c_1(n) = \frac{4Q a^2}{n^3 \pi^3} \frac{(1 - e^{-n\pi})}{(e^{-n\pi} - e^{n\pi})}$$

and

$$c_2(n) = \frac{-4Qa^2}{n^3 \pi^3} \frac{(1 - e^{n\pi})}{(e^{-n\pi} - e^{n\pi})}$$

A characteristic feature of the solution is that $T(X, Y)$ is proportional to Q .

It is obvious that the maximum temperature will occur at the position $X = a/2, y = a/2$. With these values of X and Y one gets

$$\frac{\pi^3}{4 a^2 Q} T_{\max} = \sum_1^{\infty} \frac{\sin(\frac{n\pi}{2})}{n^3} \left[\frac{2(e^{\frac{n\pi}{2}} - e^{-n\pi/2})}{(e^{-n\pi} - e^{n\pi})} + 1 \right] \quad n = 1, 3, 5, \dots$$

It can be shown that the right hand side sums to 0.571. Thus

$$T_{\max} = \frac{4 \times 0.571 \times a^2 Q}{\pi^3}$$

in particular, if $a = 0.1$ metres

$$T_{\max} = 7.366 \times 10^{-4} Q$$

END

FILMED

4-85

DTIC